Doctorate Program in Molecular Oncology
and Endocrinology
Doctorate School in Molecular Medicine

XX cycle - 2004–2007
Coordinator: Prof. Giancarlo Vecchio

"The role of *ped/pea-15* gene in the regulation of glucose homeostasis"

Gregory Alexander Raciti

University of Naples Federico II
Dipartimento di Biologia e Patologia Cellulare e Molecolare
"L. Califano"

Administrative Location

Dipartimento di Biologia e Patologia Cellulare e Molecolare "L. Califano"
Università degli Studi di Napoli Federico II

Partner Institutions

Italian Institutions
Università di Napoli "Federico II", Naples, Italy
Istituto di Endocrinologia ed Oncologia Sperimentale "G. Salvatore", CNR, Naples, Italy
Seconda Università di Napoli, Naples, Italy
Università del Sannio, Benevento, Italy
Università di Genova, Genoa, Italy
Università di Padova, Padua, Italy

Foreign Institutions
Johns Hopkins School of Medicine, Baltimore, MD, USA
Johns Hopkins Krieger School of Arts and Sciences, Baltimore, MD, USA
National Institutes of Health, Bethesda, MD, USA
Ohio State University, Columbus, OH, USA
Université Paris Sud XI, Paris, France
Universidad Autonoma de Madrid, Spain
Centro de Investigaciones Oncologicas (CNIO), Spain
Universidade Federal de Sao Paulo, Brazil
Albert Einstein College of Medicine of Yeshiwa University, USA

Supporting Institutions
Università di Napoli "Federico II", Naples, Italy
Ministero dell'Istruzione, dell'Università e della Ricerca
Istituto Superiore di Oncologia (ISO)
Terry Fox Foundation, Canada
Istituto di Endocrinologia ed Oncologia Sperimentale "G. Salvatore", CNR, Naples, Italy
Centro Regionale di Competenza in Genomica (GEAR)

Faculty

Italian Faculty

Giancarlo Vecchio, MD, Co-ordinator
Salvatore Maria Aloj, MD
Francesco Beguinot, MD
Maria Teresa Berlingieri, PhD
Angelo Raffaele Bianco, MD
Bernadette Biondi, MD
Francesca Carlomagno, MD
Gabriella Castoria, MD
Angela Celetti, MD
Annamaria Cirafici, PhD
Mario Chiariello, MD
Vincenzo Ciminale, MD
Annamaria Colao, MD
Alma Contegiacomo, MD
Sabino De Placido, MD
Monica Fedele, PhD
Pietro Formisano, MD
Alfredo Fusco, MD
Massimo Imbriaco, MD
Paolo Laccetti, MD
Antonio Leonardi, MD
Barbara Majello, PhD
Rosa Marina Melillo, MD
Claudia Miele, PhD
Francesco Oriente, MD
Roberto Pacelli, MD
Giuseppe Palumbo, PhD
Silvio Parodi, MD
Giuseppe Portella, MD
Giorgio Punzo, MD
Antonio Rosato, MD
Massimo Santoro, MD
Giampaolo Tortora, MD
Donatella Tramontano, PhD
Giancarlo Troncone, MD
Bianca Maria Veneziani, MD
Giuseppe Viglietto, MD
Roberta Visconti, MD

Foreign Faculty

National Institutes of Health (USA)
Michael M. Gottesman, MD
Silvio Gutkind, PhD
Stephen Marx, MD
Ira Pastan, MD
Phil Gorden, MD

Johns Hopkins School of Medicine (USA)
Vincenzo Casolaro, MD
Pierre Coulombe, PhD
James G. Herman MD
Robert Schleimer, PhD

Johns Hopkins Krieger School of Arts and Sciences (USA)
Eaton E. Lattman, MD

Ohio State University, Columbus (USA)
Carlo M. Croce, MD

Albert Einstein College of Medicine of Yeshiwa University (USA)
Luciano D'Adamio, MD
Nancy Carrasco

Université Paris Sud XI (France)
Martin Schlumberger, MD

Universidad Autonoma de Madrid (Spain)
Juan Bernal, MD, PhD
Pilar Santisteban

Centro de Investigaciones Oncologicas (Spain)
Mariano Barbacid, MD

Universidade Federal de Sao Paulo (Brazil)
Janete Maria Cerutti
Rui Maciel

“The role of *ped/pea-15* gene in the regulation of glucose homeostasis”

Table of contents

List of Publications

This dissertation is based upon the following publications:

1. Formisano P, Perruolo G, Libertini S, Santopietro S, Troncone G, Raciti GA, Oriente F, Portella G, Miele C, Beguinot F. Raised expression of the antiapoptotic protein PED/PEA-15 increases susceptibility to chemically induced skin tumor development. Oncogene 2005; 24:7012-21.

2. Valentino R, Lupoli GA, Raciti GA, Oriente F, Marinaro E, Della Valle E, Salomone M, Riccardi G, Vaccaro O, Donnarumma G, Sesti G, Hribal ML, Cardellini M, Miele C, Formisano P, Beguinot F. The PEA-15 gene is overexpressed and related to insulin resistance in healthy first-degree relatives of patients with type 2 diabetes. Diabetologia 2006; 49:3058-3066.

3. Miele C*, Raciti GA*, Cassese A, Romano C, Giacco F, Oriente F, Paturzo F, Andreozzi F, Zabatta A, Troncone G, Bosch F, Pujol A, Chneiweiss H, Formisano P, Beguinot F. PED/PEA-15 regulates glucose-induced insulin secretion by restraining potassium channel expression in pancreatic beta-cells. Diabetes 2007; 56:622-33.
   * equal contribution

Abstract

The role of *ped/pea-15* gene in the regulation of glucose homeostasis.

The hyper-expression of Phosphoprotein Enriched in Diabetes/ Phosphoprotein Enriched in Astrocytes (*Ped/Pea-15*) gene is commonly found in human diabetic patients and causes impaired glucose tolerance in transgenic mice. Aim of this study was to investigate: i) PED/PEA-15 expression levels in first degree relatives (FDR) of patients with T2D and the possible correlation between PED/PEA-15 levels and diabetes subphenotypes; ii) the role of PED/PEA-15 in beta cell function *in vivo*.

i) In Peripheral Blood Leucocytes (PBL) from the first degree relatives (FDR) of patients with T2D, PED/PEA-15 expression was two-fold higher than in euglycaemic individuals with no family history of diabetes (control subjects), both at the protein and the mRNA level ($p<0.001$). PED/PEA-15 expression was independent of sex and unrelated to age, Body Mass Index (BMI), waist circumference, systolic and diastolic Blood Pressure (BP), and fasting cholesterol, triacylglycerol and glucose levels. However, in euglycaemic FDR of T2 diabetic subjects, PED/PEA-15 expression was inversely correlated with insulin sensitivity ($r=-557$, $p=0.01$). ii) Transgenic mice with beta cell specific overexpression of *ped/pea-15* (beta-tg) exhibited decreased glucose tolerance and impaired insulin response to hyperglycemia. Islets from the beta-tg also exhibited little response to glucose. Furthermore, overexpression of PED/PEA-15 reduce mRNAs encoding the *Sur1* and *Kir6.2* potassium channel subunits and their upstream regulator *Foxa2*, and inhibited the activity of the atypical PKCzeta by glucose both in mouse islets and in beta cells lines. Rescue of PKCzeta activity elicited recovery of the expression of the *Sur1, Kir6.2* and *Foxa2* genes and of glucose-induced insulin-secretion in PED/PEA-15 overexpressing beta cells. Interestingly, islets from *ped/pea-15* null mice exhibited a 2-fold increased activation of PKCzeta by glucose and abundance of the *Sur1*, *Kir6.2* and *Foxa2* mRNAs and enhanced glucose effect on insulin secretion.

Thus, PED/PEA-15 overexpression represents a common defect in FDR and is correlated with reduced insulin sensitivity in these individuals, and its beta cell specific overexpression dysregulates beta cell function, restraining potassium channel expression in pancreatic beta cells and resulting in impaired glucose tolerance *in vivo*.

Background

1 Glucose homeostasis

Despite periods of feeding and fasting, plasma glucose remains in a narrow range between 4 and 7 mM in normal individuals. This tight control is governed by the balance between glucose absorption from the intestine, production by the liver and uptake and metabolism by peripheral tissues (Saltiel and Kahn 2001).

Carbohydrate metabolism is regulated by several hormones, and also by sympathetic and parasympathetic nervous system activity (Table 1). The increasing glucose concentration after feeding (80/150 mg/dl) determines an increase of insulin release from pancreatic beta cells and a decrease of glucagon release from pancreatic alpha cells (Kahn 1994). Insulin lowers blood glucose levels both by suppressing glycogenolysis and gluconeogenesis in the liver (thereby decreasing hepatic glucose output), and by stimulating glucose uptake into skeletal muscle and adipose tissue. These actions are opposed by the "counter-regulatory" hormones, which are secreted continuously but whose release is enhanced during physiological "stress" (Pickup 2005).

Thus, the correct efficiency of pancreatic beta cells in insulin synthesis and secretion represents a fundamental role in glucose homeostasis maintenance.

Table 1. Main hormones affecting carbohydrate metabolism

	Liver Gluconeogenesis	Glycogenolisys	HGO	Peripheral Glucose uptake
Insulin	↓	↓↓	↓↓	↑↑
Glucagon	↑↑§	↑↑	↑↑	-
Catecholamines	↑↑*§	↑	↑↑	↓
Growth hormone	↑*	-	↑	↓
Cortisol	↑*§	-	↑	↓

HGO, hepatic glucose output.
*Indirect enhancement of gluconeogenesis due to increased supply of glycerol and fatty acids by enhanced lipolysis
§Increased gluconeogenesis by effects on hepatic enzymes and increased supply of glucogenic amino acids.

2 Insulin

Insulin is the most potent anabolic hormone known. Secreted by pancreatic beta cells in response to increase of plasmatic glucose and amino acids levels after feeding, insulin promotes the synthesis and storage of carbohydrates, lipids and proteins, while inhibiting their degradation and release into the circulation. Insulin stimulates the uptake of glucose, amino acids and fatty acids into cells, and increases the expression and activity of enzymes that catalyse glycogen, lipid and protein synthesis, while inhibiting the activity or expression of those that catalyse degradation.

Insulin increases glucose uptake in muscle and fat, and it inhibits hepatic glucose production (glycogenolyisis and gluconeogenesis) in liver, thus serving as the primary regulator of blood glucose concentration. Insulin also stimulates cell growth and differentiation, and promotes the storage of substrates in fat,

liver and muscle by stimulating lipogenesis, glycogen and protein synthesis, and inhibiting lipolysis, glycogenolysis and protein breakdown (Figure 1) (Saltiel and Kahn 2001).

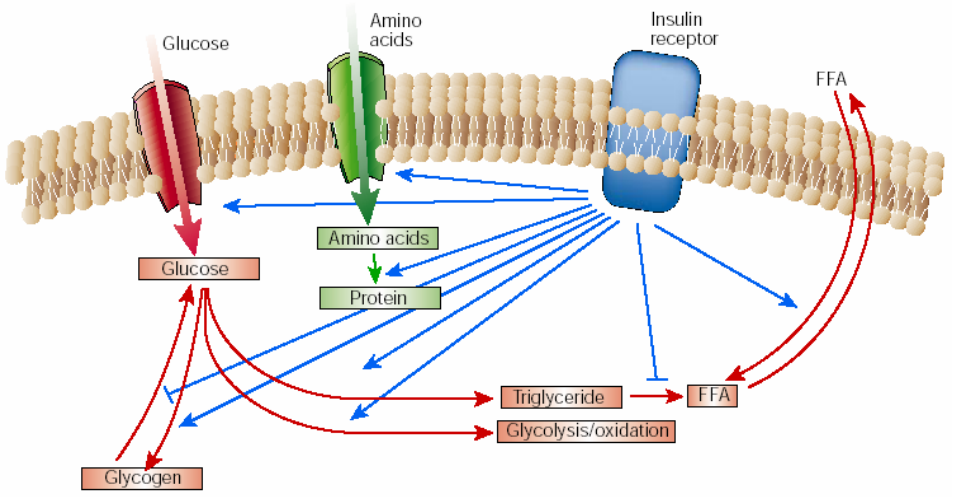

Figure 1 The regulation of metabolism by insulin.
Insulin promotes the synthesis and storage of carbohydrates, lipids and proteins. Indeed, insulin stimulates the uptake of glucose, amino acids and fatty acids into cells, and increases the expression or activity of enzymes that catalyse glycogen, lipid and protein synthesis, while inhibiting the activity or expression of those that catalyse degradation.

Insulin is an hormone of 51 amino acids and is synthesized as a precursor protein (preproinsulin) in the beta cells. Preproinsulin presents a signal sequence at N-terminus that permits its entrance in secretion vesicles. The cut of the signal sequence by proteolytic enzymes produces proinsulin. When the increase of plasmatic glucose concentrations stimulates insulin secretion, proinsulin is converted in the mature hormone by specific proteases that hydrolyse two peptide bond and generate mature insulin (Taylor, et al. 1999).

Insulin is a little protein formed by two polypeptide chains, termed respectively "A" of 21 amino acids, and "B" of 30, linked by two interchain sulphide bond.

Once beta cells are stimulated by glucose, insulin is released in blood circulation and is distributed to target tissues, where it can bind a specific receptor at high affinity, essential for insulin signalling transduction.

3 Insulin signaling system

Insulin action is mediated through the insulin receptor (IR), a transmembrane glycoprotein with intrinsic protein tyrosine kinase activity. The insulin receptor belongs to a subfamily of receptor tyrosine kinases that includes the insulin-like growth factor (IGF)-I receptor and the insulin receptor-related receptor (IRR). These receptors are tetrameric proteins consisting of two α- and two β-subunits that function as allosteric enzymes where the α-subunit

inhibits the tyrosine kinase activity of the β-subunit. Insulin binding to the α-subunit leads to derepression of the kinase activity of the β-subunit followed by transphosphorylation of the β-subunits and conformational change of the α subunits that further increases kinase activity (Patti and Kahn 1998).

Several intracellular substrates of the insulin receptor kinases have been identified (Figure 2). Four of these belong to the family of insulin-receptor substrate (IRS) proteins (White, et al. 1998). Other substrates include Gab-1 and isoforms of Shc10 (Pessin and Saltiel 2000). The phosphorylated tyrosines in these substrates act as 'docking sites' for proteins that contain SH2 (Src-homology-2) domains. Many of these SH2 proteins are adaptor molecules, such as the p85 regulatory subunit of PI(3)K and Grb2, or CrkII, which activate small G proteins by binding to nucleotide exchange factors. Others are themselves enzymes, including the phosphotyrosine phosphatase SHP2 and the cytoplasmic tyrosine kinase Fyn.

PI(3)K has a pivotal role in the metabolic and mitogenic actions of insulin (Shepherd, et al. 1995). It consists of a p110 catalytic subunit and a p85 regulatory subunit that possesses two SH2 domains that interact with tyrosine-phosphorylated motifs in IRS proteins (Myers MG Jr, et al. 1992). PI(3)K catalyses the phosphorylation of phosphoinositides on the 3-position to produce phosphatidylinositol-3-phosphates, especially PtdIns(3,4,5)P3, which bind to the pleckstrin homology (PH) domains of a variety of signalling molecules thereby altering their activity, and subcellular localization (Lietzke, et al. 2000). Phosphotidylinositol-3-phosphates regulate three main classes of signalling molecules: the AGC family of serine/threonine protein kinases, the Rho family of GTPases, and the TEC family of tyrosine kinases. PI(3)K also might be involved in regulation of phospholipase D, leading to hydrolysis of phosphatidylcholine and increases in phosphatidic acid and diacylglycerol. The best characterized of the AGC kinases is phosphoinositide-dependent kinase 1 (PDK1), one of the serine kinases that phosphorylates and activates the serine/threonine kinase Akt/PKB (Alessi, et al. 1997). Akt/PKB has a PH domain that also interacts directly with PtdIns(3,4,5)P3, promoting membrane targeting of the protein and catalytic activation. Akt/PKB has a pivotal role in the transmission of the insulin signal, by phosphorylating the enzyme GSK-3, the forkhead transcription factors and cAMP response element-binding protein. Other AGC kinases that are downstream of PI(3)K signaling include the atypical PKCs, such as PKC-ζ. Akt/PKB and/or the atypical PKCs are required for insulin stimulated glucose transport (Standaert, et al. 1997).

As is the case for other growth factors, insulin stimulates the mitogen-activaed protein (MAP) kinase extracellular signal regulated kinase (ERK) (Figure 2). This pathway involves the tyrosine phosphorylation of IRS proteins and/or Shc, which in turn interact with the adapter protein Grb2, recruiting the Son-of-sevenless (SOS) exchange protein to the plasma membrane for activation of Ras. The activation of Ras also requires stimulation of the tyrosine phosphatase SHP2, through its interaction with receptor substrates such as Gab-1 or IRS1/2. Once activated, Ras operates as a molecular switch,

stimulating a serine kinase cascade through the stepwise activation of Raf, MEK and ERK. Activated ERK can translocate into the nucleus, where it catalyses the phosphorylation of transcription factors such as p62TCF, initiating a transcriptional programme that leads to cellular proliferation or differentiation (Boulton, et al. 1991).

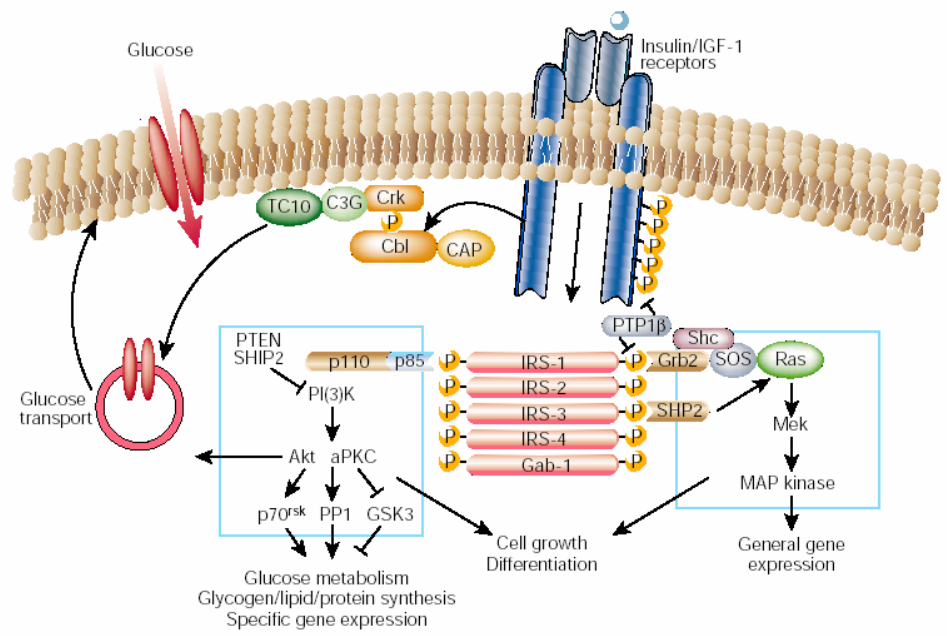

Figure 2 Signal transduction in insulin action.
The insulin receptor is a tyrosine kinase that undergoes autophosphorylation, and catalyses the phosphorylation of cellular proteins such as members of the IRS family, Shc and Cbl. Upon tyrosine phosphorylation, these proteins interact with signaling molecules through their SH2 domains, resulting in a diverse series of signaling pathways, including activation of PI(3)K and downstream PtdIns(3,4,5)P3-dependent protein kinases, ras and the MAP kinase cascade. These pathways act in a concerted fashion to coordinate the regulation of vesicle trafficking, protein synthesis, enzyme activation and inactivation, and gene expression, which results in the regulation of glucose, lipid and protein metabolism.

4 Insulin secretion

Insulin concentration is normally determined by a feed-back control system that is responsive to the prevailing level of plasma glucose (Polonsky, et al. 2001). The overall sensitivity of the pancreatic beta cell to glucose is determined by the sensitivity of peripheral tissues to the action of insulin with insulin-resistant subjects having higher insulin levels and insulin secretion rates than insulin sensitive subjects. Insulin is also secreted in response to amino acids and fatty acids and the magnitude of this response is modulated by a variety of neuronal (sympathetic and parasympathetic autonomic tone) and hormonal factors (glucagon, glp-1, and somatostatin). Glucose, however, is the overriding influence. Normal insulin secretion shows a rapid response to glucose and a complex profile. The increase in insulin secretion that occurs after the intravenous administration of glucose is virtually instantaneous; even after

oral glucose ingestion, increases in insulin secretion occur within minutes. The temporal profile of insulin secretion consists of small-amplitude pulses of insulin occurring every 5-10 minutes, superimposed on slower, larger-amplitude oscillations that occur every 1-2 hours.

After a glucose loading, it is possible to distinguish two insulin secretion phases. The first phase is characterized by a rapid increase of insulin release, immediately followed by a rapid fall of hormone plasmatic levels. The second phase, instead, is characterized by a prolonged insulin release up to 60 minutes after stimulation. At molecular level, the first phase requires ATP and Ca^{++}, and it reflects exocytosis profile of pool granules immediately disposable; second phase secretion also requires ATP and it results largely from exocytosis of insulin granules newly recruited to the plasma membrane (Mac Donald, et al. 2005).

Pancreatic beta cells secretion can be roughly divided into two components: (i) the proximal events of glucose entry and metabolism and (ii) the distal mechanism of insulin secretion, spanning from mitochondrial signal generation and initiation of electrical activity to the ultimate effectors of insulin granule exocytosis.

Glucose is transported into beta cells by the glucose transporter 2 (GLUT2). Here, GK catalyses the transfer of phosphate groups from ATP to glucose to form glucose-6-phosphate, that enters glycolysis. ATP produced by glycolysis and the Krebs cycle is the conjunction ring between glucose catabolism and electric phenomena, that occur on plasma membrane and that are responsible, ultimately, for insulin release. ATP increase, indeed, leads to closure of the ATP-sensitive K^+ (K_{ATP}) channel- a hetero-octamer formed by four subunits of the sulphonylurea 1 receptor (SUR1) and four subunits of the inwardly rectifying K^+ channel Kir6.2, responsible for the regulation of the resting membrane potential. The closing of K_{ATP} channel leads to depolarization of the plasma membrane to a value of –40mV, and influx of extracellular calcium by the opening of type L voltage-dependent calcium channels (VDCC). Ca^{++} entrance from extracellular space and the significant increase of its intracellular concentrations are considered the key events in the cascade events that leads to insulin secretion. Together with Ca^{++} mobilized from intracellular stores, this leads to fusion of insulin-containing secretory granules with the plasma membrane and the release of insulin into the circulation (Figure 3).

More than the increase of intracellular Ca^{++} concentrations, insulin secretion is sustained by the oscillation of Ca^{++} intracellular levels, paradigmatic of glucose metabolism oscillation. Three different types of Ca^{++} concentration oscillation can be observed during glucose stimulation: rapid and regular, slow and regular, or mixed, characterized by rapid oscillation superimposed to slow oscillation (Gilon, et al. 2002). According to recent hypothesis, metabolic oscillation depends on change of intracellular Ca^{++} concentration: Ca^{++} entrance determines an increase consumption of ATP and a reduction of its mitochondrial production. This, together with the direct inhibition of glycolysis by Ca^{++} , results in the decrease of ATP/ADP ratio, causing the reopening of

K_{ATP} channels. The consequent repolarization of beta cells determines the restore of Ca^{++} levels to basal values with the possibility that secretory process can be restarted (Kennedy, et al. 2002).

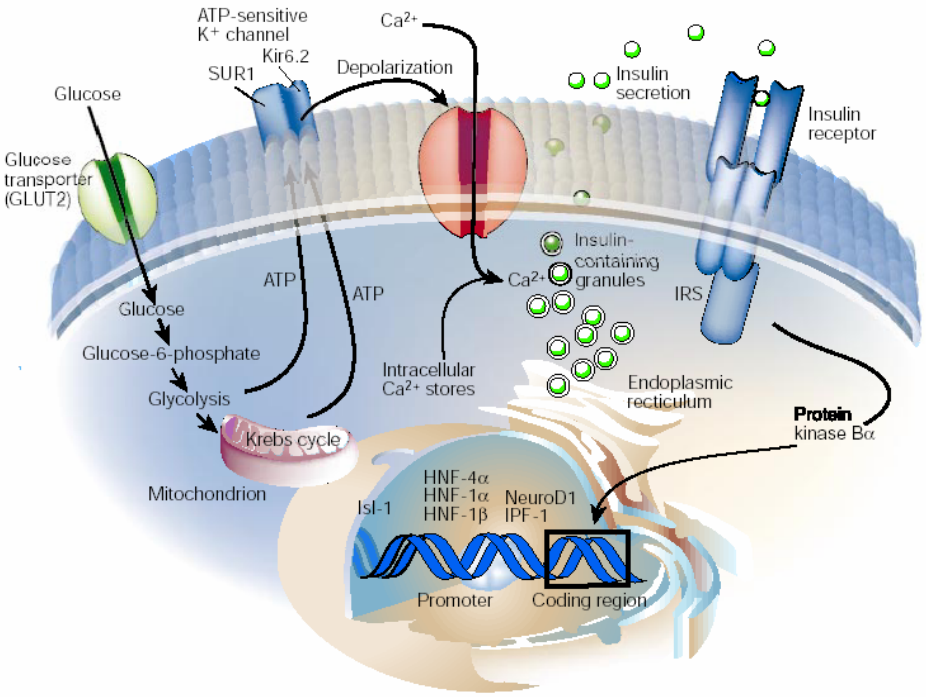

Figure 3 The regulation of glucose induced insulin secretion.
Glucose is transported into the beta cell by GLUT2, and is converted in glucose-6-phosphate by GK. The generation of ATP by glycolysis and the Krebs cycle leads to closure of the ATP-sensitive K+ channel. The closing of the K_{ATP} channel leads to depolarization of the plasma membrane and influx of extracellular calcium. Together with calcium mobilized from intracellular stores, this leads to fusion of insulin-containing secretory granules with the plasma membrane and the release of insulin into the circulation.

4.1 Regulation of insulin secretion: glucose sensors

Glucose is required as an energy substrate, but it also functions as a signaling molecule in primary processes. Glucose sensors, molecular systems that accurately detect glucose concentrations in the extracellular space, contribute to maintain glucose homeostasis by controlling several key processes.

Beta cells of pancreatic islets act as glucose-sensors, adjusting insulin output depending on the prevailing blood glucose level (MacDonald, et al. 2005). It is possible in relation to existence of a beta cellular glucose-sensing mechanism able to measure extracellular glucose. The glucose sensor is constituted by the glucose transporter 2 (GLUT2) and glucokinase (GK). These proteins are both characterized by a low affinity to glucose and they are involved in high Km glucose transport and high Km phosphorylation of glucose, respectively, which allows increased glucose utilization as its concentration rises. Indeed, since GLUT2 and GK have a Km for glucose of 5 mmol/L, glucose uptake by

GLUT2 and glucose phosphorylation in glucose-6-phosfate by GK are rapid only after feeding, when glucose concentration are elevated, and this permits to glucose-sensing unit to be extremely sensitive to plasmatic glucose levels variation. Moreover, pancreatic beta cells appear to sense glucose concentrations through its catabolic products, such that the glucose catabolism rate must be proportional to glucose levels in the extracellular space (Mac Donald, et al. 2005).

However, glucose sensing does not directly depend on GLUT-2 activity. This glucose transporter plays a more permissive role in glucose catabolism, as glucose transport in beta cells is 100-fold higher than the rates of glucose metabolism. By contrast, GK catalyses the rate-limiting step of glucose catabolism, and controls glucose oxidation and adenosine triphosphate (ATP) formation, thus acting as a true glucose sensor (Mac Donald, et al. 2005).

4.2 Regulation of insulin secretion: ATP-sensitive potassium channels

As early as 1970, ATP generation was implicated in the initiation of beta cell electrical activity based on the ability of 2,4-dinitrophenol (an uncoupler of oxidative phosphorylation) to prevent glucose-induced electrical responses in mouse islets. Subsequently, in mouse beta cells it was demonstrated the existence of K^+ channels that were closed by glucose and ATP (Mac Donald, et al. 2005).

K_{ATP} channels are now known to be expressed in numerous tissues including smooth and skeletal muscle, neurons, peripheral axons and epithelial cells. The beta cell K_{ATP} channel was the first K^+ channels cloned from insulinoma cells in 1995, along with its regulatory sulphonylurea receptor (SUR) subunit (Aguilar-Bryan, et al. 1995). There are currently two genes known for each of the K_{ATP} pore-forming subunits (Kir6.1 and 6.2) and the associated regulatory subunits (SUR1, 2), although diversity is further increased by alternative splicing of the SUR2 gene (Ashcroft and Gribble 1999). K_{ATP} channels are composed of four pore forming inward-rectifier potassium channel subunits (Kir6.2 in beta cells; two transmembrane domains) and four regulatory sulphonylurea receptor subunits (SUR1 in beta cells; total 17 transmembrane domains; Aguilar-Bryan and Bryan 1999).

In the absence of glucose K_{ATP} channels have a high open probability and mediate an outward K^+ flux that holds the membrane potential near the equilibrium potential for K^+ (approximately -70 mV). ATP can inhibit K_{ATP} channels at the Kir6.2 subunit in the absence of SUR1 and point mutations within Kir6.2 can attenuate the effect of ATP. A similar effect is mediated by the anti-diabetic sulphonylurea drugs through an interaction with SUR1, a member of the ATP-binding cassette super-family, stimulating insulin secretion even in the absence of glucose. The SUR1 subunit also binds ATP (both with and without Mg) and MgADP via the presence of two cytoplasmic nucleotide binding domains. Binding of MgADP to SUR1 is thought to stabilize the channel in the open configuration, and when the ATP-to-ADP ratio increases,

MgADP is displaced, and the Kir6.2 subunit becomes available for block by ATP (Mac Donald, et al. 2005).

4.3 Regulation of insulin secretion: Protein Kinase C

The Protein Kinase C (PKC), identified for the first time as a Serine/Threonine kinase activated by Ca^{2+} and phospholipids, up to now can be divided in three subgroups based on cofactors requirements: classical PKCs (α, β, and γ), which are dependent on Ca^{2+} and diacylglycerol (DAG); novel PKCs (δ, ε, η and θ), activated by DAG; and atypical PKCs (ζ, λ, ι), which are not dependent on Ca^{2+} and DAG (Formisano, et al. 1998).

Several studies demonstrated that PKCs play an important role in controlling beta cell insulin secretion. These kinases, indeed, act in the beta cell amplifying the metabolic signals responsible for insulin release. In particular, PKC activation develops the insulin response to metabolic and not metabolic (sulphonylurea) stimuli, and it is necessary to observe the typical biphasic profile of insulin secretion. Eight isoforms of PKCs have been identified in the beta cells (α, γ, δ, ε, η, θ, ζ, λ), and two of these, PKCα and PKCε translocate to the membrane in response to glucose with different kinetics. PKCα migrates into the nucleus after two minutes from glucose stimulation, and subsequently localizes to the plasma membrane. The block of PKCα translocation determines a 40% decrease of glucose induced insulin secretion. This depends on the role of PKCα in phosphorilating and, thus, activating several components of SNARE complex involved in the exocytosis process (Nesher, et al. 2002). Instead, PKCε colocalizes, in response to glucose, with insulin containing granules, but its translocation to the plasma membrane is slower (15 minutes) compared to PKCα. Probably PKCε is involved in the pro-insulin processing and in the mobilization of granules. Moreover, *in vitro* studies have demonstrated that PKCε is necessary for glucose and sulphonylurea induced insulin secretion since the expression of a negative double mutant of the protein abolished completely insulin secretion. On the other hand, the overexpression of the kinase determined a significant increase of insulin secretion (Mendez, et al. 2005).

Atypical PKCs have been reported to control also the function of a number of transcription factors. PKCλ has recently been shown to play a major role in regulating glucose-induced insulin secretion by modulating the expression of genes involved in this process (Hashimoto, et al. 2005). Indeed, islets from mice that lack PKCλ in pancreatic beta cells show impaired insulin secretion in response to hyperglycaemia whereas the basal rate of insulin release is increased. This depends on the ability of PKCλ to regulate glucose-induced insulin release by modulating the transcriptional expression of genes important for beta cell function such as Glut-2, Foxa2, Sur1, Kir6.2, and hexokinase 1 and 2.

5 Diseases with insulin secretion deficiencies

Maturity-onset diabetes of the young (MODY), Persistent Hyperinsulinemic Hypoglycemia of Infancy (PHHI), mitochondrial diabetes, Type 1 (T1D) and Type 2 Diabetes (T2D) are a heterogeneous group of disorders characterized by insulin secretory abnormalities and by high blood glucose levels.

In subjects with MODY, PHHI, or mitochondrial diabetes, the elevation in blood glucose levels is due to genetically determined defects in processes that are critical for the normal signaling pathways in the beta cell. The effects of these mutations on insulin secretion are so severe that diabetes develops in people with normal or relatively normal insulin sensitivity and without the contribution of environmental factors. In T1D, instead, insulin secretory abnormalities results from an absolute deficiency of insulin due to autoimmunological destruction of the insulin-producing pancreatic beta cell. Finally, in T2D, more moderate abnormalities of secretion are present that cause glucose intolerance only if insulin resistance is also present. The genetic basis of beta cell dysfunction in this form of diabetes is more complex, involving both multiple interacting genes and environmental factors, which determine whether diabetes will develop and at what age. Here no genetic abnormalities profoundly affect beta-cell function, but rather the inability of the pancreatic beta cell to adapt to the reductions in insulin sensitivity that occur over a lifetime precipitates the onset of hyperglycaemia (Bell and Polonsky 2001).

5.1 MODY, PHHI, and mitochondrial diabetes

MODY is a clinically heterogeneous group of disorders characterized by non-ketotic diabetes mellitus, an autosomal dominant mode of inheritance, onset usually before 25 years of age and frequently in childhood or adolescence, and a primary defect in pancreatic beta cell function. MODY can result from mutations in any one of at least six different genes that encode the glycolytic enzyme glucokinase and five transcription factors: hepatocyte nuclear factor (HNF)-4α, HNF-1α, insulin promoter factor-1 (IPF-1), HNF-1β and neurogenic differentiation 1/beta cell E-box transactivator 2 (NeuroD1/BETA2) (Table 2). All the mentionated genes are expressed in the pancreatic beta-cell and mutations lead to beta cell dysfunction and diabetes mellitus in the heterozygous state (Bell and Polonsky 2001).

Table 2 MODY classification and genes

MODY	Gene involved
MODY 1	HNF-4α
MODY 2	GK
MODY 3	HNF-1 α
MODY 4	IPF-1
MODY 5	NEURO D1/BETA 2

GK is expressed at highest levels in the pancreatic beta cell and in the liver. It catalyses the transfer of phosphate groups from ATP to glucose to generate glucose-6-phosphate: the first rate-limiting step in glucose metabolism. GK functions as the glucose sensor in the beta cell and influences the ability to store glucose as glycogen in the liver. Heterozygous mutations leading to partial deficiency of GK are associated with MODY and homozygous mutations usually result in complete deficiency of this enzyme, leading to PHHI (Bell and Polonsky 2001)..

The transcription factors HNF-1α, HNF-1β and HNF-4α are involved in the tissue-specific regulation of gene expression in the liver, pancreatic beta cells and other tissues. HNF-1α and HNF-1β are members of the homeodomain-containing family of transcription factors and HNF-4α is an orphan nuclear receptor. They are part of a network of transcription factors that controls gene expression during embryonic development and also in adult tissues where they are co-expressed. In the pancreatic beta cell, they regulate the expression of genes important in the regulation of insulin secretion. Mutations in these genes produce defects in insulin secretory responses to a variety of factors, particularly glucose, which are present before the onset of hyperglycaemia. In mice lacking the gene for HNF-1α, beta cell mass fails to increase despite the presence of hyperglycaemia, suggesting that this transcription factor may regulate beta cell mass (Bell and Polonsky 2001).

IPF-1 is a homeodomain-containing transcription factor involved in pancreatic development, transcriptional regulation of a number of beta cell genes including insulin, glucokinase, islet amyloid polypeptide and GLUT2, and mediation of glucose-stimulated insulin gene transcription. Mutations in the heterozygous state are associated with MODY, whereas mouse and human homozygotes fail to develop a pancreas and suffer congenital diabetes mellitus. IPF-1 mutations have also been discovered in a small fraction of patients with typical adult-onset type 2 diabetes. Subjects with heterozygous mutations in IPF-1 demonstrated reduced insulin secretory responses to glucose and glucagon-like peptide-1, consistent with a defect in the signalling pathways that regulate secretion in the beta cell and/or a defect in beta cell mass.

The basic helix–loop–helix transcription factor NeuroD1/BETA2 is involved in the regulation of transcription of the insulin gene and is required for normal pancreatic islet development. Mutations in NeuroD1 are a rare cause of MODY and result in reduced serum insulin concentrations, either due to a signalling defect in the beta cell, or a reduction in beta cell mass, or both (Bell and Polonsky 2001).

PHHI, also known asfamilial hyperinsulinism, pancreatic nesidioblastosis or hyperinsulinemic hypoglycemia, is a rare genetic disease, that can be inherited in a dominant or recessive way. It is mainly characterized by the presence of inappropriately high levels of insulin in parallel with low or very low glucose levels. This disease affects newborns and infants and it is as frequent as 1:50000 for unselected populations. Mutations in four different genes have been identified: the K_{ATP} channel genes *SUR1* and *Kir6.2*, glucokinase (*GK*), and

glutamate dehydrogenase (*GLUD1*). Nevertheless, in as many as 60% of patients, the genetic basis of the condition has not been elucidated. The most common and most severe forms of PHHI arise from *SUR1* (40 different mutations) and/or *Kir6.2* (three mutations) gene defects and alterations of beta cellular K_{ATP} channels are responsible for PHHI physiopathology. Using both recombinant expression systems and beta cells isolated from patients after surgery, investigators have shown these mutations to lead to impaired trafficking or assembly of K_{ATP} channels or to cause defects in the ADP-dependent regulation of channel activity, and it results in depolarized beta cells with unregulated Ca^{2+} channel activity, that determines hypoglycaemia and impaired insulin secretion (Kane, et al. 1996; Straub, et al. 2001).

In addition to mutations in the nuclear genome, abnormal mitochondrial function resulting from mutations in the mitochondrial genome can lead to diabetes. The most common diabetes-associated mutation is an A-to-G transition in the mito-chondrial $tRNA^{Leu(UUR)}$ gene at base pair 3,243. This mutation results in defects in insulin secretion including failure of glucose to prime the insulin secretory response and abnormal insulin secretory oscillation (Bell and Polonsky 2001).

5.2 Type 1 diabetes

T1D accounts for 10% of all diabetes cases. The disease can affect people of any age, but usually occurs in children or young adults. T1D is caused by an auto-immune reaction againist the insulin-producing cells. The reason why this occurs is not fully understood. T1D pathogenesis involves environmental triggers that may activate autoimmune mechanisms in genetically susceptible individuals. It is characterized by insulitis, an infiltration of the pancreatic islets by lynphocytes, macrophages and neutrophil granulocytes, resulting in auto-immune destruction of the beta cells since chronic exposure to pro-inflammatory cytokines such as IL-1, TNFα, and interferon γ is cytotoxic to beta cells. The clinical manifestation of T1D is typically late-stage, when majority of beta cells (90%) have been destroyed and its onset is often sudden and dramatic. The lives of people with this form of diabetes are entirely dependent on injections of insulin every day for survival in order to prevent the development of ketoacidosis. (Diabetes Atlas 2006)

5.3 Type 2 diabetes

T2D is the most common type of diabetes and accounts for 90% of all forms of diabetes. T2D is most common in people older than 45 who are overweight. However, as a consequence of increased obesity among young people, it is becoming more common in children and young adults.

T2D is a heterogeneous syndrome with many possible causes. This is due to the interaction of environmental factors with a genetic susceptibility to the disease (Table 3), and it is becoming more and more evident that the relative contribution of genes and environment can differ considerably, even among individual whose clinical phenotype is similar (Diabetes Atlas 2006).

The maintenance of normal glucose homeostasis depends on a precisely balanced and dynamic interaction between tissue sensitivity to insulin and insulin secretion. Type 2 diabetes develops because of defects in both insulin secretion and action, both of these with a genetic as well as an acquired component. Thus, T2D is made up of different forms each of which is characterized by variable degrees of insulin resistance and beta cell dysfunction, and which together lead to hyperglycaemia.

Insulin resistance, typically, is an early feature of T2D. It results from a genetically determined reduction in insulin sensitivity, compounded by exposure to the environmental factors, which further impair insulin action. Major sites of insulin resistance include liver and the peripheral tissues, skeletal muscle and fat. In muscle and fat, insulin resistance is manifested by decreased glucose uptake; in muscle, it impaired utilization of glucose by non-oxidative pathways as well as by decrease in glucose oxidation; in the liver, insulin resistance leads to failure of insulin to suppress hepatic glucose production, which is fulled by glycogen breakdown and particularly by gluconeogenesis (Pickup 2005) (Figure 4).

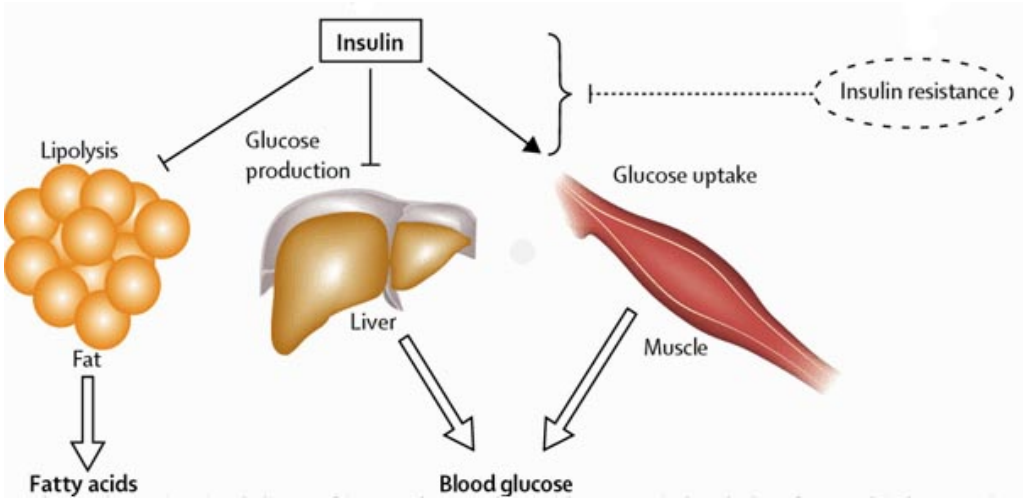

Figure 4. Insulin resistance on tissue targets.
The main sites of insulin resistance are liver and the peripheral tissue, skeletal muscle and fat. insulin resistance is manifested by decreased glucose uptake in muscle and fat, and by failure of insulin to suppress hepatic glucose production in the liver.

The beta cell dysfunction ,the other key component of T2D pathophysiology, involves a relatively selective defect in the ability of glucose to provoke insulin secretion by beta cells, a temporal irregularity in the pulse and oscillations of insulin secretion, and a loss of the tight coupling between pulses of insulin secretion and pulse in glucose. This defect accounts for the failure of beta cells to compensate for increasing insulin-resistance and for the ultimate development of overt hyperglycaemia.

The disease often remains asymptomatic and undetected for years. People with T2D do not usually require injections of insulin, and they control their blood glucose levels by watching their diet, taking regular exercise, oral medication, and possibly insulin. But if T2 diabetic people are not diagnosed and treated, they can develop serious complications, which can result in early death. Indeed, as glycaemic control deteriorates over time, patients are at increased risk of microvascular complications (disease of the small blood vessels) including retinopathy, neuropathy and nephropathy, and macrovascular complications (disease of the large blood vessels) including coronary heart disease, myocardial infarction and stroke. As a result, diabetes affects almost every element of the human body, as can be seen in figure 5.

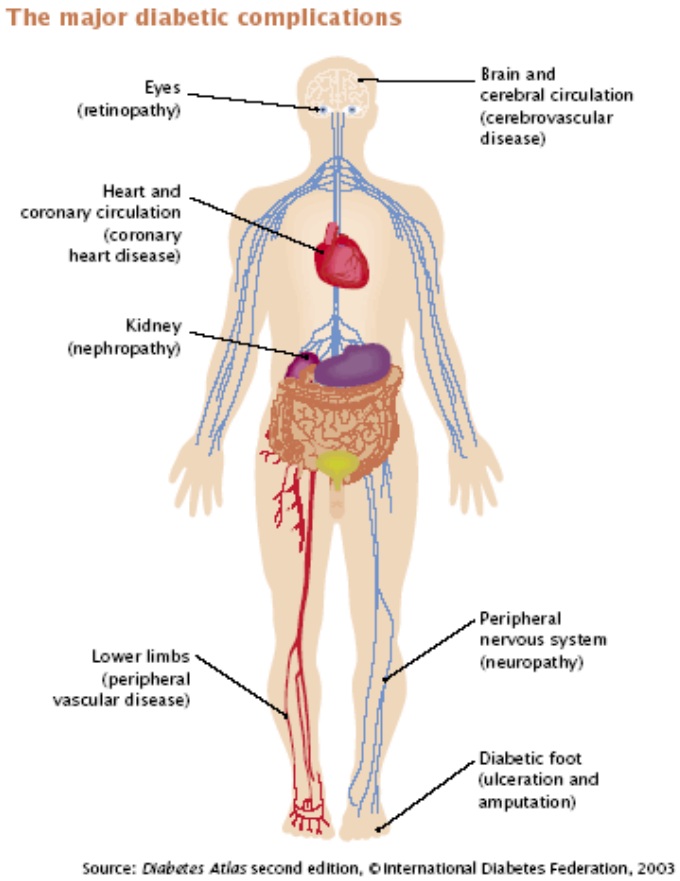

Figure 5. The major diabetic complications.
Diabetic patients are at increased risk of microvascular complications (disease of the small blood vessels) including retinopathy, neuropathy and nephropathy, and macrovascular complications (disease of the large blood vessels) including coronary heart disease, myocardial infarction and stroke.

Table 4. T2D risk factors

Major risk factor
Demographic factors - Race and ethnic background (native American, Polynesian islanders, African-American) - Age ≥ 45 years Family history: first-degree relatives with type 2 diabetes Obesity: BMI ≥ 27 Kg/m^2 with central fat distribution History of impaired fasting glucose or impaired glucose tolerance Hypertension (blood pressure ≥ 140/90 mmHg) HDL cholesterol level ≤ 0.90 mmol/l and/or a triglyceride level ≥2.8 mmol/l
Other risk factors
Malnutrition in the first year of life, and particularly in utero Lifestyle factors - Physical inactivity - High-fat, low-carbohydrate diet - Alcohol (heavy consumpition) - Smoking

5.4 Genes in type 2 diabetes

As mentioned above, insulin resistance and impaired beta cell function are the prominent features of T2D, and it is contributed by genetic and environmental factors. These factors might affect either the process of insulin signal transmission across the plasma membrane and/or the biochemical pathways allowing glucose uptake and metabolism by the cells, or might affect the pathways regulating beta cell function, including those for beta cell compensation. While several environmental factors have been identified, discovery and characterization of the genes involved in T2D has been an arduous task and has proceeded slowly. In the past 10 years, indeed, geneticists have devoted a large amount of effort to finding T2D genes. These efforts have included many candidate-gene studies, extensive efforts to fine map linkage signals, and an international linkage consortium that was perhaps the best example of a multi-centre collaboration in common-disease genetics (Genome Wide Association Studies, GWAS). Of these efforts, only the candidate-gene studies produced unequivocal evidence for common variants involved in T2D. These are the E23K variant in the potassium inwardly-rectifying channel, subfamily J, member 11 (*KCNJ11*) gene (Nielsen, et al. 2003), the P12A variant in the peroxisome proliferator-activated receptor-γ (*PPARG*) gene (Altshuler, et al. 2000), and common variation in the transcription factor 2, hepatic (*TCF2*) (Gudmundsson, et al. 2007) and the Wolfram syndrome 1 (*WFS1)*10 genes (Sandhu, et al. 2007). All of these genes encode proteins that have strong biological links to diabetes. Rare, severe mutations in these four genes cause monogenic forms of diabetes, and two of them are targets of anti-diabetic therapies: *KCNJ11* encodes a component of a potassium channel with a key role in beta cell physiology and it is targeted by the sulphonylurea class of drugs; *PPARG* encodes a transcription factor involved in adipocyte differentiation and it is targeted by the thiazolodinedione class of drugs (Figure 6).

A common amino-acid polymorphism (Pro12Ala) in peroxisome proliferator-activated receptor-γ (PPARγ) has been associated with T2D. People homozygous for the Pro12 allele are more insulin resistant than those having one Ala12 allele and have a 1.25-fold increased risk of developing diabetes. Moreover, there is also evidence for interaction between this polymorphism and fatty acids, thereby linking this locus with diet (Altshuler, et al. 2000).

In 2006, by far the most spectacular recent development in the field of multifactorial T2D genetics has been the identification of TCF7L2 (encoding transcription factor 7-like 2) as the most important T2D-susceptibility gene to date (Owen, et al. 2007). The estimate of effect size (an odds ratio for T2D of 1.4-fold per allele) was identified in an intronic SNP with uncertain functional credentials (rs7903146). TCF7L2 variation is strongly associated with rates of progression from impaired glucose tolerance to diabetes (with a hazard ratio of 1.55 between homozygote groups). TCF7L2 is widely expressed and involved in the Wnt signalling cascade. Most studies suggest that the predominant intermediate phenotype associated with TCF7L2 variation is impaired insulin secretion, consistent with the replicated observation that the TCF7L2 association is greater among lean than obese T2D subjects. Early mechanistic hypotheses have focused on the known role of TCF7L2 in the gut, postulating the involvement of impaired release of glucagon-like peptide-1 (an important islet secretagogue), reduced beta cell mass or intrinsic beta cell dysfunction. Body mass index data and some preliminary associations with leptin and ghrelin levels, however, could point towards a central mechanism.

TCF7L2 result was encouraging for two reasons. First, this study analysed more than 200 markers across a region of linkage on chromosome 10q, but the variants that were found to alter risk did not explain the linkage signal, suggesting that a non-candidate-gene or region-based association effort (such as a GWAS) could work. Second, *TCF7L2* was a completely unexpected gene-this showed that a genome-wide approach could uncover previously unexpected disease pathways.

6 PED/PEA-15 identification

In our laboratory, to identify genes whose expression is altered in T2D, we have used a differential display approach (Condorelli, et al. 1998). We analysed pools of mRNA extracted from fibroblasts derived from six T2 diabetics and six non-diabetic individuals. We obtained forty-five bands appeared to be differentially expressed in the two groups of fibroblasts. Out of these, eight bands were confirmed to be overexpressed and 12 were expressed at lower levels in T2 diabetic fibroblasts compared with those from the non-diabetic individuals. The clones, termed 10.1, was selected, and the expression profile analyzed by dot-blot analysis. The 10.1 probe hybridized 2-fold more intensely to RNA preparations from fibroblasts, skeletal muscle and adipose tissues in the T2 diabetics compared with the non-diabetics. Northern blot analysis are fibroblasts RNA showed that the 10.1 probe hybridized to a major 2.8 kb band. To obtain the full-length cDNA, we have screened a human heart library with

the 10.1 clone. One of nine positive clones isolated corresponds to the protein kinase C (PKC) substrate PEA-15 (phosphoprotein enriched in astrocytes) (Condorelli, et al. 1998).

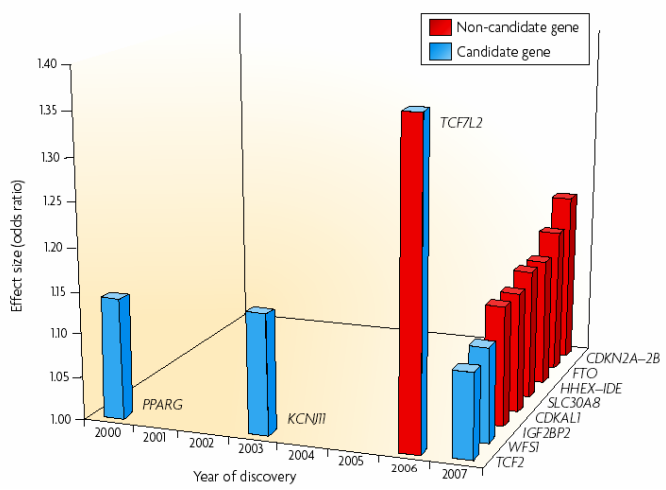

Figure 6. Effect sizes of the 11 common variants confirmed to be involved in type 2 diabetes risk.
The x axis shows the year when published evidences reached the levels of statistical confidence that are now accepted as necessary for genetic association studies. CDKAL1, CDK5 regulatory subunitassociated protein 1-like 1; CDKN2, cyclin-dependent kinase inhibitor 2A; FTO, fat mass and obesity-associated; HHEX, haematopoietically expressed homeobox; IDE, insulin-degrading enzyme; IGF2BP2, insulin-like growth factor 2 mRNA-binding protein 2; KCNJ11, potassium inwardly-rectifying channel, subfamily J, member 11; PPARG, peroxisome proliferator-activated receptor-γ gene; SLC30A8, solute carrier family 30 (zinc transporter), member 8; TCF2, transcription factor 2, hepatic; TCF7L2, transcription factor 7-like 2 (T-cell specific, HMg-box); WFS1, Wolfram syndrome 1.

7 PED/PEA-15

Phosphoprotein enriched in diabetes/phosphoprotein enriched in astrocytes (PED/PEA-15) was originally identified as a major astrocytes phosphoprotein and it was found to be widely expressed in different tissue and highly conserved among mammals. PED/PEA-15 is a 15 kDa cytosolic protein whose gene maps on human chromosome 1q21-22 (Condorelli, et al. 1998). It is a highly regulated protein with two major phosphorylation sites on Ser_{104} and Ser_{116}. Indeed, PED/PEA-15 is phosphorylated at Ser_{104} by protein kinase C (PKC) and at Ser_{116} by calcium-calmodulin kinase II (CaMKII) and by Akt/PKB (Kubes, et al. 1998; Trencia, et al. 2003). Thus, PED/PEA-15 is present in the cell in the unphosphorylated (N), singly phosphorylated (Pa), and doubly phosphorylated (Pb) form. Moreover, it presents at N-terminus the protein-protein interaction domain DED (Death Effector Domain) and a Nuclear Export Sequence (NES), that localizes the protein prevalently in the cytosol.

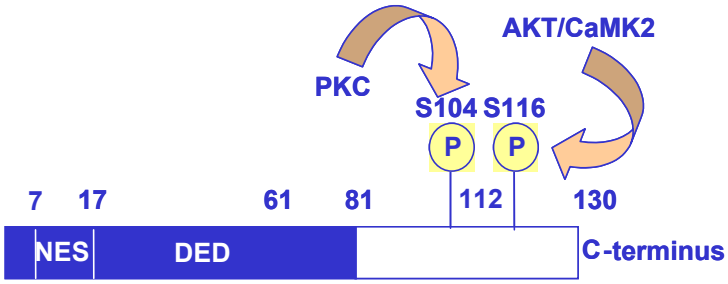

Figure 7. PED/PEA-15 structure.
PED/PEA-15 protein presents at N-terminus the protein-protein interaction domain DED (Death Effector Domain) and a Nuclear Export Sequence (NES), that localizes the protein prevalently in the cytosol. The two major phosphorylation sites on Ser_{104} and $Ser_{116.}$ are visualized.

Several studies in cultured cells and in rodent tissues have revealed that PED/PEA-15 is a multifunctional protein. i) it regulates multiple cellular functions by binding to distinct components of major intracellular transduction pathways (Formstecher, et al. 2001; Vaidyanathan and Ramos 2003). These include ERK1/2, Akt/PKB, and RSK2. ii) it has been shown to exert antiapoptotic action through distinct mechanisms. First, PED/PEA-15 inhibits the formation of the death-inducing signaling complex (DISC) and caspase 3 activation by different apoptotic cytokines including FASL, tumor necrosis factor alpha, and tumor necrosis factor-related apoptosis-inducing ligand (TRAIL) (Condorelli, et al. 1999, Hao, et al 2001). At least in part, this action is accomplished through the death-effector-domain of PED/PEA-15 upon PED/PEA-15 recruitment to the DISC. Secondly, PED/PEA-15 inhibits the induction of different stress-activated protein kinases (SAPKs) triggered by growth factor deprivation, hydrogen peroxide, and anisomycin (Condorelli, et al. 2002). This action of PED/PEA-15 is exerted by the blocking of an upstream event in the SAPK activation cascade and requires the interaction of PED/PEA-15 with ERK1/2. Thirdly, PED/PEA-15 modulates apoptosis upon UVC exposure in a dose-dependent fashion. Indeed, at least in part, apoptosis following Omi/HtrA2 mitochondrial release is mediated by reduction in PED-PEA15 cellular levels (Trencia, et al. 2004). Thus, the ability of Omi/HtrA2 to relieve XIAP inhibition on caspases is modulated by the relative levels of Omi/HtrA2 and PED/PEA-15. iii) it plays an important role in tumor development and sensitivity to antineoplastic agents (Formisano, et al. 2005).

Indeed, the expression levels of PED/PEA-15 control Caspase-3 function and epidermal cell apoptosis *in vivo* and determine susceptibility to skin tumor development. iiii) PED/PEA-15 also binds to and increases the stability of phospholipase D, enhancing its activity and controlling important mechanisms in cell metabolism (Zhang, et al. 2000). In cultured muscle and adipose cells and in peripheral tissues from transgenic mice, high levels of PED/PEA-15 impair insulin-stimulated GLUT4 translocation and glucose transport, suggesting that PED/PEA-15 overexpression may contribute to insulin resistance in Type 2 diabetes (Condorelli, et al. 2001; Vigliotta, et al. 2004).

Moreover, other studies have demonstrated that PED/PEA-15-induced resistance to insulin action on glucose disposal is accompanied by PLD-dependent activation of the classical protein kinase C isoform PKCalpha. In turn, the induction of PKCalpha by PED/PEA-15 prevents subsequent activation of the atypical PKCzeta by insulin. Rescue of PKCzeta activity in cells overexpressing PED/PEA-15 restores normal sensitivity to insulin of the glucose transport machinery (Condorelli, et al. 2001). Thus, in muscle and adipose cells, PED/PEA-15 generates resistance to insulin action on glucose disposal by impairing normal regulation of PKCzeta. Transgenic mice ubiquitously overexpressing *ped/pea-15* (Tg-PED) to levels similar to those found in many type 2 diabetics exhibited mildly elevated random-fed blood glucose levels and decreased glucose tolerance. Treatment with a 60% fat diet led *ped/pea-15* transgenic mice to develop diabetes. Consistent with insulin resistance in these mice, insulin administration reduced glucose levels by only 35% after 45 min, compared to 70% in control mice, and insulin-stimulated glucose uptake was decreased by almost 50% in fat and muscle tissues. In addition to insulin resistance, *ped/pea-15* transgenic mice showed a 70% reduction in insulin response to glucose loading (Figure 8). Thus, in vivo, overexpression of *ped/pea-15,*in addition to generating insulin resistance and altered glucose tolerance, may impair beta-cell function and glucose-induced insulin secretion (Vigliotta, et al. 2004).

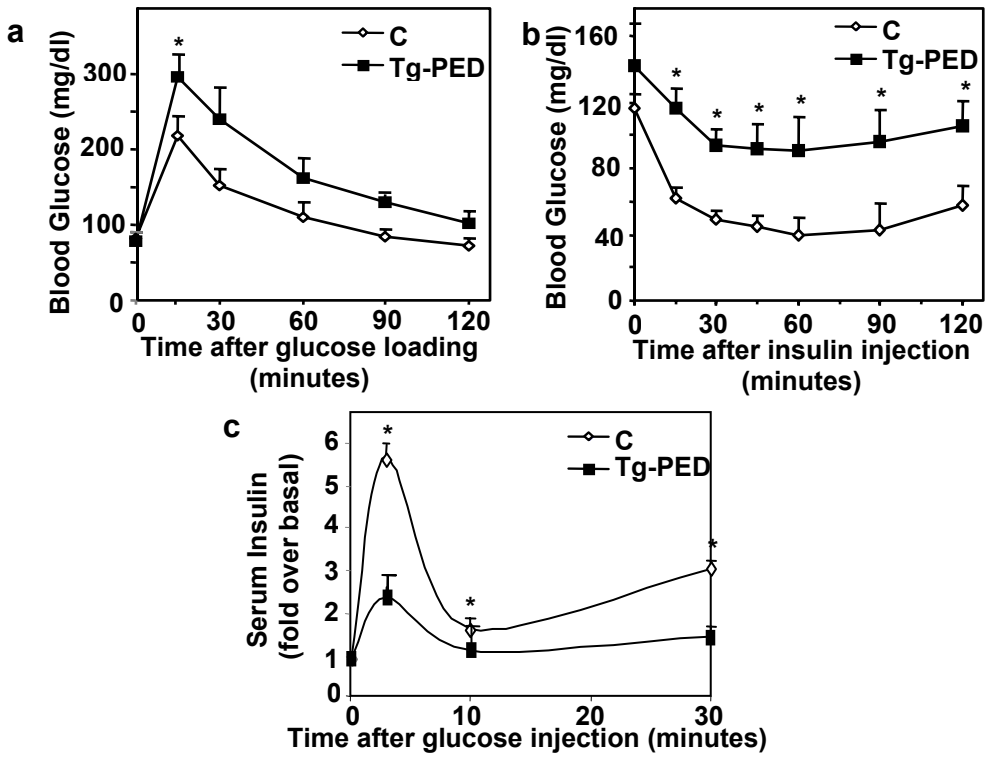

Figure 8. Tg-PED metabolic phenotype.
a) Glucose Tolerance Test, **b**) Insulin Tolerance Test and **c**) glucose-induced insulin secretion were performed in Tg-PED and in their control mice (C).

Aims of the study

This thesis concerns the study of the role of *ped/pea-15* gene in the regulation of glucose homeostasis.

The hyper-expression of Phosphoprotein Enriched in Diabetes/ Phosphoprotein Enriched in Astrocytes gene is commonly found in human diabetic patients. Earlier findings in humans, indeed, evidenced that the PED/PEA15 gene is overexpressed in skeletal muscle and fat tissues as well as in cultured skin fibroblasts from individuals with type 2 diabetes, and this effect occurs independently of obesity, suggesting that it may be a primary component of insulin resistance in these subjects. Moreover, PED/PEA-15 overexpression causes insulin-resistance and impaired glucose tolerance in transgenic mice (TgPED). In these mice, PED/PEA-15 overexpression determines also an increase of insulin fasting levels. Furthermore, insulin levels do not change after glucose injection, suggesting a defect on insulin secretion regulation. However, the physiologic function of PED/PEA-15 and the mechanism through which PED/PEA-15 overexpression can impair glucose tolerance are not clear.

In this context, I have investigated: i) whether PEA15 overexpression occurs in individuals at high risk of diabetes and whether it is associated with specific type 2 diabetes subphenotypes, ii) the role of PED/PEA-15 in beta-cell function.

For the first point, I analysed PED/PEA15 expression in euglycaemic first-degree relatives (FDR) of type 2 diabetic subjects, and evaluated the possible correlation between PED/PEA-15 levels and diabetes subphenotypes

For the second point, I generated and characterized a transgenic mice featuring selective overexpression of PED/PEA-15 in the beta-cells (beta-Tg), and I tried to identify the molecular mechanism through which PED/PEA-15 induces beta-cell dysfunction on pancreatic islets isolated from beta-Tg mice and on a beta cell cellular model stably overexpressing PED/PEA-15 cDNA.

Materials and Methods

Subjects

The subjects investigated in the present study were recruited at the outpatient facilities of the Metabolic Unit at the University of Catanzaro 'Magna Graecia' (offspring from the European Network on Functional Genomics of Type 2 Diabetes [EUGENE2] study). Written informed consent was obtained from all participants. The study protocol was approved by the ethics committee of the institution and conducted in accordance to the principles of the Declaration of Helsinki as revised in 2000. The euglycaemic individuals were healthy employees of the Campania Region. The presence of type 2 diabetes affected first-degree relatives (FDR) was ascertained through a written questionnaire and further verified through the medical history. The average number of relatives with type 2 diabetes in the subgroup of FDR was 1.1. Anthropometric indexes (BMI was calculated by dividing the weight in kilograms by the square of the height in metres; waist circumference was measured midway between the lowest rib margin and the iliac crest to the nearest 0.5 cm) and detailed medical history were obtained from all of the participants. Blood pressure, plasma glucose, total cholesterol, HDL cholesterol, and serum insulin levels were determined. The OGTT and euglycaemic–hyperinsulinaemic clamp procedures were performed. Briefly, for clamp studies, insulin (Humulin; Eli Lilly, IN) was given as a prime contiuous infusion to produce plasma insulin levels of 420 pmol/l. Thereafter, the insulin infusion rate was fixed at 40 mU m^{-2} min^{-1}. Blood glucose was maintained at a constant level throughout the study by infusing 20% glucose at varying rates according to blood glucose measurements performed at 5-min intervals. Lean body mass was assessed by bioimpedence. Duration of the clamp was 120 min. Glucose disposal is expressed as milligrams per kilogram of lean body per mass per minute. Insulin secretion was estimated by the homeostasis model assessment of pancreatic beta cell function (HOMA-B) index and the insulinogenic index as the difference between the 30- and 0-min OGTT plasma insulin values divided by the difference between the corresponding plasma glucose values, ($\Delta I_{30}/\Delta G_{30}$).

Separation of white blood cells

For peripheral blood leucocyte (PBL) separation, EDTA-treated whole-blood samples were first centrifuged at 300 ×g for 10 min and the plasma removed. PBLs were separated using a 6% dextran gradient in filtered PBS, pH 7.4, washed in PBS three times, counted and resuspended in 1 ml of PBS for subsequent use. Neutrophils and other major leucocyte subpopulations were further separated, as described (Metcalfe and Waters 1992). The purity of the different cell populations was confirmed by microscopic examination.

Generation of transgenic mice

The *rip-I/ped/pea-15* chimeric gene was obtained by introducing a 2.3-Kb *EcoRI* fragment containing the entire human *ped/pea-15* cDNA at the *EcoRI*

site in a pB5-RIP-β-globin expression vector (kindly provided by Prof. D. Accili, Columbia University, N.Y.). This chimeric gene was microinjected into fertilized C57BL6/SJL mouse eggs. The general procedures used for microinjection and animal selection have been previously described (Devedjian, et al. 2000). Six F_0 founders were identified by PCR as in (Vigliotta, et al. 2004). Mice were fed ad libitum with a standard diet (Research Diets formulas D12328; Research Diets, Inc., N.J.) and kept under a 12 hour-light/12 hour-dark cycle. All procedures described below were approved by the Institutional Animal Care and Utilization Committee.

Determination of glucose and insulin tolerance, assessment of insulin secretion and of glucose utilization.

Glucose tolerance tests, insulin tolerance tests and insulin secretion were measured as previously described (Kulkarni, et al. 1999; Bruning, et al. 1998). For analysing glucose utilization by skeletal muscle, an intravenous injection of 1 μCi of the nonmetabolizable glucose analog 2-[1-^{3}H]deoxy-D-glucose (2-DG) (Amersham Pharmacia Biotech, NJ) and an intraperitoneal injection of insulin (0.75 mU/g of body weight) were administered to random fed mice. The specific blood 2-DG clearance was determined with 25μl blood samples (tail vein) obtained 1, 15, and 30 min after injection as previously reported (Somogyi 1945). Skeletal muscles were removed 30 min after the injections. Glucose utilization index was determined by measuring the accumulation of radiolabeled compound (Ferre, et al. 1985). The amount of 2-DG-6 phosphate per milligram of protein was then divided by the integral of the concentration ratio of 2-DG to the measured unlabeled glucose. Glucose utilization indexes were expressed as picomoles/milligram of protein/minute.

Immunoistochemistry and morphometric analysis

PED/PEA-15 antibody has been previously reported (Condorelli, et al. 1998). Immunoistochemical detection of PED/PEA-15, insulin and glucagon in pancreases from control and transgenic mice were analysed as described (Vigliotta, et al. 2004). Analysis of serial consecutive islet sections stained with either insulin or PED/PEA-15 antibodies was used to confirm *ped/pea-15* expression in insulin-immunopositive beta cells. Sections were also stained with hematoxylin and eosin. For morphometry, pancreases were obtained from 6-month-old control and transgenic mice, and immunohistochemical detection of insulin was performed in 3 sections (2-3 μm) separated by 200 μm as in (Devedjian, et al. 2000).

Islet isolation, ex vivo insulin secretion assessment

Islets were isolated from 6-month-old mice by collagenase digestion and subsequent centrifugation on a Histopaque (Sigma-Aldrich, MO) gradient as in (Kitamura, et al. 2001). 20 islets were manually selected and preincubated in Dulbecco's modified Eagle's medium (DMEM, Life Technologies, Germany) at 37°C in a 5% CO_2 atmosphere for 24 hours. Islets were then further

incubated in Krebs-Ringer Buffer (KRB, 120 mM NaCl, 1.2 mM $MgSO_4$, 5 mM KCl, 10 mM $NaHCO_3$, 1.3 mM $CaCl_2$, 1.2 mM KH_2PO_4) for 30 min, and then stimulated at 37°C with various concentrations of either glucose for 1 hour, KCl for 30 min, or glyburide (Sigma-Aldrich, MO) for 1 hour. Islets were subsequently collected by centrifugation and supernatants were assayed for insulin content by RIA.

Cell culture procedures and transfection.

MIN-6 cells were cultured in DMEM containing 25 mM glucose, 50 μM 2-mercaptoethanol, and 10% fetal calf serum (Biochrom, Germany) at 37°C in a 5% CO_2 atmosphere (Miyazaki, et al. 1990). INS-1 cells were cultured in RPMI 1640 medium (Life Technologies, Germany) containing 11 mM glucose, 50 μM 2-mercaptoethanol, and 10% fetal bovin serum (Biochrom, Germany) at 37°C in a 5% CO_2 atmosphere (Wang, et al. 2002). Stable transfection of the ped/pea-15 cDNA was performed with the lipofectamine method according to manufacturer's instructions. Transient transfection of the PKCzetącDNA was also performed with the lipofectamine method. By using PCAGGS-β-Gal as a reporter, transfection efficiency was between 65 and 85%, staining with the chromogenic substrate 5-bromo-4-chloro-3-indolyl b-D-galactopyranoside.

RNA extraction and Real-Time RT-PCR analysis.

Total cellular RNA was isolated from pancreatic islets and tissue samples by using the RNeasy kit (QIAGEN Sciences, Germany), and from white blood cells were immediately extracted following cell isolation using the QIAamp RNA Blood Mini Kit according to the manufacturer's instructions. For Real-time RT-PCR analysis, 1 μg of islet or cell RNA was reverse-transcribed using Superscript II Reverse Transcriptase (Invitrogen, CA). PCR reactions were analyzed using SYBR Green mix (Invitrogen, CA). Reactions were performed using Platinum SYBR Green qPCR Super-UDG using an iCycler IQ multicolor Real Time PCR Detection System (Biorad, CA). All reactions were performed in triplicatę and β-actin was used as an internal standard.

Western blot analysis and PKC assay.

Tissues homogenates and cell lysates were separated by sodium dodecyl sulfate-polyacrylamide gel electrophoresis (SDS-PAGE) and analysed by western blot as previously described (Vigliotta, et al. 2004; Laemmli 1970). Membranes were probed with antibodies to PED/PEA-15, PKCζ (Santa Cruz Biotechnology, Inc., CA), or tubulin (Santa Cruz Biotechnology, Inc., CA). For analyzing atypical PKC activity, cells were incubated with KRB for 30 min and then incubated with either 2.8 or 16.7 mM glucose containing medium for 1h at 37°C in a 5% CO_2 atmosphere. Cells were solubilized in lysis buffer (25 mM Tris-HCL, pH 7.4, 0.5 mM EDTA, 0.5 mM EGTA, 0.05% Triton X-100, 10 mM beta-mercaptoethanol, 1mg/ml leupeptin, 1 mg/ml aprotinin) for 1 h at 4°C. Lysates were precipitated with a PKCzeta antibody and PKC activity was assayed using the SignaTECT™ PKC assay system (Promega, WI), according

to manufacturer's instructions. Determination of PKC activity using the Ac-MBP(4-14) or the pseudosubstrate region of PKCepsilon (specific for atypical PKC) provided consistent results.

Statistical procedures.

Data were analysed with Statview software (Abacus-concepts) by one-factor analysis of variance. *p* values of less than 0.05 were considered statistically significant (Vigliotta, et al. 2004).

Results and discussion

As I mentioned before, the hyper-expression of Phosphoprotein Enriched in Diabetes/Phosphoprotein Enriched in Astrocytes gene is commonly found in human diabetic patients. Previous studies in humans, indeed, have reported that PED/PEA15 gene is overexpressed in skeletal muscle and fat tissues as well as in cultured skin fibroblasts from individuals with T2D, and this effect occurs independently of obesity and drug treatment (Condorelli, et al. 1998), suggesting that it may be a primary component of insulin resistance in these subjects.

In this context, I investigated whether PED/PEA15 overexpression occurs in individuals at high risk of diabetes and whether it is associated with specific T2D subphenotypes.

I addressed these questions by measuring PED/PEA-15 protein and mRNA expression levels in First Degree Relatives (FDR) of T2 diabetic subjects. These individuals have a very high risk of T2D and develop different diabetes-related phenotypes years before diabetes onset, independently of the metabolic abnormalities associated with this disorder. PED/PEA15 levels were measured in the Peripheral Blood Leucocytes (PBLs) of these individuals. Indeed, PED/PEA-15 levels in PBLs are closely correlated with those in fat and skeletal muscle tissues. Thus, although PBLs do not represent a classical target for insulin, they represent a non-invasive investigation to quantify PED/PEA15 expression.

In FDR-subjects, there was a two-fold increase both in PED/PEA-15 protein and mRNA levels compared to control euglycaemic individuals (Eu) ($p<0.001$; Figure 9a, b), suggesting that PED/PEA-15 overexpression is caused, at least in part, by a transcriptional abnormality. Furthermore, this increase was of a similar magnitude to that observed in a group of T2 diabetic patients. As in the case of T2 diabetic patients, one-third of the FDR-subjects expressed amounts of PED/PEA15 protein that were more than two SDs higher than the mean for the Eu-subjects. It appears therefore that increased PED/PEA15 levels represent a common abnormality in both T2 diabetic subjects and individuals at increased risk of this disease, suggesting that it might precede diabetes onset.

To address the functional significance of PED/PEA15 overexpression in T2 diabetic FDR, we searched for associations with diabetes-related phenotypes. We analysed a group of 25 euglycaemic offspring of T2D-affected couples. PBL expression levels of PED/PEA15 in these offspring were comparable to those of the other T2 diabetic FDR investigated previously (Table 4). A negative correlation was evidenced between the individual levels of PED/PEA15 in PBLs and insulin-stimulated glucose disposal according to fat-free mass, as determined by the euglycaemic–hyperinsulinaemic clamp ($r=-557$, $p=0.01$; Figure 10), suggesting that high levels of PED/PEA15 protein contribute to development of skeletal muscle resistance to insulin action in these individuals. Furthermore, PED/PEA15 levels were also weakly correlated with fasting plasma insulin in these FDR, but not in euglycaemic individuals lacking

a family history of type 2 diabetes. By contrast, in these FDR, PED/PEA15 levels were not related to BMI, waist circumference, systolic and diastolic blood pressure, HDL cholesterol, triacylglycerol and glucose levels, indicating that expression of the PED/PEA15 gene is independent of the main variables associated with the metabolic syndrome in humans, and they were not related to age, or to reduced physical activity, two recognised risk factors for T2D and insulin resistance.

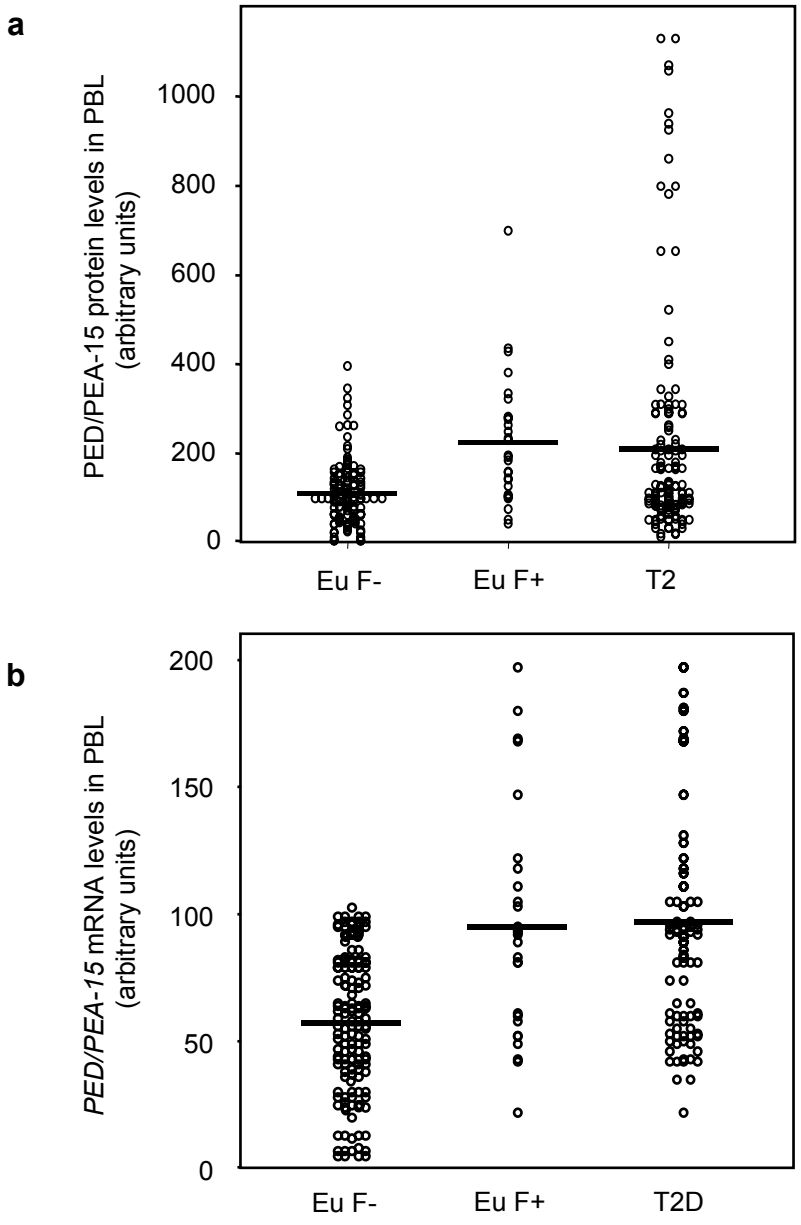

Figure 9 Expression of PED/PEA15 in PBLs from euglycaemic subjects.
PBLs from euglycaemic individuals with at least one T2 diabetic FDR (EuF+) and euglycaemic subjects lacking a family history of diabetes (EuF-) were consecutively collected. For comparison, PBLs from T2 diabetic patients (T2D) were also analysed. Cells were solubilised and PED/PEA15 protein (**a**) and mRNA levels (**b**) were quantified.

Table 4 Clinical and biochemical features of the type 2 diabetic offspring

Parameter	Mean ± SEM
Number (male/female)	13/12
Age (years)	30.1±8.3
BMI (kg/m2)	24.5±4.1
Waist circumference (cm)	83.5±12.2
Systolic BP (mmHg)	112±11
Diastolic BP (mmHg)	75±6
Total cholesterol (mmol/l)	4.8±0.9
HDL cholesterol (mmol/l)	1.5±0.3
Triacylglycerol (mmol/l)	1±0.7
Fasting plasma glucose (mmol/l)	4.8±0.5
2-h glucose (mmol/l)	5.8±1.4
Fasting plasma insulin (pmol/l)	55.6±20.8
Fat-free mass glucose disposal (mg kg LBM-1 min-1)	12±3
HOMA-IR	1.8±0.9
HOMA-B	174±65
Insulinogenic index (ΔI30/ΔG30)	18±12
PEA15 (arbitrary units)	257±35

Data are presented as the means ± SEM
HOMA-B Homeostasis model assessment of pancreatic beta cell function, HOMA-IR homeostasis model assessment of insulin resistance, LBM lean body mass

Thus, in euglycaemic FDR of T2 diabetic patients, high PED/PEA15 levels are strongly correlated with resistance to insulin action in the lean mass, suggesting that PEA15 contributes to the early appearance of insulin resistance in these individuals.

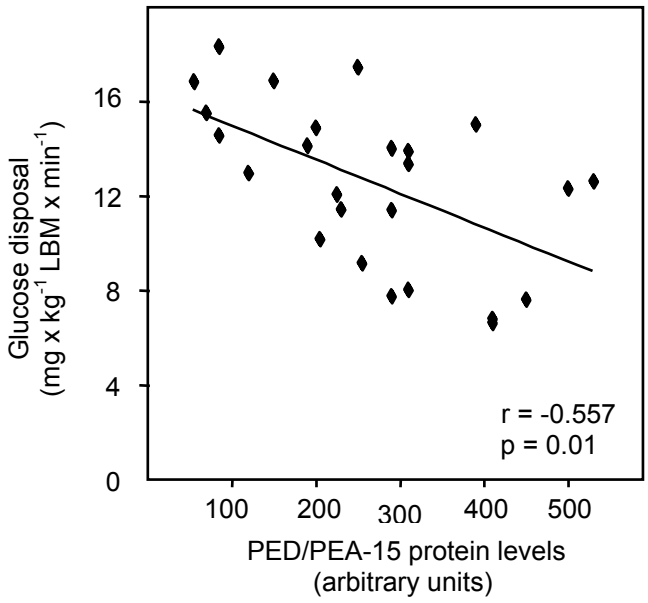

Figure 10 Risk-factors related to PED/PEA15 expression.
PED/PEA15 protein levels were determined in PBLs from 25 euglycaemic offspring of couples, one of which was affected by T2D. Glucose disposal was assessed by the euglycaemic–hyperinsulinaemic clamp as described in material and methods section and corrected for fat-free mass.

Nevertheless, PED/PEA15 levels were not correlated with any index of beta cell function in the offspring. Overexpression of the gene may impair glucose-triggered insulin secretion in transgenic mice but not in humans. This is unlikely, however, as transfection of a PED/PEA15 cDNA in human beta cell lines grossly impairs the insulin response to glucose. Alternatively, in the T2 diabetic FDR, the consequence of the high PED/PEA15 levels on insulin action might occur earlier during life than the PED/PEA15 effect on beta cell function.

To investigate the relevance of PED/PEA-15-induced beta cell dysfunction to glucose tolerance, I generated and characterized a transgenic mouse featuring selective overexpression of PED/PEA-15 in the beta cells (beta-tg). To this aim, the entire human *ped/pea-15* cDNA was cloned under the control of the RAT Insulin promoter (RIP I), that allows a beta cells specific expression of the transgene.

I obtained three lines of beta-tg mice (L5, L8, and L9) in which PED/PEA-15 protein and mRNA showed a 10 to 20-fold increased expression in the pancreatic islets compared to their non-transgenic littermates (c) (Figure 11a, b); by contrast there were no difference in PED/PEA-15 expression between beta-tg and controls in the other tissues taken in account such as the skeletal muscle, the liver and the adipose tissue. Moreover, beta-tg mice, were fertile and generated viable offsprings showing no significant growth alterations or other apparent abnormalities compared to controls.

First of all, I studied the glucose homeostasis of beta tg-mice, analysing their blood glucose levels and their glucose tolerance. Beta-tg mice, both male and female, exhibited slightly reduced fasting blood glucose levels compared to control mice (males, 84 ± 6 vs. 91 ± 7 mg/dl; females, 82 ± 8 vs. 92 ± 6 mg/dl; significant at the $p < 0.05$ level). However, during a glucose tolerance test (GTT), glucose loading (2 g/kg) rendered the beta-tg mice significantly more hyperglycemic during the following 120 min compared to control mice (Figure 12), suggesting the presence of a severe impairment of glucose tolerance. Furthermore, gender and aging (3 to 14 months) had no effect on the impairment of glucose tolerance caused by beta cell overexpression of PED/PEA-15. This indicates that the selective overexpression of PED/PEA-15 in beta cell is sufficient to impair glucose tolerance in mice.

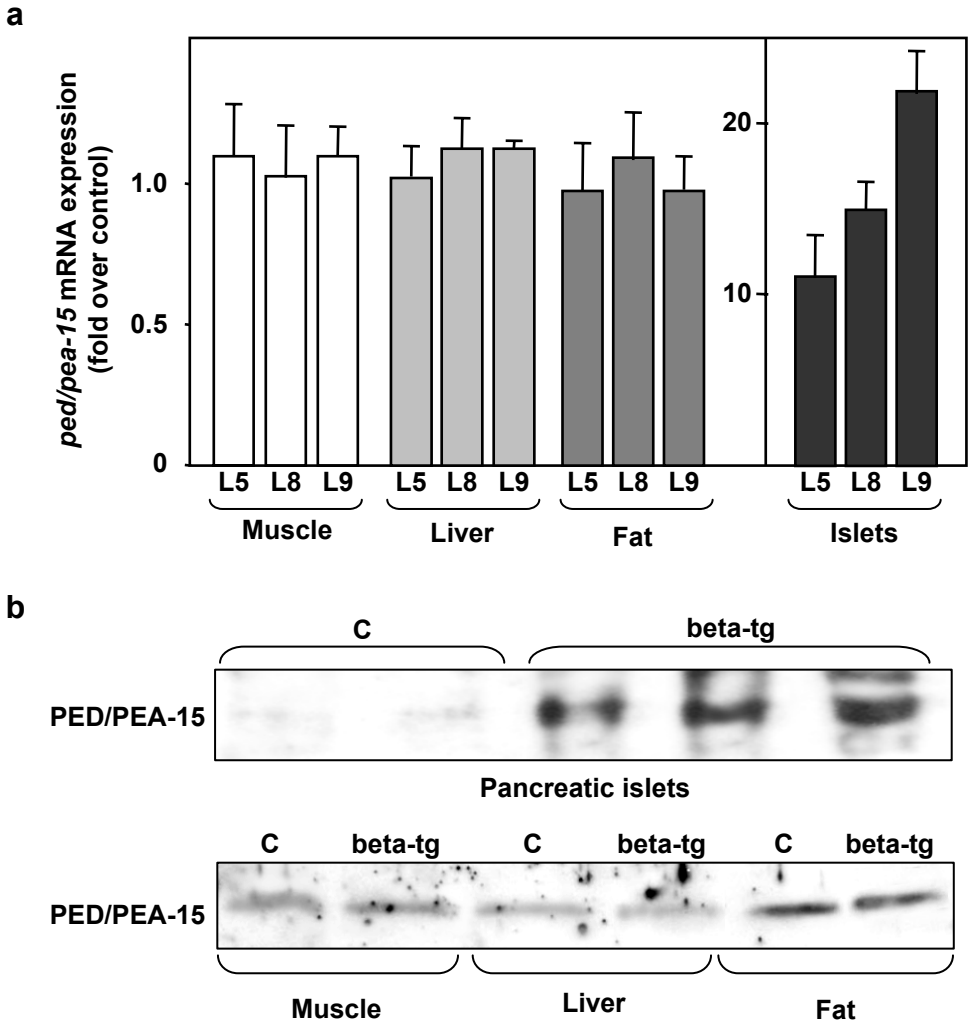

Figure 11 - PED/PEA-15 expression in beta-tg mice

Tissues from three lines of beta-tg mice (L5, L8, L9) and from their non transgenic littermates (C) were subjected to Northern (**a**) or Western (**b**) blotting. Northern blots (30 μg of RNA/lane) were probed with *ped/pea-15* cDNA. Loading of the same amount of RNA in each lane was ensured by further blotting the filters for beta-actin. Quantitation was performed by densitometric analysis. Data are plotted as increase of *ped/pea-15* mRNA expression in transgenic versus control mice. For Western blotting, tissue lysates (100 μg of proteins/lane) were blotted and incubated with the PED/PEA-15 antiserum. The autoradiographs shown are representative of 5 (top) and 6 (bottom) independent experiments.

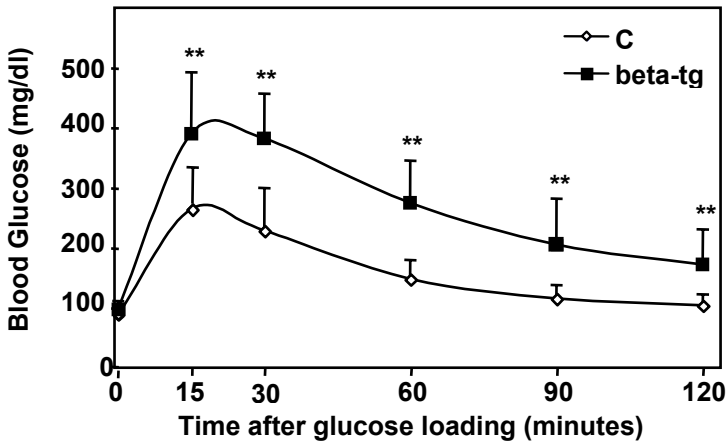

Figure 12 Glucose tolerance in beta-tg mice.

Three-month-old beta-tg (beta-tg) mice and their non transgenic littermates (C) were fasted for 16 h and subjected to IP glucose loading (2 g/kg of body weight). Blood glucose levels were determined before and at the indicated times following the load. Values are expressed as means ± SD. Asterisks denote statistically significant differences (*, $p < 0.05$; **, $p < 0.01$).

Then, to verify whether beta cell overexpression of PED/PEA-15 is accompanied by reduced insulin sensitivity, I performed insulin tolerance tests. After intraperitoneal injection of insulin (0.75 mU/g), blood glucose levels were comparable between beta-tg and control mice (Figure 13), with no significant difference in glucose areas under the curve between beta-tg and control mice (C: 9180 ± 1900 mg/dl/120 min; beta-tg: 8805 ± 1600 mg/dl/120 min). Furthermore, beta-tg mice featured no significant differences in fasting nonesterified free fatty acid and triglyceride blood concentrations compared to their controls (FFAs: 0.82 ± 0.03 mmol/l vs. 0.78 ± 0.05 mmol/l; Triglyceride: 115 ± 7 mg/dl vs. 111 ± 8 mg/dl). Moreover, insulin-dependent glucose uptake in quadriceps and tibialis muscles from beta-tg and control mice exhibited no difference, suggesting that beta-tg mice present an intact insulin sensitivity.

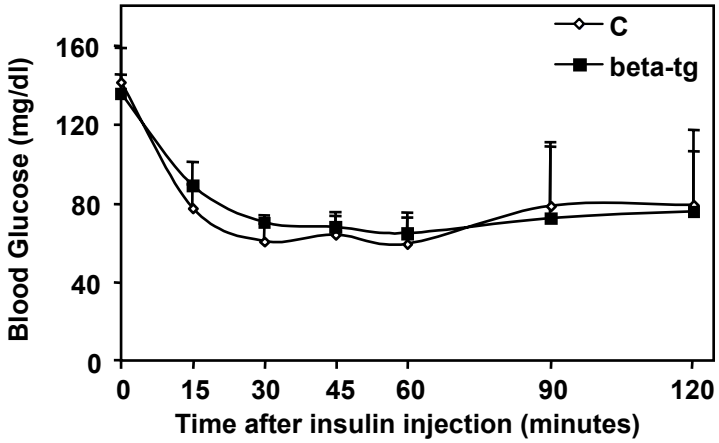

Figure 13 Insulin sensitivity in beta-tg mice.

Three-month old random-fed beta-tg mice and their non transgenic littermates (C) (n = 12/group; 6M, 6F) were injected intraperitoneally with insulin (0.75 mU/g of body weight), followed by determinations of blood glucose levels at the indicated times. Blood glucose levels were determined before and at the indicated times following the load. Values are expressed as means ± SD.

I than investigated: i) the effect of beta cellular PED/PEA-15 overexpression on beta-tg insulin secretion *in vivo* and *in vitro*; and ii) on their islets morphometry.

i) Concerning glucose induced insulin secretion, the control mice presented a 7-fold increase in insulin secretion 3 min after intraperitoneal glucose injection, and their levels remained higher than baseline values for up to 30 min, indicating a second phase response (Figure 14); by contrast beta tg mice presented a 80% increase of fasting insulin levels compared to controls (0.31 ± 0.07 ng/ml vs. 0.17 ± 0.03, $p < 0.001$), and they have no significant insulin secretion in response to glucose either at 3 or at 30 minutes. Indeed, both their acute first-phase insulin secretory response to glucose and their second phase response were significantly impaired compared to control mice ($p < 0.001$). Thus, *in vivo*, isolated beta cell overexpression of PED/PEA-15 increases fasting insulinemia but impairs further insulin secretion response to hyperglycemia.

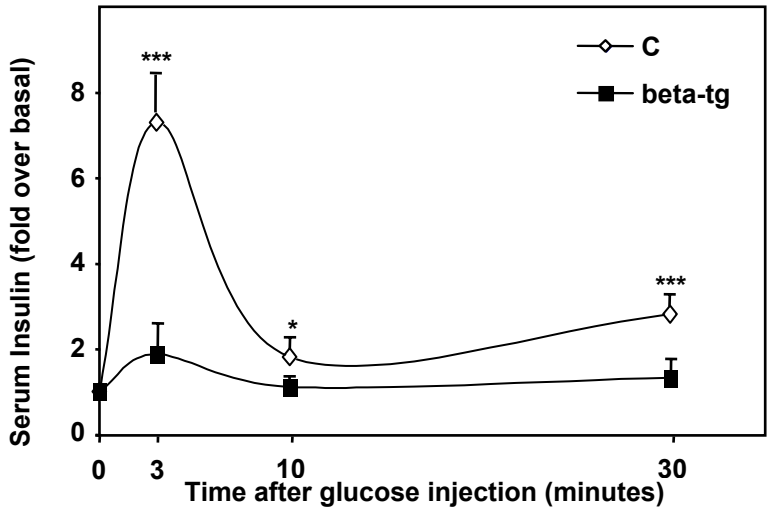

Figure 14 Insulin secretion *in vivo*.
Beta-tg and control mice (C) were fasted overnight and then injected with glucose (3 g/kg of body weight) intraperitoneally. Serum insulin concentrations were measured at the indicated times by radioimmunoassay. Data points represent the mean ± SD. Asterisks denote statistically significant differences (*, $p < 0.05$; ***, $p < 0.001$).

Then, to clarify the role of PED/PEA-15 overexpression in the impairing of glucose induced insulin secretion, I evaluate the insulin secretion in isolated pancreatic islets of beta-tg mice. In particular I analysed the insulin secretion induced by high glucose levels and by potassium chloride. Similar as in intact mice, beta-tg mouse islets exhibited a 2-fold increased insulin release when incubated in medium containing 2.8 mM glucose compared to control islets (Figure 15a; $p < 0.001$). Furthermore, raising glucose concentration did not further increase the insulin release by these islets, while enhancing that from control mice by 3.9-fold ($p < 0.001$). At variance with glucose, exposure to the membrane depolarising agent potassium chloride (33 mM) caused a

comparable release of insulin by both the beta-tg and the control islets (Figure 15), suggesting that PED/PEA-15 action on glucose-induced secretion affects earlier events of beta cell response to glucose upstream the membrane depolarisation step.

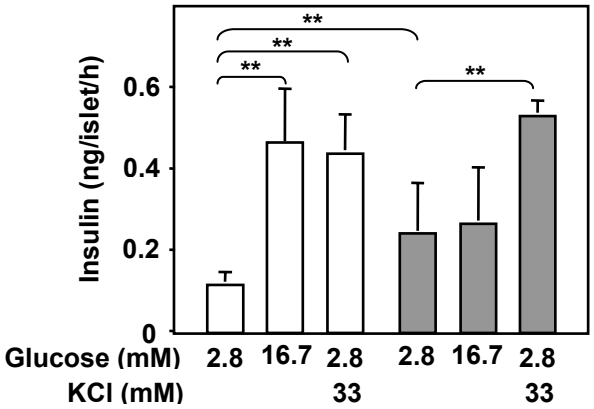

Figure 15 Insulin secretion *ex vivo*.
Islets were isolated from 6-month old mice from the beta-tg and their non transgenic littermates (C). Insulin release was determined upon exposure to the indicated concentrations of glucose, potassium chloride as described in materials and methods. Bars represent the means ± SD. Asterisks denote statistically significant differences (**, $p < 0.01$).

ii) Concerning islet morphometry, I found that PED/PEA-15 overexpression determines islet hyperplasia with a specific increase in beta cell mass. Indeed, beta-tg islets were larger and showed a more elongated and irregular shape but featured normal distribution of alpha and beta cells as compared to control islets. Quantitative morphometry revealed a 2-fold increase in islet and beta cell mass per unit of total pancreatic area in the beta-tg mice ($p < 0.01$; Table 5) with no significant difference in their pancreas weight. This may result from a direct effect on beta cell survival as PED/PEA-15 exerts a broad anti-apoptotic action, and it may suggest that the increased beta cell mass observed may be responsible for the increased fasting serum insulin levels detected in the beta-tg mice.

Table 5 Morphometric analysis of beta-tg pancreas

	Control	beta-tg
% islet area/pancreatic area	0.52 ± 0.06	1.04 ± 0.11 **
% beta cells/islet	76.87 ± 4.66	81.33 ± 2.08 *
% alpha cells/islet	17.23 ± 1.92	14.54 ± 1.85 n.s.
% other cells/islet	5.90 ± 0.71	4.13 ± 0.41 n.s.
Pancreas weight (mg)	182 ± 16	188 ± 12 n.s.
Islet cell mass (mg)	0.95 ± 0.08	1.96 ± 0.06 **
Beta-cell mass (mg)	0.73 ± 0.05	1.59 ± 0.06 **

Mice were analyzed as described in materials and methods. Data are the means ± SD of determinations in six beta-tg and six control (non transgenic littermates) mice. * and ** denote statistically significant differences, respectively at the $p < 0.05$ and 0.01 levels.

Thus, this first part of results shows that beta-tg mice present grossly impaired glucose tolerance and reduced insulin secretion in response to hyperglycemia. This latter defect is comparable to that occurring in mice with PED/PEA-15 ubiquitous overexpression (Vigliotta, et al. 2004), suggesting that beta cell overexpression of PED/PEA-15 is sufficient to impair glucose tolerance in mice.

To gain further insights into the mechanisms leading to dysfunction of beta cells overexpressing PED/PEA-15, I evaluated the expression of several genes relevant to the glucose sensory apparatus by real-time RT-PCR analysis of total RNA isolated from islets of beta-tg mice.

The amounts of mRNAs for the *Sur1* and *Kir6.*2, the ATP-sensitive K^+ channel subunits, and the *Sur1/Kir6.2* upstream regulator *Foxa2* were reduced by 30-35% in the islets from beta-tg compared with those in control mice ($p < 0.001$; Figure 16a). Furthermore, islets from beta-tg mice exhibited no secretory response to the K^+ channel locking agent glyburide (Figure 16b), suggesting that PED/PEA-15 overexpression in beta cells induces impairing of glucose induced insulin secretion reducing both the expression and the function of the channel. At variance, the abundance of *glucokinase, HK1, HK2,* and *GLUT2* mRNAs, genes encoding key components of the glucose-sensitive insulin secretion machinery were unaffected by PED/PEA-15 in both transgenic and control mice (Figure 16a).

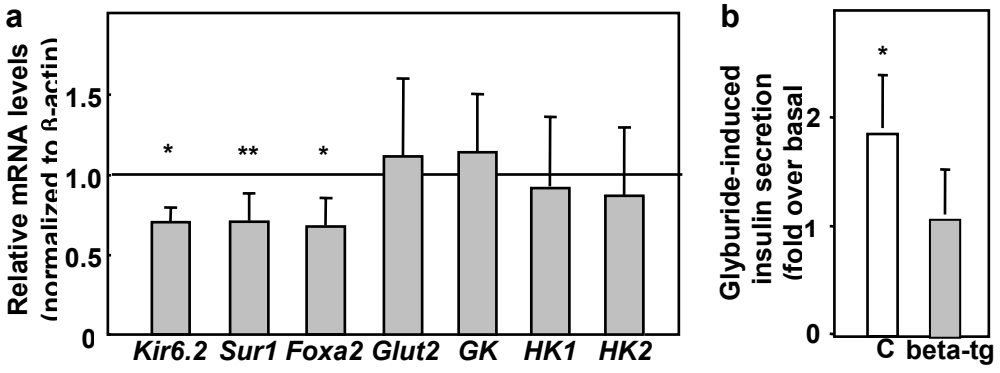

Figure 16 Gene expression profile and glyburide induced insulin secretion in isolated islets from beta-tg and controlmice.

a) The abundance of mRNAs for the indicated proteins was determined by real-time RT-PCR analysis of total RNA isolated from islets of beta-tg mice and their non transgenic littermates, using beta-actin as internal standard. The mRNA levels in beta-tg islets are relative to those in control animals (C). Each bar represents the mean ± SD. Asterisks denote statistically significant differences (*, $p < 0.05$; **, $p < 0.01$). **b**) Islets were isolated from 6-month old beta-tg and their non transgenic littermates mice (C). Insulin release was determined upon exposure to 10 μM glyburide. Bars represent the means ± SD. Asterisks denote statistically significant differences (*, $p < 0.05$).

Previous studies in mice evidenced that ablation of either the *Sur1* or the *Kir6.2* genes results in a phenotype reminiscent of that characterizing the beta-tg mice (Miki, et al. 1998; Nenquin, et al. 2004; Seghers, et al. 2000). Indeed, both the *Sur1*$^{-/-}$ and the *Kir6.2*$^{-/-}$ mice feature blunted insulin secretion response to sulfonylureas, and impaired glucose tolerance and glucose-induced first and second phase insulin secretion. Furthermore, fasted *Sur1*$^{-/-}$ mice are more hyperinsulinemic than control animals due to persistent activation of voltage-gated calcium channels (Nenquin, et al. 2004; Seghers, et al. 2000). Thus, at least in part, the loss of potassium channels caused by beta cell overexpression of PED/PEA-15 may account for the abnormalities in basal and glucose-stimulated insulin secretion and in glucose tolerance observed in the beta-tg mice.

As in the mouse islets, the same results were obtained in the glucose-responsive MIN-6 and INS-1 beta cell lines upon transfection with *ped/pea-15* cDNA (Min-$6_{ped/pea-15}$, INS-$1_{ped/pea-15)}$. A close to 35% decrease in the abundance of the *Sur1*, *Kir6.2* and *Foxa2* mRNAs has been observed compared to control cells ($p < 0.001$). These changes were accompanied by a significantly greater release of insulin when in low-glucose medium (2.8 mM glucose) with no further insulin secretion upon exposure to 16.7 mM glucose ($p < 0.001$).

Recent evidence in skeletal muscle and in fat indicated that high cellular levels of PED/PEA-15 impair the function of the atypical PKC isoform PKCzeta through a phospholipase D-mediated mechanism. Furthermore, atypical PKCs have been reported to control the function of a number of transcription factors (Furukawa, et al. 1999; Matsumoto, et al. 2003). In particular, very recent data by Hashimoto evidenced that, in *PKClambda* null mice, the expression of *Foxa2, Sur1* and *Kir6.2* mRNA in the pancreatic beta cells is significantly reduced (Hashimoto, et al. 2005). Thus, I evaluated glucose induced PKCzeta activity in beta cells overexpressing PED/PEA-15 and in mouse islets. In both mouse islets and cultured beta cell lines, the effect of glucose on insulin release was paralleled by a 2-fold increase in immunoprecipitated PKCzeta activity, with no measurable change in its expression (Figure 17). By contrast, the effect of glucose was almost completely abolished in cells overexpressing PED/PEA-15 and in the beta-tg mouse islets, suggesting an important role of atypical PKCs in regulating genes of the insulin secretion pathway.

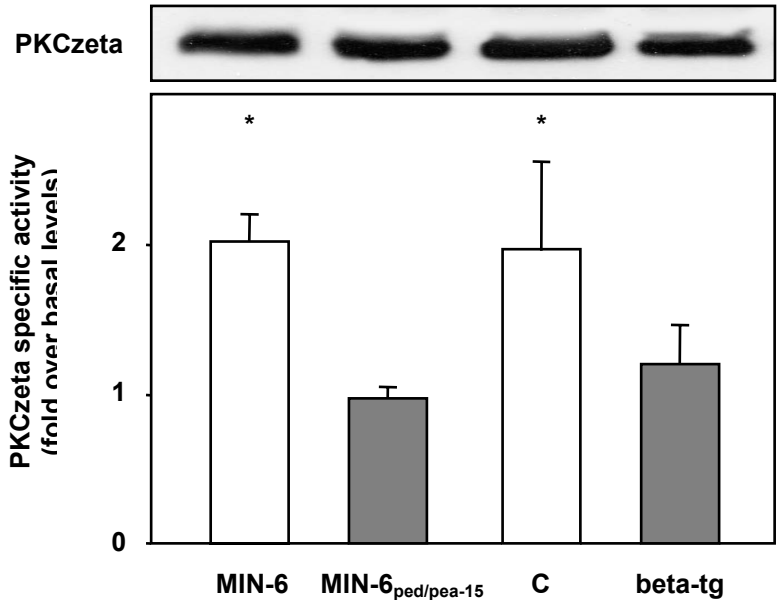

Figure 17 PKCzeta activity in beta cell lines overexpressing PED/PEA-15.
Islet from beta-tg and control mice (right) and wild-type MIN-6 cells and those stably expressing the *ped/pea-15* cDNA (MIN-$6_{ped/pea-15}$; left) were exposed to 16.7 mM glucose for 60 min. 100 μg of proteins were then precipitated with PKCzeta antibody and PKC activity was assayed as described under Research design and methods. PKC activity is expressed as fold-increase over basal activity (measured in the presence of 2.8 mM glucose). Bars represent the mean ± SD. For control, aliquots of the cell lysates were normalized for protein and directly blotted with PKCzeta antibodies. Asterisks indicate statistically significant differences (*, $p < 0.05$).

To further analyze this issue, the expression of PKCzeta was forced in the MIN-$6_{ped/pea-15}$ and the INS-$1_{ped/pea-15}$ cells. The overexpression largely rescued PKCzeta activity in the precipitates from glucose-exposed PED/PEA-15 overexpressing cells (Figure 18a), and this rescue was accompanied by recovery of the *Sur1, Kir6.2* and *Foxa2* gene expression (Figure 18b), and in part by a recovery of glucose-induced insulin secretion (Figure 18c), indicating that the changes in atypical PKC function caused by PED/PEA-15 overexpression represent upstream abnormalities impairing the function of multiple genes involved in regulating insulin secretion by the beta cell.

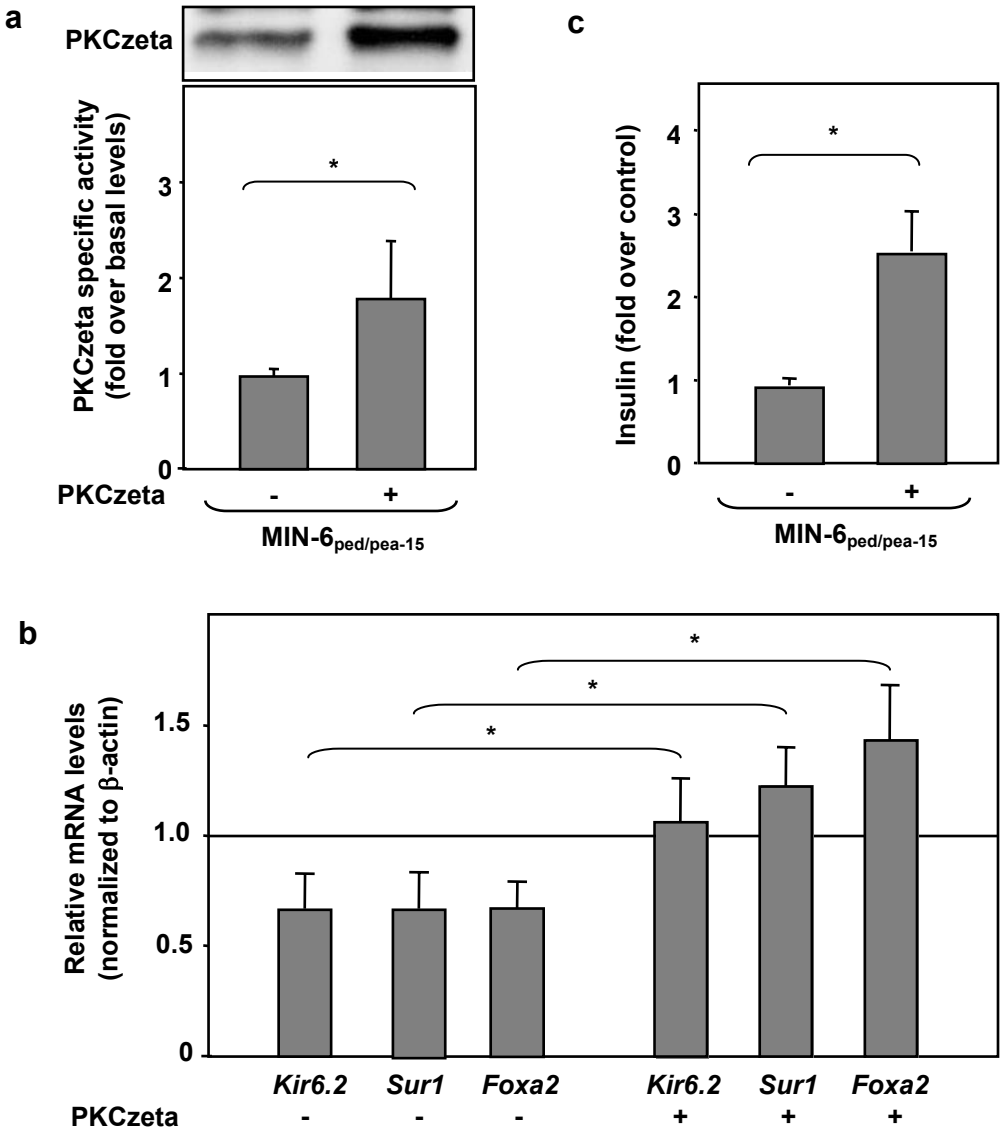

Figure 18 Rescue of PKCzeta activity, gene expression profile and glucose-stimulated insulin secretion in MIN$_{ped/pea-15}$ cells.
a) MIN-6$_{ped/pea-15}$ cells were transiently transfected with a PKCzeta cDNA, solubilized and lysates immunoprecipitated with a PKCzeta antibody. PKC activity was assayed in the immunoprecipitates. For control, aliquots of the lysates were blotted with the PKCzeta antibody (inset). Bars represent the means ± SD; **b**) the abundance of mRNAs for the indicated proteins was determined by real-time RT-PCR analysis of total RNA isolated from MIN-6 and MIN-6$_{ped/pea-15}$ cells. Bars represent the mRNA levels in the MIN-6$_{ped/pea-15}$ cells and are relative to those in the untransfected cells (MIN-6). Data are expressed as means ± SD; **c**) the MIN-6$_{ped/pea-1}$, either those transiently transfected with the PKCzeta cDNA and the untransfected cells, were exposed to 16.7 mM glucose for 60 min and insulin release in the culture medium was assayed by radioimmunoassay. Bars represent the means ± SD. Asterisks indicate statistically significant differences (*, $p < 0.05$).

To gain further insight into the role of PED/PEA-15 in the regulation of beta cell function, islets from *ped/pea-15* null mice were used. These animals

feature no PED/PEA-15 expression in beta cells. Islets from these animals evidenced a 2-fold increased PKCzeta activation following glucose exposure, as compared to islets from control mice ($p < 0.01$; Figure 19a). The enhanced PKCzeta activity is accompanied by 45% increases in the abundance of *Kir6.2*, *Sur1* and *Foxa2* mRNAs ($p < 0.001$; Figure 19b), and by a significant 2-fold increase in sensitivity to glucose induced insulin secretion compared to controls ($p < 0.01$; Figure 19c). These data evidence that PKCzeta activation is sufficient to upregulate these genes, indicating that these genes represent major effectors through which PED/PEA-15 physiologically controls insulin secretion.

Thus, *Foxa2*-mediated control of glucose sensitivity represents a physiological function of PED/PEA-15 in the beta cell, and dysregulation of this mechanism may be relevant for Type 2 Diabetes in humans.

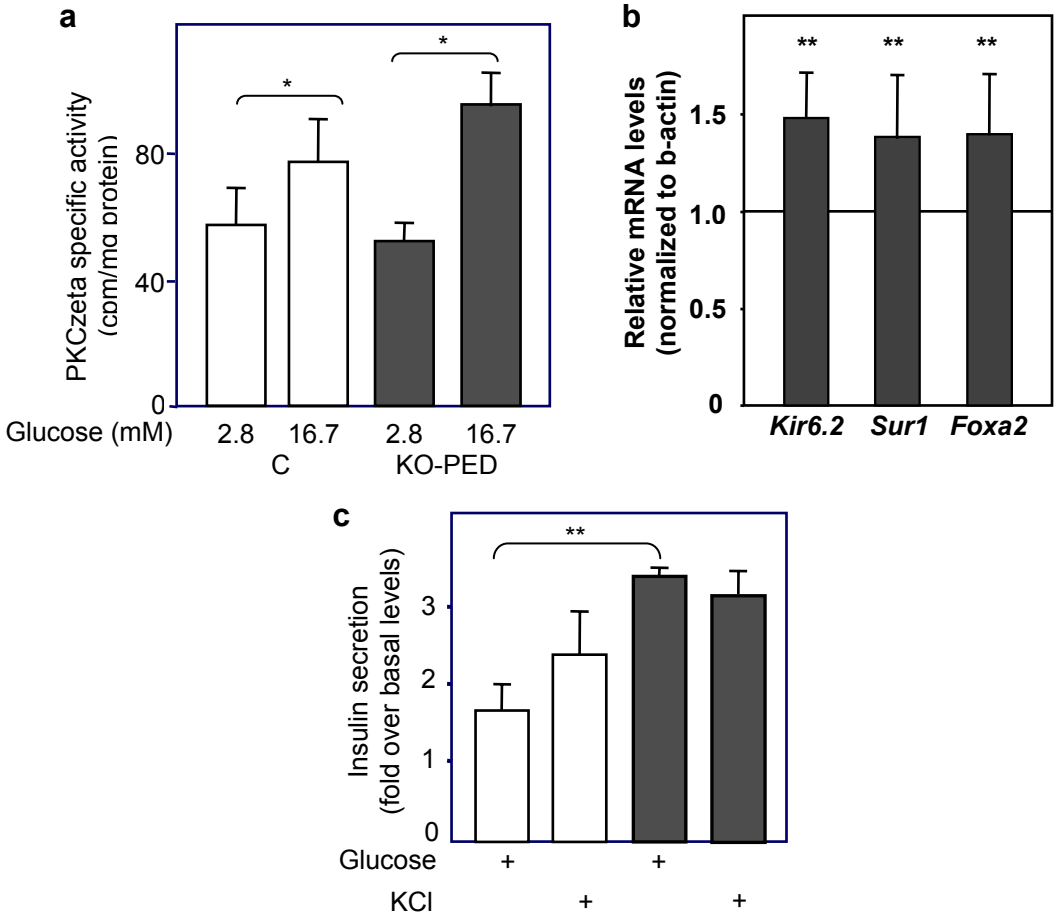

Figure 19 PKCzeta activity, insulin secretion and gene expression profile in isolated islets from KO-PED mice.

a) PKC activity was assayed in islets isolated from 6-month old *ped/pea-15* null mice (KO) and from their unmodified littermates (C), and it is expressed as fold-increase over basal activity; **b**) the abundance of mRNAs was determined by real-time RT-PCR analysis of total RNA isolated from islets of KO-PED and control mice using beta-actin as internal standard; **c**) islets from KO-PED and control mice were exposed to glucose and potassium. Insulin release is expressed as fold-increase in medium insulin concentration over the basal; bars represent the mean ± SD Asterisks denote statistically significant differences (**, $p < 0.01$; ***, $p < 0.001$).

Conclusions

From the first part of experiments (work in human), I can conclude that PED/PEA15 overexpression represents not only a common abnormality in T2 diabetic patients, but also in their First Degree Relatives. In these individuals, PED/PEA15 levels are strongly correlated with resistance to insulin action in the lean mass, suggesting that PED/PEA15 contributes to the early appearance of insulin resistance.

From the second part of experiments (work in mice), I can conclude that PED/PEA-15 can be considered as an endogenous regulator of glucose-induced insulin secretion, which restrains potassium channel expression in pancreatic beta-cells. Indeed, *Foxa2*-mediated control of glucose sensitivity represents a physiological function of PED/PEA-15 in the beta cell, and dysregulation of this mechanism is sufficient to impair glucose tolerance in mice, and it may be relevant for T2D in humans.

We might hypothesize that in T2 diabetic FDR the consequence of the high levels of PED/PEA15 on insulin action might occur earlier during life than the effects of PED/PEA15 on beta cell function. Thus, follow-up studies of FDR individuals are necessary to further elucidate the effect of PED/PEA15 levels in the progression to T2D.

Acknowledgements

I thank *Prof Francesco Beguinot* to give me the opportunity to work in his laboratory, to be an example of life, and for the care that he has for our work and for our future.

I would like to thank *Prof. Giancarlo Vecchio* for letting to attend this Doctorate program under his supervision.

I thank *Prof. Pietro Formisano* for his scientific suggestions and for his availability.

I thank *Dr. Claudia Miele* to be all that I want to be.

I thank *Dr. Alessia Paola Maria Barbagallo* for taking with me this way, sometimes difficult, full of beautiful and also sad moments, and being as a sister for me.

I would like to thank *my family* for supporting me and all my decisions and for having taught me to love life and to believe in its values.

I would like to thank *Miele's family* for having welcomed me as a member of their family.

I would like to thank my colleagues of *Diablab laboratory* for the time spent together.

References

Aguilar-Bryan L, Nichols CG, Wechsler SW, Clement JP, Boyd AE, González G, Herrera-Sosa H, Nguy K, Bryan J, Nelson DA. Cloning of the beta cell high-affinity sulfonylurea receptor: a regulator of insulin secretion. Science 1995; 268:423–426.

Aguilar-Bryan L, Bryan J. Molecular biology of adenosine triphosphate-sensitive potassium channels. Endocr Rev 1999; 20:101–135.

Alessi DR, James SR, Downes CP, Holmes AB, Gaffney PR, Reese CB, Cohen P. Characterization of a 3-phosphoinositide-dependent protein kinase which phosphorylates and activates protein kinase Balpha Curr Biol 1997; 7:261–269.

Altshuler D, Hirschhorn JN, Klannemark M, Lindgren CM, Vohl MC, Nemesh J, Lane CR, Schaffner SF, Bolk S, Brewer C, Tuomi T, Gaudet D, Hudson TJ, Daly M, Groop L, Lander ES. The common PPARγ Pro12Ala polymorphism is associated with decreased risk of type 2 diabetes. Nature Genet 2000; 26 :76–80.

Ashcroft FM, Gribble FM. ATP-sensitive K^+ channels and insulin secretion: their role in health and disease. Diabetologia 1999; 42:903–919.

Bell GI, Polonsky KS. Diabetes mellitus and genetically programmed defects in β-cell function. Nature 2001; 414:788-791.

Boulton TG, Nye SH, Robbins DJ, Ip NY, Radziejewska E, Morgenbesser SD, DePinho RA, Panayotatos N, Cobb MH, Yancopoulos GD. ERKs: a family of protein-serine/threonine kinases that are activated and tyrosine phosphorylated in response to insulin and NGF. Cell 1991; 65:663–675.

Bruning JC, Michael MD, Winnay JN, Hayashi T, Horsch D. Accili D, Goodyear LJ, Kahn CR: A muscle-specific insulin receptor knockout exhibits features of the metabolic syndrome of NIDDM without altering glucose tolerance. Mol Cell 1998; 2:559-569.

Condorelli G, Vigliotta G, Iavarone C, Caruso M, Tocchetti CG, Andreozzi F, Cafieri A, Tecce MF, Formisano P, Beguinot L, Beguinot F. PED/ PEA-15 gene controls glucose transport and is overexpressed in type 2 diabetes mellitus. The EMBO Journal 1998; 17: 3858–3866.

Condorelli G, Vigliotta G, Cafieri A, Trencia A, Andalo P, Oriente F, Miele C, Caruso M, Formisano P, Beguinot F. PED/PEA-15: an anti-apoptotic molecule that regulates FAS/TNFR1-induced apoptosis. Oncogene 1999; 18:4409-4415.

Condorelli G, Vigliotta G, Trencia A, Maitan MA, Caruso M, Miele C, Oriente F, Santopietro S, Formisano P, Beguinot F: Protein kinase C (PKC)-alpha activation inhibits PKC-zeta and mediates the action of PED/PEA-15 on glucose transport in the L6 skeletal muscle cells. Diabetes 2001; 50:1244-1252.

Condorelli G, Trencia A, Vigliotta G, Perfetti A, Goglia U, Cassese A, Musti AM, Miele C, Santopietro S, Formisano P, Beguinot F. Multiple members of the mitogen-activated protein kinase family are necessary for PED/PEA-15 anti-apoptotic function. J Biol Chem 2002.; 277: 11013–11018.

Devedjian JC, George M, Casellas A, Pujol A, Visa J, Pelegrin M, Gros L, Bosch F: Transgenic mice overexpressing insulin-like growth factor-II in beta cells develop type 2 diabetes. J Clin Invest 2000; 105:731-740.

Diabetes Atlas 2006, 3rd ed., International Diabetes Federation, 2006.

Ferre P, Leturque A, Burnol AF, Penicaud L, Girard J: A method to quantify glucose utilization in vivo in skeletal muscle and white adipose tissue of the anaesthetized rat. Biochem J 1985; 228:103-110.

Formstecher E, Ramos JW, Fauquet M, Calderwood DA, Hsieh JC, Canton B, Nguyen XT, Barnier JV, Camonis J, Ginsberg MH, Chneiweiss H: PEA-15 mediates cytoplasmic sequestration of ERK MAP kinase. Dev Cell 2001; 1:239-250.

Formisano P, Oriente F, Miele C, Caruso M, Auricchio R, Vigliotta G, Condorelli G, Beguinot F. In NIH-373 fibrolasts, insulin receptor interaction with specific protein kinase C isoforms controls receptor intracellular routine. J Biol Chem 1998; 273:13197-13202.

Formisano P, Perruolo G, Libertini S, Santopietro S, Troncone G, Raciti GA, Oriente F, Portella G, Miele C, Beguinot F. Raised expression of the antiapoptotic protein ped/pea-15 increases susceptibility to chemically induced skin tumor development. Oncogene 2005; 24:7012-7021.

Furukawa N, Shirotani T, Araki E, Kaneko K, Todaka M, Matsumoto K, Tsuruzoe K, Motoshima H, Yoshizato K, Kishikawa H, Shichiri M: Possible involvement of atypical protein kinase C (PKC) in glucose-sensitive expression of the human insulin gene: DNA-binding activity and transcriptional activity of pancreatic and duodenal homeobox gene-1 (PDX-1) are enhanced via calphostin C-sensitive but phorbol 12-myristate 13-acetate (PMA) and Go 6976-insensitive pathway. Endocr J 1999; 46:43-58.

Gilon P, Ravier MA, Jonas JC, Henquin JC. Control mechanisms of the oscillations of insulin secretion in vitro and in vivo. Diabetes 2002; 51 Suppl 1: S144-151.

Gudmundsson J, Sulem P, Steinthorsdottir V, Bergthorsson JT, Thorleifsson G, Manolescu A, Rafnar T, Gudbjartsson D, Agnarsson BA, Baker A, Sigurdsson A, Benediktsdottir KR, Jakobsdottir M, Blondal T, Stacey SN, Helgason A, Gunnarsdottir S, Olafsdottir A, Kristinsson KT, Birgisdottir B, Ghosh S, Thorlacius S, Magnusdottir D, Stefansdottir G, Kristjansson K, Bagger Y, Wilensky RL, Reilly MP, Morris AD, Kimber CH, Adeyemo A, Chen Y, Zhou J, So WY, Tong PC, Ng MC, Hansen T, Andersen G, Borch-Johnsen K, Jorgensen T, Tres A, Fuertes F, Ruiz-Echarri M, Asin L, Saez B, van Boven E, Klaver S, Swinkels DW, Aben KK, Graif T, Cashy J, Suarez BK, van Vierssen Trip O, Frigge ML, Ober C, Hofker MH, Wijmenga C, Christiansen C, Rader DJ, Palmer CN, Rotimi C, Chan JC, Pedersen O, Sigurdsson G, Benediktsson R, Jonsson E, Einarsson GV, Mayordomo JI, Catalona WJ, Kiemeney LA, Barkardottir RB, Gulcher JR, Thorsteinsdottir U, Kong A, Stefansson K. Two variants on chromosome 17 confer prostate cancer risk, and the one in TCF2 protects against type 2 diabetes. Nature Genet 2007; 39:977–983.

Hao C, Beguinot F, Condorelli G, Trencia A, Van Meir EG, Yong VW, Parney IF, Roa WH, Petruk KC. Induction and intracellular regulation of tumor necrosis factor-related apoptosis-inducing ligand (TRAIL) mediated apoptosis in human malignant glioma cells. Cancer Res 2001; 61:1–9.

Hashimoto N, Kido Y, Uchida T, Matsuda T, Suzuki K, Inoue H, Matsumoto M, Ogawa W, Maeda S, Fujihara H, Ueta Y, Uchiyama Y, Akimoto K, Ohno S, Noda T, Kasuga M: PKClambda regulates glucose-induced insulin secretion through modulation of gene expression in pancreatic beta cells. J Clin Invest 2005; 115:138-145.

Kahn CR. Insulin action, diabetogenes, and the cause of type II diabetes. Diabetes 1994; 43:1066-1084.

Kane C, Shepard RM, Squires PE, Johson PR, James RF, Milla PJ, Aynsley-Green A, Lindley KJ, Dunne MJ. Loss of function KATP channels in pancreatic β-cells causes persistent hyperinsulinemic hypoglicemia of infancy. Nat Med 1996;. 2: 1301-1302.

Kennedy RT, Kauri LM, Dahlgren GM, Jung SK. Metabolic oscillations in beta cells. Diabetes 2002; 51 Suppl 1: S 152-61.

Kitamura T, Kido Y, Nef S, Merenmies J, Parada LF, Accili D: Preserved pancreatic beta-cell development and function in mice lacking the insulin receptor-related receptor. Mol Cell Biol 2001; 21:5624-5630.

Kubes M, Cordier J, Glowinski J, Girault JA, Chneiweiss H. Endothelin induces a calcium-dependent phosphorylation of PEA-15 in intact astrocytes: identification of Ser104 and Ser116 phosphorylated, respectively, by protein kinase C and calcium/calmodulin kinase II in vitro. J Neurochem 1998; 71:1303–1314.

Kulkarni RN, Bruning JC, Winnay JN, Postic C, Magnuson MA, Kahn CR: Tissue-specific knockout of the insulin receptor in pancreatic beta cells creates an insulin secretory defect similar to that in type 2 diabetes. Cell 1999; 96: 329-339.

Laemmli UK: Cleavage of structural proteins during the assembly of the head of bacteriophage T4. Nature 1970; 227:680-685.

Lietzke SE, Bose S, Cronin T, Klarlund J, Chawla A, Czech MP, Lambright DG. Structural basis of 3-phosphoinositide recognition by pleckstrin homology domains. Mol Cell 2000; 6:385–394.

MacDonald PE, Joseph JW, Rorsman P. Glucose-sensing mechanisms in pancreatic β-cells. Phil Trans R Soc 2005; 360:2211-2225.

Matsumoto M, Ogawa W, Akimoto K, Inoue H, Miyake K, Furukawa K, Hayashi Y, Iguchi H, Matsuki Y, Hiramatsu R, Shimano H, Yamada N, Ohno S, Kasuga M, Noda T: PKCλ in liver mediates insulin-induced SREBP-1c expression and determines both hepatic lipid content and overall insulin sensitivity. J Clin Invest 2003; 112:935-944.

Mendez CF, Leibiger IB, Leibiger B, Hoy M, Gromada J, Berggren PO, Bertorello AM. Rapid association of protein kinase C-epsilon with insulin granules is essential for insulin exocytosis. J Biol Chem 2003; 278:44753-44757.

Metcalfe P, Waters AH. Location of the granulocyte-specific antigen LAN on the Fc-receptor III. Transfus Med 1992; 2:283–287.

Miki T, Nagashima K, Tashiro F, Kotake K, Yoshitomi H, Tamamoto A, Gonoi T, Iwanaga T, Miyazaki J, Seino S: Defective insulin secretion and enhanced insulin action in KATP channel-deficient mice. Proc Natl Acad Sci USA 1998; 95:10402-10406.

Miyazaki J, Araki K, Yamato E, Ikegami H, Asano T, Shibasaki Y, Oka Y, Yamamura K: Establishment of a pancreatic beta cell line that retains glucose-inducible insulin secretion: special reference to expression of glucose transporter isoforms. Endocrinology 1990; 127:126-132.

Myers MG Jr, Backer JM, Sun XJ, Shoelson S, Hu P, Schlessinger J, Yoakim M, Schaffhausen B, White MF. IRS-1 activates phosphatidylinositol 38-kinase by associating with src homology 2 domains of p85. Proc Natl Acad Sci USA 1992; 89 :10350–10354.

Nenquin M, Szollosi A, Aguilar-Bryan L, Bryan J, Henquin JC: Both triggering and amplifying pathways contribute to fuel-induced insulin secretion in the absence of sulfonylurea receptor-1 in pancreatic beta-cells. J Biol Chem 2004; 279:32316-32324.

Nesher R, Anteby E, Yedovizky M, Warwar N, Kaiser N, Cerasi E. β-cell protein kinases and the dynamics of the insulin response to glucose. Diabetes 2002;. 51 Suppl. 1: S68-73.

Nielsen EM, Hansen L, Carstensen B, Echwald SM, Drivsholm T, Glumer C, Thorsteinsson B, Borch-Johnsen K, Hansen T, Pedersen O. The E23K variant of Kir6.2 associates with impaired post-OGTT serum insulin response and increased risk of type 2 diabetes. Diabetes 2003; 52 :573–577.

Owen KR, McCarthy MI. Genetics of type 2 diabetes. Current Opinion in Genetics & Development 2007; 17:239–244.

Patti ME, Kahn CR. The insulin receptor-a critical link in glucose homeostasis and insulin action. J Basic Clin Physiol Pharmacol 1998; 9: 89–109.

Pessin JE, Saltiel AR. Signaling pathways in insulin action: molecular targets of insulin resistance. J Cli. Invest 2000; 106:165–169.

Pickup JC, Williams G, editors.Textbook of Diabetes: selected chapters. 3rd ed. Oxford: Blackwell Publishing; 2005.

Polonsky KS, O'Meara NM. DeGroot LJ, Jameson LJ, editors. Endocrinology. 4th ed. Philadelphia: Saunders; 2001. p. 697–711.

Saltiel AR, Kahn CR. Insulin signalling and the regulation of glucose and lipid metabolism. Nature 2001; 414:799-806.

Sandhu MS, Weedon MN, Fawcett KA, Wasson J, Debenham SL, Daly A, Lango H, Frayling TM, Neumann RJ, Sherva R, Blech I, Pharoah PD, Palmer CN, Kimber C, Tavendale R, Morris AD, McCarthy MI, Walker M, Hitman G, Glaser B, Permutt MA, Hattersley AT, Wareham NJ, Barroso I. Common variants in WFS1 confer risk of type 2 diabetes. Nature Genet 2007; 39:951–953.

Seghers V, Nakazaki M, DeMayo F, Aguilar-Bryan L, Bryan J: Sur1 knockout mice. A model for K(ATP) channel-independent regulation of insulin secretion. J Biol Chem 2000; 275:9270-9277.

Shepherd PR, Nave BT, Siddle K. Insulin stimulation of glycogen synthesis and glycogen synthase activity is blocked by wortmannin and rapamycin in 3T3-L1 adipocytes: evidence for the involvement of phosphoinositide 3-kinase and p70 ribosomal protein-S6 kinase. Biochem J 1995; 305:25–28.

Somogyi M: Determination of blood sugar. J Biol Chem 1945; 160:69-73.

Standaert ML, Galloway L, Karnam P, Bandyopadhyay G, Moscat J, Farese RV. Protein kinase C-ζ as a downstream effector of phosphatidylinositol 3-kinase during insulin stimulation in rat adipocytes. Potential role in glucose transport. J Biol Chem 1997; 272:30075–30082.

Straub SG, Cosgrove KE, Ämmälä C, Shepherd RM, O'Brien RE, Barnes PD, Kuchinski N, Chapman JC, Schaeppi M, Glaser B, Lindley KJ, Sharp GWG, Aynsley-Green A, Dunne MJ. Hyperinsulinism of Infancy. The Regulated Release of Insulin by KATP Channel–Independent Pathways. Diabetes 2001; 50:329:339.

Taylor IS. Deconstructing Type 2 Diabetes. Cell Press 1999; 97:9-12.

Trencia A, Fiory F, Maitan MA, Vito P, Barbagallo AP, Perfetti A, Miele C, Ungaro P, Oriente F, Cilenti L, Zervos AS, Formisano P, Beguinot F. Omi/HtrA2 Promotes Cell Death by Binding and Degrading the Anti-apoptotic Protein ped/pea-15. J Biol Chem 2004; 279: 46566–46572.

Vaidyanathan H, Ramos JW: RSK2 activity is regulated by its interaction with PEA-15. J Biol Chem 2003; 278:32367-32372.

Vigliotta G, Miele C, Santopietro S, Portella G, Perfetti A, Maitan MA, Cassese A, Oriente F, Trencia A, Fiory F, Romano C, Tiveron C, Tatangelo L, Troncone G, Formisano P, Beguinot F: Overexpression of the ped/pea-15 gene causes diabetes by impairing glucose-stimulated insulin secretion in addition to insulin action. Mol Cell Biol 2004; 24:5005-5015.

Wang H, Gauthier BR, Hagenfeldt-Johansson KA, Iezzi M, Wollheim CB: Foxa2 (HNF3beta) controls multiple genes implicated in metabolism-secretion coupling of glucose-induced insulin release. J Biol Chem 2002; 277:17564-17570.

White MF. The IRS-signalling system: a network of docking proteins that mediate insulin action. Mol Cell Biochem 1998; 182: 3–11.

Zhang Y, Redina O, Altshuller YM, Yamazaki M, Ramos J, Chneiweiss H, Kanaho Y, Frohman MA. Regulation of expression of phospholipase D1 and D2 by PEA-15, a novel protein that interacts with them. J Biol Chem 2000; 275:35224-35232.

Oncogene (2005) 24, 7012–7021

www.nature.com/onc

Raised expression of the antiapoptotic protein ped/pea-15 increases susceptibility to chemically induced skin tumor development

Pietro Formisano[1], Giuseppe Perruolo[1], Silvana Libertini[1], Stefania Santopietro[1], Giancarlo Troncone[2], Gregory Alexander Raciti[1], Francesco Oriente[1], Giuseppe Portella[1], Claudia Miele[1] and Francesco Beguinot*[,1]

[1]*Dipartimento di Biologia e Patologia Cellulare e Molecolare, Università di Napoli Federico II, Istituto di Endocrinologia ed Oncologia Sperimentale del CNR, Via Sergio Pansini, 5, Naples 80131, Italy;* [2]*Dipartimento di Scienze Biomorfologiche e Funzionali of the Federico II University of Naples, Naples, Italy*

ped/pea-15 is a cytosolic protein performing a broad antiapoptotic function. We show that, upon DMBA/TPA-induced skin carcinogenesis, transgenic mice overexpressing *ped/pea-15* ($Tg_{ped/pea-15}$) display early development of papillomas and a four-fold increase in papilloma number compared to the nontransgenic littermates ($P<0.001$). The malignant conversion frequency was 24% for the $Tg_{ped/pea-15}$ mice and only 5% in controls ($P<0.01$). The isolated application of TPA, but not that of DMBA, was sufficient to reversibly upregulate *ped/pea-15* in both untransformed skin and cultured keratinocytes. ped/pea-15 protein levels were also increased in DMBA/TPA-induced papillomas of both $Tg_{ped/pea-15}$ and control mice. Isolated TPA applications induced Caspase-3 activation and apoptosis in nontransformed mouse epidermal tissues. The induction of both Caspase-3 and apoptosis by TPA were four-fold inhibited in the skin of the $Tg_{ped/pea-15}$ compared to the nontransgenic mice, accompanied by a similarly sized reduction in TPA-induced JNK and p38 stimulation and by constitutive induction of cytoplasmic ERK activity in the transgenics. *ped/pea-15* expression was stably increased in cell lines from DMBA/TPA-induced skin papillomas and carcinomas, paralleled by protection from TPA apoptosis. In the A5 spindle carcinoma cell line, antisense inhibition of *ped/pea-15* expression simultaneously rescued sensitivity to TPA-induced Caspase-3 function and apoptosis. The antisense also reduced A5 cell ability to grow in semisolid media by 65% ($P<0.001$) and increased by three-fold tumor latency time ($P<0.01$). Thus, the expression levels of *ped/pea-15* control Caspase-3 function and epidermal cell apoptosis *in vivo* and determine susceptibility to skin tumor development.

Oncogene (2005) **24,** 7012–7021. doi:10.1038/sj.onc.1208871; published online 25 July 2005

Keywords: ped/pea-15; transgenic mice; chemical carcinogenesis; skin cancer; apoptosis

*Correspondence: F Beguinot; E-mail: beguino@unina.it
Received 26 January 2005; revised 6 May 2005; accepted 20 May 2005; published online 25 July 2005

Introduction

There is evidence that deregulation of apoptosis plays an important role in tumorigenesis. Indeed, alterations of apoptosis-related genes have been identified in a number of human cancers (Debatin and Krammer, 2004). ped/pea-15 is a 15 kDa, death effector domain (DED)-containing protein featuring ubiquitous expression, and originally identified as a major astrocytic phosphoprotein (Araujo *et al*., 1993; Condorelli *et al*., 1998). ped/pea-15 exerts a broad antiapoptotic action through at least three distinct mechanisms. Firstly, it inhibits the formation of the death-inducing signaling complex (DISC) and Caspase-3 activation triggered by FASL, tumor necrosis factor alpha, and the tumor necrosis factor-related apoptosis-inducing ligand (TRAIL) (Condorelli *et al*., 1999; Kitsberg *et al*., 1999; Hao *et al*., 2001). Secondly, ped/pea-15 inhibits stress-induced apoptosis by simultaneously blocking stress-activated protein kinases (SAPK) and increasing the function of cytosolic extracellular signal-regulated kinases (ERK1/2) (Condorelli *et al*., 2002). Thirdly, ped/pea-15 prevents degradation of the antiapoptotic protein XIAP caused by release of proapoptotic mitochondrial proteins (Trencia *et al*., 2004).

Studies in our own and other laboratories have shown that elevated expression of *ped/pea-15* occurs in several tumor-derived cell lines. Indeed, *ped/pea-15* is highly expressed in human glioma and metastatic breast cancer cell lines and induces resistance to chemotherapic agents in these cells (Ramos *et al*., 2000; Hao *et al*., 2001; Condorelli *et al*., 2002; Trencia *et al*., 2004). *ped/pea-15* is also expressed at high levels in tumor cell lines derived from human larynx, cervix, and skin tumors (Condorelli *et al*., 1998), and in human mammary carcinomas as well (Tsukamoto *et al*., 2000). Finally, the *ped/pea-15* gene was demonstrated to be increasingly expressed during tumor progression in murine squamous carcinomas (Dong *et al*., 2001). However, despite these mounting evidence supporting the role of *ped/pea-15* in neoplastic transformation and tumor progression, whether *ped/pea-15* has a direct role in tumorigenesis and progression *in vivo* has not been investigated yet.

Transgenic mice overexpressing *ped/pea-15* ubiquitously have recently been generated (Vigliotta *et al*., 2004). These mice feature reduced glucose tolerance due to both impaired insulin action and secretion. We have now used these transgenics and a well-characterized mouse model of chemically induced multistep skin carcinogenesis (Balmain and Harris, 2000) to explore the role of *ped/pea-15* in the initiation, promotion and progression of skin tumors. Our study shows, for the first time, that *ped/pea-15* expression level has a significant impact on skin tumor development in a mouse model of chemically induced skin carcinogenesis.

Results

Skin carcinogenesis in ped/pea-15 *transgenic mice*

We have investigated whether the variation in *ped/pea-15* expression levels affects skin tumorigenesis. To this end, we have used transgenic mice overexpressing the human cDNA of *ped/pea-15* ($Tg_{ped/pea\text{-}15}$; Vigliotta *et al*., 2004). Based on Western blot analysis, ped/pea-15 protein was overexpressed by about four-fold ($P<0.001$) in the epidermis of these transgenics, as compared to their nontransgenic littermates (WT) (Figure 1a).

$Tg_{ped/pea\text{-}15}$ and control mice ($n=40$/group; M/F = 1) were subjected to a single DMBA topical application followed by repeated applications of the tumor promoter TPA. This treatment resulted in the development of papillomatous lesions. Visible papillomas began to appear on the dorsal skin of both the $Tg_{ped/pea\text{-}15}$ and WT mice at 7 weeks of promotion, indicating no difference in the benign tumor latency between the two groups of mice (Figure 1b). The incidence of papilloma development reached 100% at 10 weeks of promotion in the $Tg_{ped/pea\text{-}15}$, and at week 12 in the WT mice ($P<0.001$; Figure 1b). Interestingly, there was a significant increase in the average number of papillomas per mouse in the $Tg_{ped/pea\text{-}15}$ compared to WT mice throughout the entire promoter treatment period. The difference in papilloma number was already significant at week 8. By the end of promotion (week 15), $Tg_{ped/pea\text{-}15}$ mice showed 18.4 ± 10.7 papillomas per mouse compared to 4.9 ± 4.8 in the WT mice ($P<0.001$) (Figure 1c). No gender-related difference was evidenced in either the incidence or the number of papillomas in transgenic and control mice (data not shown).

At 35 weeks after promoter treatment suspension, the lesions from $Tg_{ped/pea\text{-}15}$ and WT mice were subjected to histological examination. The malignant conversion frequency was 24% in the $Tg_{ped/pea\text{-}15}$ mice (12 out of 50 analysed lesions, Figure 2A). As in previous studies (Burns *et al*., 1978), the frequency was only 5% (two out of 40 analysed lesions) in the control mice ($P<0.001$), however. Sections of the lesions from $Tg_{ped/pea\text{-}15}$ mice more frequently showed the presence of a poorly differentiated epithelial neoplasm composed of nests of small undifferentiated cells with minimal keratinization, occasional squamous pearl formation and extremely

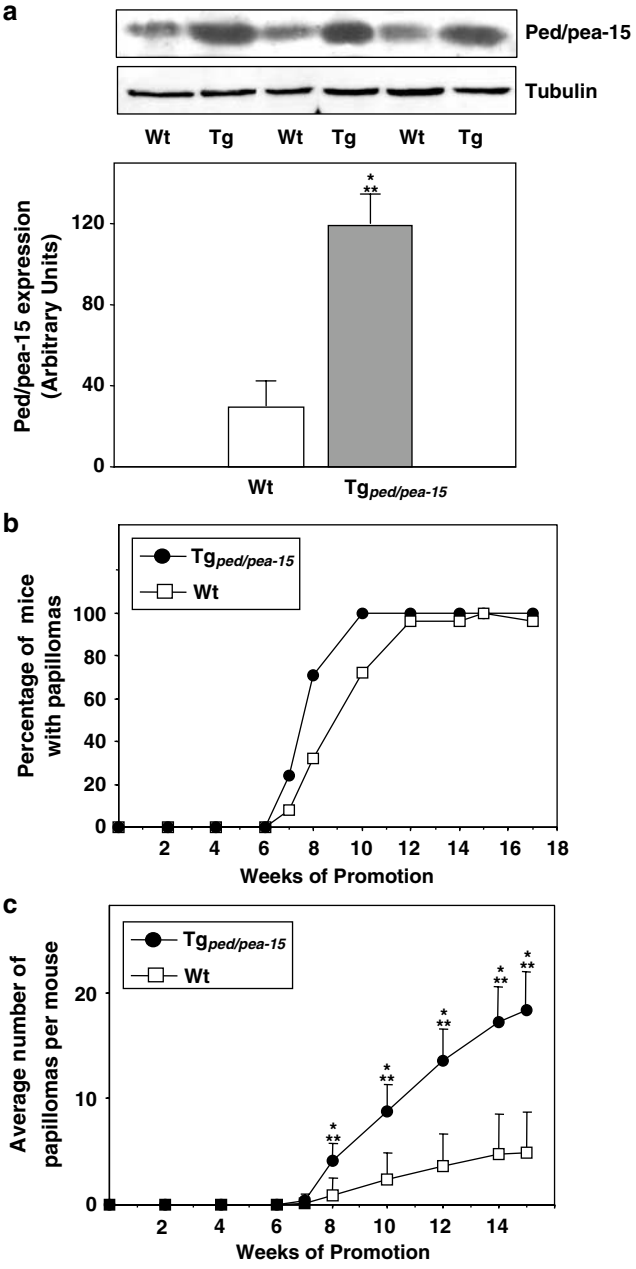

Figure 1 Chemically induced skin carcinogenesis in $Tg_{ped/pea\text{-}15}$ mice. (**a**) Duplicate samples from the dorsal skin of *ped/pea-15* transgenic mice ($Tg_{ped/pea\text{-}15}$) and the nontransgenic littermates ($n=40$ animals/group; male/female = 1) were solubilized and proteins (50 μg) analysed by Western blotting with ped/pea-15 antibodies as in Vigliotta *et al*. (2004). To ensure normalization, aliquots from the samples were also blotted with tubulin antibodies. Bars represent the average values ($\pm$s.d.) obtained from ped/pea-15 band densitometry, normalized for tubulin band densitometry. A representative blot is also shown on the top. (**b** and **c**) $Tg_{ped/pea\text{-}15}$ and control mice (three independent experiments; $n=40$ animals/group in each; male/female = 1) were subjected to skin carcinogenesis as described under Materials and methods. The number of papillomas was recorded weekly and is expressed either as percentage of mice containing at least one papilloma (**b**) or the average number ($\pm$s.d.) of papillomas per mouse (**c**). Statistical significance was assessed by *t*-test analysis

A

Mouse line	No. of mice At 35 weeks by the end of promotion	No. of carcinomas per no. of papillomas	Frequency of malignant conversion
Wt	20	2/40	5%
$Tg_{ped/pea-15}$	12	12/50	24%

B

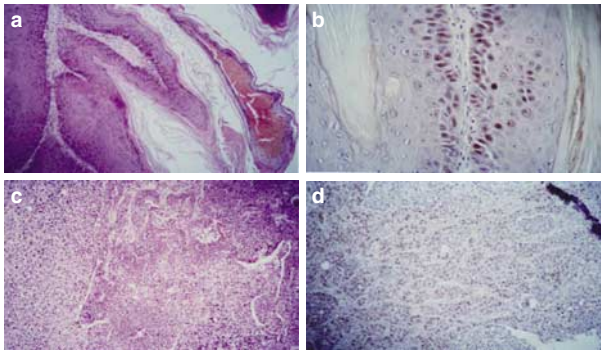

Figure 2 Malignant conversion frequency in $Tg_{ped/pea-15}$ mice. (**A**) ped/pea-15 transgenic and control mice were subjected to chemical carcinogenesis as described under Materials and methods. Total papilloma and carcinoma numbers were recorded. Carcinoma numbers were scored by morphological appearance on collection followed by histological confirmation after H&E staining of paraffin sections. (**B**) Representative H&E stained paraffin sections ($\times 100$ magnification) of tumors at 35 weeks after the end of promotion treatment from control (a) and $Tg_{ped/pea-15}$ mice (c). In the transgenics, PCNA immunostaining ($\times 100$ magnification) was scattered throughout the the tumour tissue (d), while limited to the basal cells in the control mice (b), as evidenced at higher magnification ($\times 400$). Representative microphotographs are shown

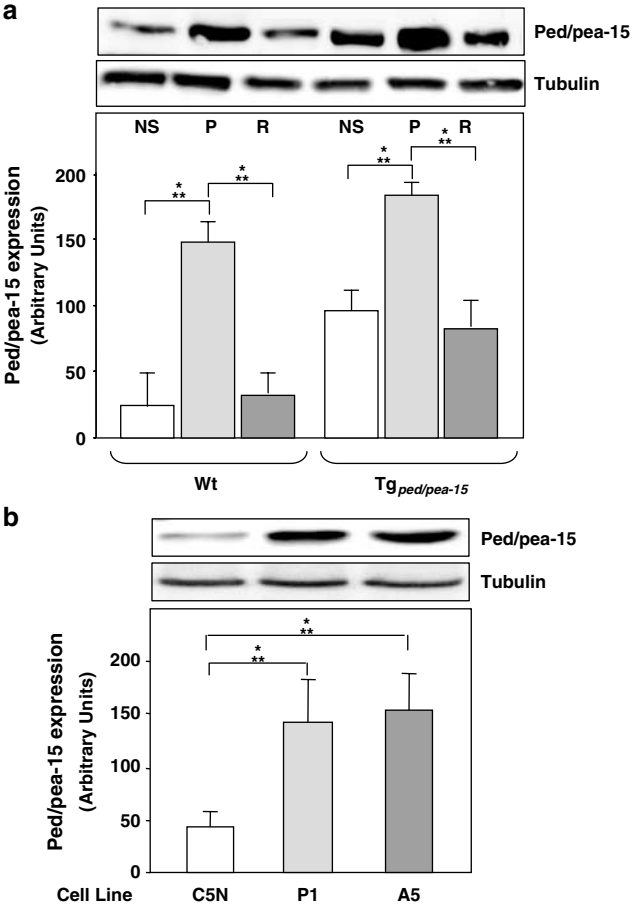

Figure 3 *ped/pea-15* expression in cell lines from chemically induced skin tumors and papillomas from $Tg_{ped/pea-15}$ mice. (**a**) Papillomatous lesions (P; $n=32$), samples from unaffected skin of the surrounding areas (NS; $n=34$), or from the skin corresponding to the papillomatous base upon regression of the lesion (R; $n=28$) from control (WT) and *ped/pea-15* transgenic mice ($Tg_{ped/pea-15}$) animals ($n=27$/group) were excised and lysed as described in the legend to Figure 1. ped/pea-15 and tubulin expression were detected in the lysates (50 μg of proteins/sample) by Western blotting and autoradiography. Blots were revealed by ECL and autoradiography and analysed by laser densitometry. Bars represent the average (values $\pm$ s.d.) of the tubulin-normalized expression of ped/pea-15 in duplicate determinations from four independent experiments. The difference between P and NS was significant at the $P=0.001$ (Wt) and $P<0.001$ (Tg). (**b**) The C5N, P1 and A5 cell lines derived, respectively, from normal keratinocytes, DMBA/TPA-induced papillomas and spindle cell carcinomas, were cultured as described under Materials and methods. Cell proteins (50 μg) were Western blotted with ped/pea-15 or tubulin antibodies as indicated. Blots were revealed and further analysed as in (**a**). Bars represent the average (values $\pm$ s.d.) of the tubulin-normalized expression of ped/pea-15 in duplicate determinations from four independent experiments. The difference between the P1 and C5N cells and between the A5 and C5N cells were significant at the $P<0.001$ level. A representative autoradiograph is also shown

intense mitotic activity (Figure 2B(c)). As shown in Figure 2B(d), the majority of the neoplastic cells displayed intense PCNA nuclear labeling, and stained cells were scattered throughout the tissue, reflecting the neoplastic modifications. At variance, lesions from WT mice more commonly showed benign hyperplastic proliferation of the epidermis, with epithelial cells featuring normal morphological characteristics, without significant nuclear atypia (Figure 2B(a)). Based on PCNA immunostaining, cycling cells were present only at the basal epidermal level (Figure 2B(b)). Differentiating squamous cells exhibited no staining, consistent with lack of dysplatic/neoplastic changes in the WT mouse skin.

ped/pea-15 levels during skin tumor initiation and promotion

To investigate the significance of *ped/pea-15* expression to skin tumor development and malignant progression, we have first analysed ped/pea-15 levels in papillomatous lesions and in the corresponding skin upon regression of the lesions. Despite the four-fold increase in the normal skin of $Tg_{ped/pea-15}$ *versus* control mice, ped/pea-15 was raised to comparable absolute levels in papillomas from WT and $Tg_{ped/pea-15}$ mice (Figure 3a). Immunohistochemical analysis with ped/pea-15 antibodies revealed comparable distribution of ped/pea-15 between the stromal and epithelial components of the epidermal tissues from transgenic and control mice (data not shown). After papilloma regression, there were no longer differences in ped/pea-15 levels between the skin

where the lesion had originated and the surrounding normal skin, in both the $Tg_{ped/pea-15}$ and the WT mice.

We next analysed mouse cell lines derived from DMBA/TPA-induced skin tumors at different stages of carcinogenesis (Portella *et al*., 1998). By Western blotting, ped/pea-15 protein was similarly overexpressed (almost three-fold; $P<0.001$) in both the P1 benign papilloma cells and the A5 highly anaplastic, invasive spindle carcinoma cells compared to the C5N immortalized nontumorigenic keratinocytes (Figure 3b). Thus, in the cell lines as well as *in vivo*, the increase in ped/pea-15 protein level appeared to occur at an early stage during skin carcinogenesis.

Repeated applications of the DMBA initiator on the mouse skin did not change ped/pea-15 levels either in the $Tg_{ped/pea-15}$ or in WT mice (Figure 4a). Also, transfection of the constitutively active H-*Ras61* mutant in keratinocytes showed no effect on ped/pea-15 levels (Figure 4b), indicating that *Ras* activation is not sufficient to upregulate ped/pea-15. At variance with DMBA, TPA treatment raised ped/pea-15 expression in skin cells, both in the absence and in the presence of the H-Ras61 mutant (Figure 4b). Indeed, exposure of the nontumorigenic C5N keratinocytes to 100 μg/ml TPA increased ped/pea-15 protein level in a time-dependent manner (Figure 5a). The effect achieved a plateau (five-fold increase) within 24 h and was maintained for 24 more hours, returning to baseline upon TPA withdrawal. Also, a single TPA application to the skin of both WT and $Tg_{ped/pea-15}$ mice caused a five-fold elevation of ped/pea-15 protein for up to 48 h, declining thereafter and returning to the pretreatment level by 144 h (still four-fold higher in transgenic compared to WT mice; Figure 5b). Previous studies showed that phosphorylation by both Akt/PKB and PKC increases intracellular stability of ped/pea-15 (Trencia *et al*., 2003). Based on immunoblotting with specific pSer116 and pSer104 ped/pea-15 antibodies, these increased ped/pea-15 levels in TPA-treated skin were accompanied by 2.5- and four-fold increased phosphorylation of ped/pea-15 on the Akt/PKB and PKC sites (Ser116 and Ser104, respectively). There were no differences in these phosphorylations in Wt and transgenic mice suggesting that increased ped/pea-15 stability may, at least in part, account for the effect of TPA in these animals (Figure 5c).

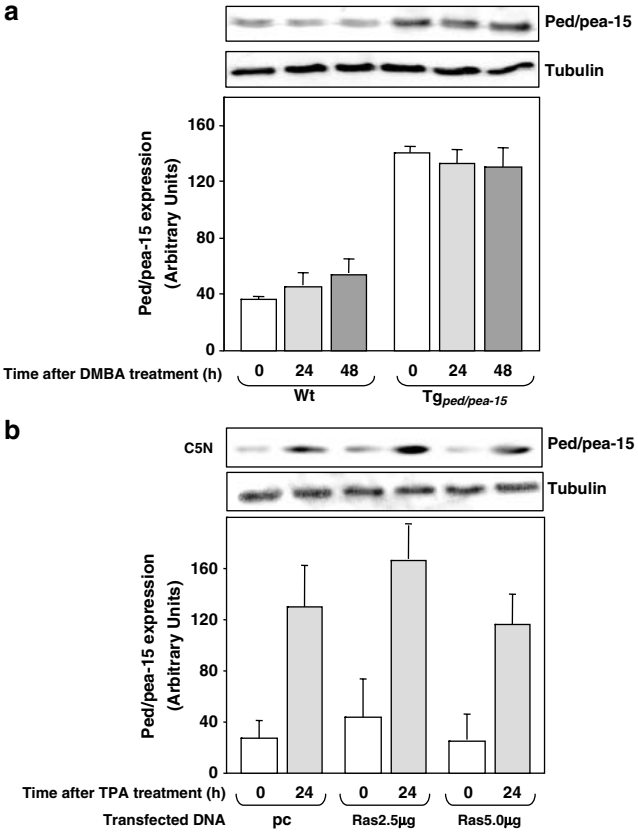

Figure 4 Effect of DMBA application and of constitutively active Ras mutant on *ped/pea-15* expression. (**a**) Mouse dorsal skin was treated by repeated DMBA applications at times 0, 6 and 12 h. ped/pea-15 and tubulin expression was determined at the indicated times upon the first application of DMBA, as described above. Bars represent the mean $\pm$ s.d. of duplicate determinations of the tubulin-normalized expression of ped/pea-15 in 2 (**a**: $n=20$ mice/time point) independent experiments. Representative blots are also shown in the insets. (**b**) The C5N cells were transfected with 2.5 or 5.0 μg of H-Ras61 or with 5.0 μg of the empty vector (pc) as described under Materials and methods. After TPA treatment, cells were lysed and cell proteins (50 μg) were Western blotted with ped/pea-15 or tubulin antibodies as indicated. Blots were revealed by ECL and autoradiography and analysed by laser densitometry. Bars represent the average (values $\pm$ s.d.) of the tubulin-normalized expression of ped/pea-15 in duplicate determinations from three independent experiments. Representative blots are also shown in the insets

Effect of ped/pea-15 on skin tissue apoptosis

To examine the consequences of *ped/pea-15* overexpression and its role in skin tumorigenesis, we compared *in vivo* apoptosis in the skin of $Tg_{ped/pea-15}$ and WT mice upon the application of TPA. Based on skin lysate determination, $Tg_{ped/pea-15}$ mice showed a significant decrease in the number of apoptotic cells compared to WT animals (Figure 6a). Importantly, TPA application to the skin of WT mice induced the appearance of the 20K fragment of the terminal caspase Caspase-3 in the lysates, evidencing Caspase-3 activation (Figure 6b). Activation of Caspase-3 by TPA was barely detectable in the skin of $Tg_{ped/pea-15}$ mice, however. Consistently, cleavage of the Caspase-3 substrate PARP was well evident upon treating WT mouse skin with TPA, but >10-fold less measurable in $Tg_{ped/pea-15}$ mice (Figure 6c).

At variance with Caspase-3, TPA treatment exhibited very little effect on the activation of the upstream caspase, Caspase-8, in both WT and $Tg_{ped/pea-15}$ mouse skin (data not shown).

In different cell types, ped/pea-15 protects the inhibitor of apoptosis XIAP from the intracellular degradation following certain apoptotic stimuli, thereby preventing Caspase-3 activation (Trencia *et al*., 2004). However, skin lysates from WT and $Tg_{ped/pea-15}$ mouse showed no difference in XIAP levels (Figure 7a),

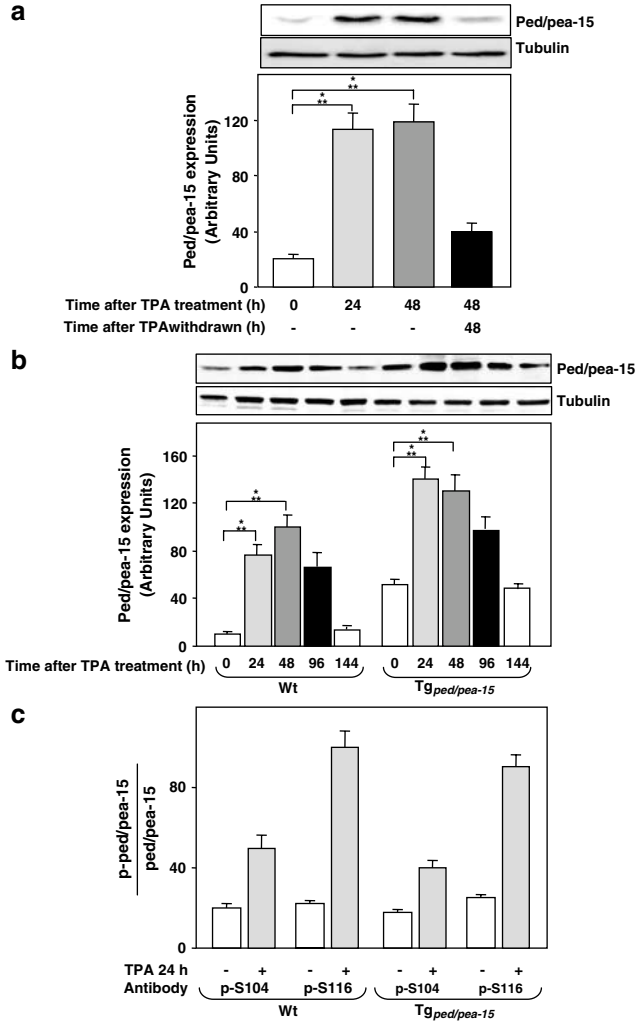

Figure 5 Effect of isolated applications of TPA on *ped/pea-15* expression and phosphorylation. C5N keratinocytes (**a**) and shaved dorsal skin of WT and Tg mice (**b**) were exposed to TPA, respectively, by addition to the culture medium (**a**) and topical application (**b**) as described under Materials and methods. Upon 48 h, TPA was removed from the cell cultures by medium replacement (**a**). At the indicated times, cells (**a**) and tissue samples (**b**) were lysed and analysed by Western blotting with ped/pea-15 and tubulin antibodies. Skin lysate filters were also reblotted with specific phosphoserine$_{104}$ and phosphoserine$_{116}$ antibodies (**c**). Blots were revealed by ECL and autoradiography and subjected to densitometric quantitation. Bars represent the mean $\pm$ s.d. of duplicate determinations of the tubulin-normalized expression of ped/pea-15 in three (**a, b**: $n = 20$ mice/time point) and two (**c**) independent experiments. Representative blots are also shown in the insets

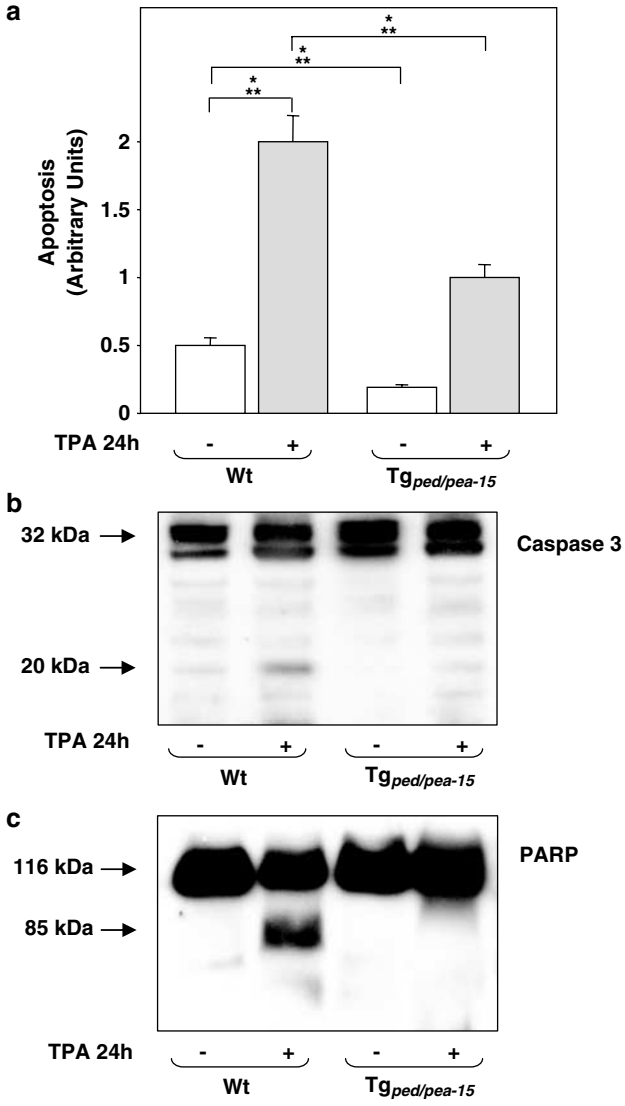

Figure 6 TPA-induced apoptosis and activation of Caspase 3 in Tg$_{ped/pea-15}$ mice. (**a**) Transgenic and control mice ($n = 30$/group; M/F ratio = 1 in each group) were subjected to TPA applications (6.25 μg of TPA in 200 μl acetone for 24 h) as described under Materials and methods. Samples of squamous stratified epithelium from the treated areas were solubilized and analysed with the ELISA^{PLUS} kit for detection of apoptosis. Bars represent the mean values ($\pm$ s.d.) of triplicate determinations in three independent experiments. (**b**) The dorsal skin of Tg$_{ped/pea-15}$ and control mice was treated with TPA as above. Samples from the treated skin were excised and analysed by Western blotting with Caspase-3 (**b**) or PARP antibodies (**c**). Blots were revealed by ECL and autoradiography. A representative autoradiography is shown; same results were obtained in three further experiments

suggesting that alternative mechanisms are responsible for the reduced apoptosis occurring in the Tg$_{ped/pea-15}$ mouse skin after TPA exposure. Indeed, previous studies in 293 cells indicated that ped/pea-15 antiapoptotic function requires ped/pea-15 simultaneous inhibition of the SAPK signaling system of JNK/p38 and activation of ERK1/2 (Condorelli *et al*., 2002). In WT mouse skin, TPA elicited a 10-fold increase in phosphorylation of the key activation sites of JNK (Thr183 and Tyr185) and those of p38 (Thr180, Thr182), indicating activation of these kinases (Figure 7b). Interestingly, the effect of TPA was five-fold reduced in Tg$_{ped/pea-15}$ mouse skin, despite normal expression of both JNK and p38. ERK1/2 phosphorylation was also constitutively increased in Tg$_{ped/pea-15}$ compared to Wt mouse skin (Figure 7c). Despite the eight-fold induction in the WT mouse, ERK phosphorylation in response to TPA showed little further increase in the transgenics, with no significant difference in ERK1/2 expression.

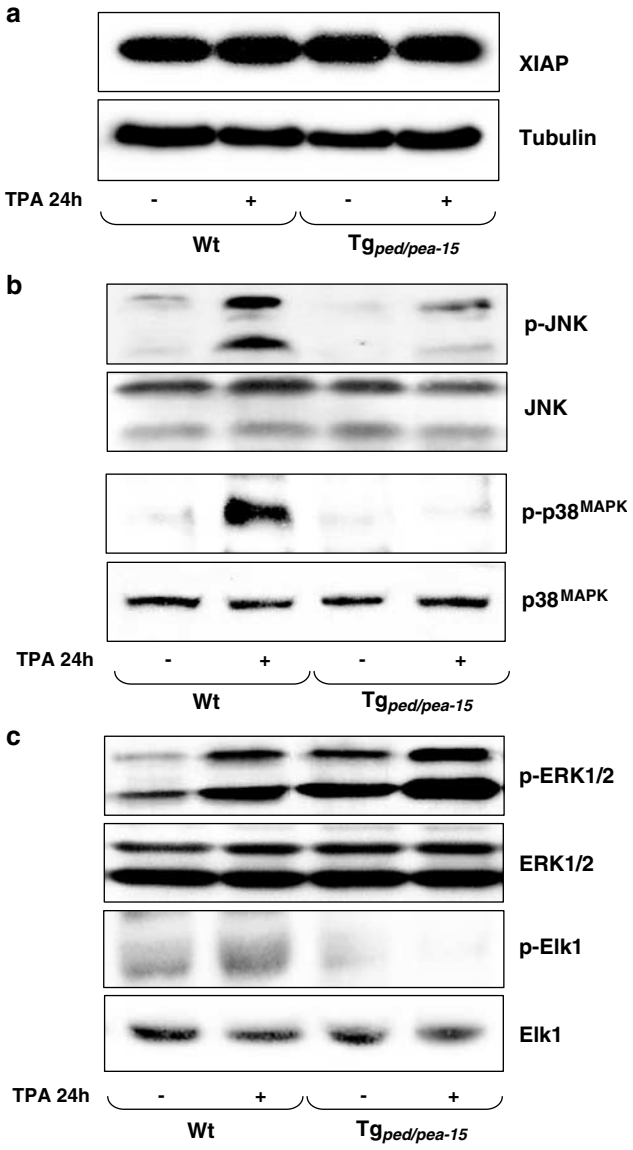

Figure 7 Effects of TPA on XIAP expression and JNK, p38, ERK1/2 and ELK1 phosphorylations. Transgenic and control mice ($n = 12$/group; M/F ratio = 1 in each group) were subjected to TPA applications (6.25 μg of TPA in 200 μl acetone for 24 h) as described under Materials and methods. Samples from the treated skin were excised and analysed by Western blotting with XIAP, tubulin (**a**), phospho-JNK, JNK, phospho-p38, p38 (**b**), phospho-ERK1/2, ERK1/2, phospho-Elk1, and Elk-1 antibodies (**c**). Blots were revealed by ECL and autoradiography. The autoradiographs shown are representative of four (**a** and **b**) and three (**c**) independent experiments

Consistent with the reported ability of ped/pea-15 to prevent nuclear migration of ERK1/2, phosphorylation of the ELK substrate in response to TPA was drastically reduced in tissues from $Tg_{ped/pea\text{-}15}$ compared to control mice. At variance with ELK, TPA phosphorylation of the H3 histone target of the ERK1/2-downstream and ped/pea-15 binding kinase RSK2 (Vaidayanathan and Ramos, 2003) showed no difference in $Tg_{ped/pea\text{-}15}$ and control mice (data not shown). Thus, at least in part, overexpression of ped/pea-15 may inhibit TPA-induced apoptosis by dysregulating selective pathways of the MAPK signaling and by inhibiting Caspase-3.

The role of caspase-3 inhibition in chemically induced skin tumorigenesis

To further address the involvement of impaired Caspase-3 activation in the increased susceptibility to skin carcinogenesis of the $Tg_{ped/pea\text{-}15}$ mice, we first compared TPA effect in the C5N nontumorigenic mouse keratinocytes and the A5 highly malignant invasive spindle carcinoma cells. Based on its own cleavage and that of the PARP substrate, TPA induction of Caspase-3 was barely detectable in the *ped/pea-15* overexpressing A5 cells, despite the evident effect occurring in the C5N keratinocytes (Figure 8a). The reduced activation of Caspase-3 in the A5 carcinoma cells was paralleled by a six-fold decrease in TPA-induced apoptosis, compared to the C5N keratinocytes (Figure 8b). We then silenced the expression of ped/pea-15 using a specific antisense cDNA (Hao *et al*., 2001). In the A5 cells, the antisense inhibited ped/pea-15 expression to levels comparable to those of the untreated C5N keratinocytes (Figure 8c). In parallel, the antisense rescued TPA apoptosis in the A5 cells, rendering the A5 as responsive to TPA as the C5N cells (Figure 8b). Caspase-3 and PARP cleavage in response to TPA was similarly rescued in antisense-transfected A5 cells (Figure 8a).

The colony growth rate in semisolid medium was also reduced in the antisense expressing A5 clones compared to cells tansfected with the empty vector (65% reduction; $P < 0.001$) (Table 1). Importantly, injection of A5 cells transfected with either the *ped/pea-15* antisense cDNA or the empty vector into athymic mice showed no significant difference in tumor incidence. However, the tumor latency period of the antisense expressing clones was almost three-fold increased compared to that of control cells ($P < 0.01$).

Discussion

There is evidence that increased expression of the antiapoptotic protein *ped/pea-15* is associated to development of malignancy (Condorelli *et al*., 1998; Ramos *et al*., 2000; Tsukamoto *et al*., 2000; Dong *et al*., 2001; Hao *et al*., 2001). However, no information is available, to date, to assess whether modulation of *ped/pea-15* expression may directly affect tumorigenesis and/or progression *in vivo*. Chemically induced skin carcinogenesis studies have provided valuable information concerning the impact of genetic alterations on multistep tumorigenesis and progression in genetically modified mice (Balmain and Harris, 2000). In the present paper, we have addressed the role of ped/pea-15 in skin tumor initiation, promotion and progression and used transgenic mice overexpressing the *ped/pea-15* gene. These mice express three- to four-fold higher skin levels of *ped/pea-15* compared to their nontransgenic littermates. We now report that, in parallel with the increased *ped/pea-15* expression, the transgenics show

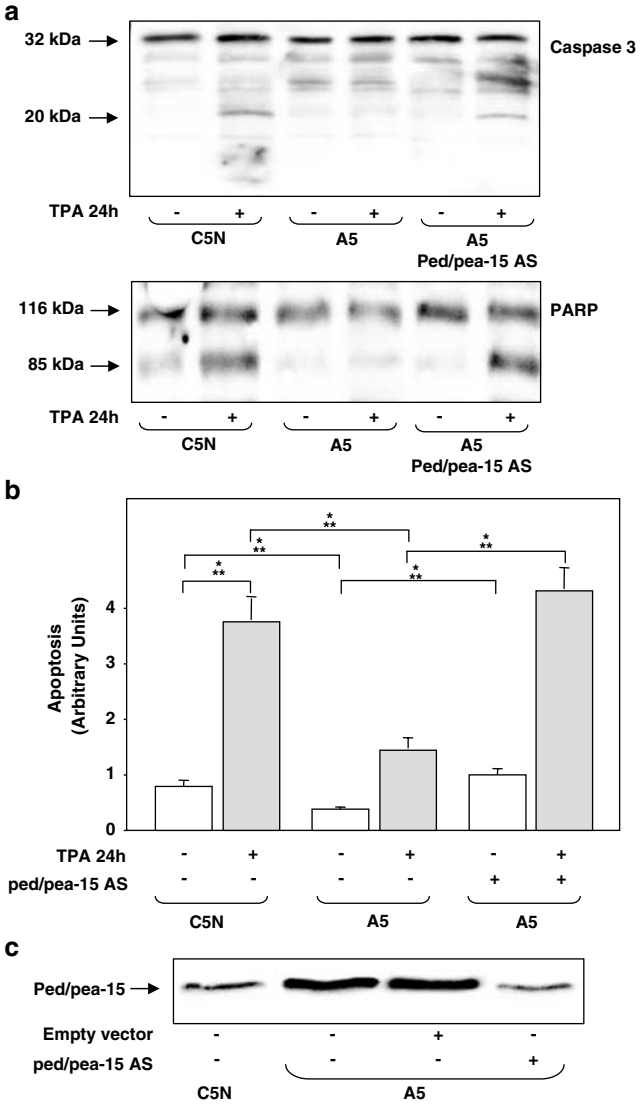

Figure 8 Effect of ped/pea-15 silencing on TPA apoptosis in C5N and A5 cells. (**a**) C5N and A5 cells stably transfected with ped/pea-15 antisense cDNA were obtained as described under Materials and methods. Antisense-expressing and control cells were exposed to TPA for 24 h and then solubilized. Cell lysates (50 μg per point) were then analysed by Western blotting with Caspase-3 or PARP antibodies, as indicated. The effect of the antisense on *ped/pea-15* expression was controlled in the same cell lysates by Western blotting with ped/pea-15 antibodies as described in the legend to Figure 3(c). Filters were revealed by ECL and autoradiography. The autoradiographs shown are representative of three independent experiments. Alternatively (**b**), TPA-stimulated cells were solubilized and analysed with the ELISA^{PLUS} kit for detection of apoptosis as described under Materials and methods. Bars represent the mean values ($\pm$s.d.) of triplicate determinations in three independent experiments

anticipated as well as increased occurrence of benign papillomatous lesions upon being topically treated with the tumor initiator DMBA followed by repeated applications of the tumor promoter TPA. Interestingly, *ped/pea-15* expression is also increased in papillomas from WT mice, compared to the adjacent normal skin. The significance of the increased ped/pea-15 levels to skin tumorigenesis is further strengthened by the finding that, upon papilloma regression, ped/pea-15 returns to basal levels in the skin where the lesions have been produced. In addition, the malignant conversion frequency of the papillomatous lesion was significantly higher in *ped/pea-15* transgenic compared to the control animals. These results indicate, for the first time, that increased levels of ped/pea-15 confer greater susceptibility to skin carcinogenesis *in vivo* and may enhance cutaneous tumor progression toward malignancy. Indeed, after suspension of TPA treatment, the transgenic mice maintain stably elevated ped/pea-15 levels compared to the WT animals where the effect of TPA vanishes.

We show that the constitutively active H-*Ras61* mutant does not affect *ped/pea-15* expression levels in keratinocytes. Consistently, DMBA application did not upregulate *ped/pea-15* in mouse skin, indicating that *Ras* mutation is not sufficient to cause *ped/pea-15* overexpression. At variance, treatment with TPA alone rapidly increased *ped/pea-15* expression levels in the skin of both transgenic and control mice, suggesting that ped/pea-15 overexpression represents an early event during cutaneous tumor promotion, though not initiation. At least in part, the effect of TPA may be mediated by induction of PKB/Akt and PKC. Indeed, (i) phosphorylation of ped/pea-15 on PKB/Akt and PKC sites is increased in TPA-treated skin; and (ii) previous studies (Trencia *et al*., 2003) demonstrated that phosphorylation of these sites increases cellular stability of ped/pea-15. In addition, transformed cell lines derived from DMBA/TPA-induced skin tumors consistently show higher ped/pea-15 levels compared to immortalized nontumorigenic keratinocytes. It is conceivable, therefore, that higher *ped/pea-15* levels may confer a distinctive advantage to the cells upon DMBA initiation, leading to selection of those overexpressing ped/pea-15.

Transgenic mice overexpressing *ped/pea-15* feature insulin-resistance and decreased glucose tolerance (Vigliotta *et al*., 2004). Considerable epidemiological evidence exists indicating that these metabolic abnormalities have a role in determining the occurrence of a

Table 1 Analysis of transformation markers of A5 carcinoma cells

Transfected DNA/caspase inhibitor	*Colony-forming efficiency (%)*[a]	*Tumor incidence*[b]	*Latency period (days)*[c]
—	58	5/5	14
pcDNA vector	56	6/6	14
pcDNA AS	20	6/6	39
Z-DEVD-FMK	14	—	—

[a]Colonies larger than 64 cells were scored after 3 weeks. Colony-forming efficiency was calculated by dividing the number of colonies formed by the number of plated cells $\times 100$. [b]Tumorigenicity was assayed by injecting 1×10^6 cells into 6-week-old athymic mice. [C]The animals were monitored for the appearance of tumors. The mean tumor latency is the time needed for tumors to reach 10 mm in diameter. The tumor latency of the antisense (AS)-transfected cells differed significantly from controls ($P<0.001$)

number of tumors in humans (Calle and Kaaks, 2004). Transgenic mice overexpressing *ped/pea-15* show no greater prevalence of spontaneous tumors, but whether insulin-resistance and/or impaired glucose tolerance contribute to the increased susceptibility to skin carcinogenesis cannot be concluded from the present study. Different mechanisms likely play a greater role, however, as TPA-induced upregulation of *ped/pea-15* also accompanies skin tumor development in nontransgenic mice featuring normal insulin sensitivity and glucose tolerance.

ped/pea-15 performs a broad antiapoptotic action in cultured cells (Condorelli *et al*., 1999, 2002; Kitsberg *et al*., 1999; Hao *et al*., 2001; Trencia *et al*., 2004). At least in part, ped/pea-15 antiapoptotic action is due to inhibition of the induction of the terminal caspase, Caspase-3 (Hao *et al*., 2001; Condorelli *et al*., 2002). In this paper, we show that TPA-induced apoptosis in squamous stratified epithelium *in vivo* is also significantly inhibited in *ped/pea-15* transgenic mice. This decrease is accompanied by reduced activation of Caspase-3 and cleavage of the Caspase-3 substrate PARP in response to TPA. Reduced apoptosis and Caspase-3 activation in response to TPA also occur in the A5 cells, which are derived from DMBA/TPA-induced spindle cell carcinomas and overexpress ped/pea-15. Consistently, in the normal C5N keratinocytes that express lower levels of endogenous *ped/pea-15*, transfection of *ped/pea-15* cDNA and treatment with the specific Caspase-3 inhibitor Z-DEVD-FMK prevented TPA apoptosis in a nonadditive manner (data not shown). Expression of a specific ped/pea-15 antisense cDNA in the A5 cells simultaneously reduced ped/pea-15 levels and rescued TPA-induced apoptosis and Caspase-3 activation. Importantly, the antisense significantly increased the latency preceding tumor formation upon A5 cell injection in nude mice. The A5 cell growth in semisolid medium was also significantly reduced by decreasing *ped/pea-15* expression. Thus, the impaired apotosis determined by inhibition of Caspase-3 activity in *ped/pea-15* overexpressing skin cells might affect the malignant progression as well as tumorigenesis.

Previous studies by other investigators and by us have shown that ped/pea-15 may inhibit Caspase-3 function by preventing the activation of Caspase-8 (Condorelli *et al*., 1999; Kitsberg *et al*., 1999) as well as by increasing stability of the inhibitor of apoptosis protein XIAP (Trencia *et al*., 2004). These events do not account for ped/pea-15 inhibition of Caspase-3 in TPA-treated skin, as *ped/pea-15* overexpression does not affect TPA action on either Caspase-8 function or XIAP levels. In certain cell types, block of the JNK and p38 members of the MAPK family also plays an important role in mediating the ped/pea-15 protection from apoptosis (Condorelli *et al*., 2002), which may lead to Caspase-3 inhibition (Kamata *et al*., 2005). Full antiapoptotic function in these cells requires concomitant *ped/pea-15* induction of the ERK1/2 MAPKs and/or ERK1/2 anchoring into the cytoplasm (Formstecher *et al*., 2001; Condorelli *et al*., 2002). Impaired JNK and p38 activation and increased ERK1/2 cytoplasmic activity have also been detected in the skin of $Tg_{ped/pea-15}$ mice upon exposure to TPA, indicating they may mediate the decreased susceptibility to apoptosis caused by overexpression of *ped/pea-15* in these cells. Indeed, same as in other cell types (Condorelli *et al*., 2002), in the A5, the rescue of JNK function by overexpression of the upstream kinase MKK6 significantly enhanced the apoptotic response to TPA (data not shown).

Intriguingly, Gaumont-Leclerc *et al*. (2004) have very recently reported evidence that *ped/pea-15* may exert a tumor suppressor function in the IMR90 fibroblasts. It is possible that this function is also exerted in the mouse keratinocyte model. Upon DMBA/TPA exposure of these cells, the antiapoptotic function of ped/pea-15 seems to prevail, however. Consistently, ped/pea-15 overexpression confers raised susceptibility to chemical carcinogenesis in the skin. Thus, different settings may lead ped/pea-15 to have its pro- or antioncogenic functions overriding.

Deregulated apoptosis has been suggested to play an important role in tumorigenesis and malignant progression of transformed cells by contributing the cells with the capability to skip cell death programs, accumulating DNA damage (Debatin and Krammer, 2004). In certain tumors, these abnormalities may occur because of loss of proapoptotic molecules such as Bax, Apaf-1 or Caspase-8 (Harada and Grant, 2003; Baldi *et al*., 2004). In other situations, impaired apoptosis has been associated to increased expression of antiapoptotic molecules of the Bcl-2 family (Harada and Grant, 2003). In this paper, we have shown that increased expression levels of the antiapoptotic protein ped/pea-15 may also determine susceptibility to skin tumorigenesis and tumor progression by inhibiting Caspase-3-dependent apoptosis in DMBA/TPA-treated mice. Several alterations occurring in these chemically induced mouse skin tumors have also been observed in the homologous cutaneous tumors in humans (Balmain and Harris, 2000). ped/pea-15 might represent a novel target for cutaneous cancer treatment and prevention.

Materials and methods

Transgenic ped/pea-15 *mice*

The C57BL/6JxDBA/2J *ped/pea-15* transgenic mice were described in Vigliotta *et al*. (2004). The animals were maintained in the animal facility at the Dipartimento di Biologia e Patologia Cellulare e Molecolare, Federico II University of Naples. Experiments involving animals were conducted in accordance with accepted standards of animal care and the Italian regulations for the welfare of animals. The study protocol was approved by the Institutional Committee on Animal Care of the University of Naples.

Two-stage skin carcinogenesis

The dorsal skin of 8-week-old mice were shaved, and, 2 days later, a single dose of 50 μg of 7,12-dimethylbenz[a]anthracene (DMBA) in 200 μl of acetone was applied. At 1 week after initiation, the mice were treated with 6.25 μg of 12-*O*-tetradecanoylphorbol-13-acetate (TPA) in 200 μl of acetone

twice a week for 15 weeks. The number of papillomas detected by palpation was recorded once a week.

At 1 week after termination of TPA treatment, mice were killed, and skin tissues snap frozen in liquid nitrogen and/or fixed in freshly prepared 4% paraformaldehyde followed by paraffin embedding. Mice were maintained for 35 additional weeks after TPA discontinuation, and tumor progression was investigated. Tumors were scored as papillomas or carcinomas by histological analysis after H&E staining of paraffin sections.

Histology

Tissues were fixed in formalin, dehydrated, blocked in paraffin and sectioned at 6 μm. The tissue sections were stained with hematoxylin and eosin. A total of 76 nonmalignant papillomas and all malignant tumors were examined. Malignant skin tumors were densely cellular spindle cell tumors in the dermis underlying the papilloma, often exhibiting invasion through skeletal muscle and sometimes associated with lymph node metastasis. Premalignant lesions were squamous cells showing atypia (enlarged nuclei, mitotic activity) but not associated with spindle cell proliferation, invasion and metastasis.

Cell culture and growth, transfection and Western blot analysis

The C5N, P1 and A5 cells have been previously described (Portella *et al*., 1998) and were kindly provided by Dr A Balmain (University of California, San Francisco, Comprehensive Cancer Center, USA). Cells were cultured in DMEM supplemented with 10% foetal calf serum, 10 000 U/ml penicillin, 10 000 μg/ml streptomycin and 2% L-glutamine in a humidified CO_2 incubator as described in Portella *et al*. (1998). Transfection of the constitutively active H-Ras61 in C5N cells, tissue collection and Western blots were performed as described in Vigliotta *et al*. (2004). The pcDNA-*ped/pea-15* antisense construct has been previously described (Hao *et al*., 2001). Clones expressing the antisense were selected as in Hao *et al*. (2001). Soft agar colony assays were performed according to a previously described technique (Macpherson and Montagnier, 1964). The antibodies used include ped/pea-15 antibodies (Vigliotta *et al*., 2004), phosphoserine$_{104}$ped/pea-15 and phosphoserine$_{116}$ped/pea-15 antibodies (Trencia *et al*., 2004), tubulin, caspase-3, XIAP and PARP antibodies (Santa Cruz Biotechnology, CA, USA).

Detection of apoptosis

Animals were subjected to topical applications of acetone-dissolved TPA (6.25 μg) or DMBA (50 μg) or acetone alone, as indicated. The animals were killed, skin tissues were removed and then solubilized as in Vigliotta *et al*. (2004) and processed for the apoptosis assay using the Cell Death Detection ELISA^{PLUS} Kit (Roche Diagnostics GmbH, Mannheim, Germany), according to the manufacturer instructions. For studies in isolated cells, apoptosis was investigated as previously described (Trencia *et al*., 2004).

Tumorigenicity assay

Experiments were performed in 6-week old male athymic mice (Charles River, Italy). A5 cells (1×10^6), either transfected with the *ped/pea-15* antisense cDNA or not, were injected into the right flank of the mice. The animals were monitored for the appearance of tumors and tumor latency was evaluated. The mean tumor latency is the time needed for tumors to reach 10 mm in diameter. All mice were maintained at the animal facility of the Dipartimento di Biologia e Patologia Cellulare e Molecolare of the Federico II University of Naples.

Densitometry and statistical analysis

Densitometric analysis was performed using a Scion Image Analyser. All the data were expressed as mean$\pm$s.d. Significance was assessed by Student's *t*-test for comparison between two means.

Acknowledgements
We thank Dr A Balmain for kindly providing C5N, P1 and A5 cells and Dr S Linardopoulos for critical reading of the manuscript. The technical help of Maria Russo, Salvatore Sequino and Dr Antonio Baiano is also acknowledged. This work was supported by the European Community's FP6 EUGENE2 (LSHM-CT-2004-512013), grants from the Associazione Italiana per la Ricerca sul Cancro (AIRC) to FB and PF, and the Ministero dell'Università e della Ricerca Scientifica (PRIN to FB, GiPo and PF and FIRB RBNE0155LB to FB). The financial support of Telethon – Italy is gratefully acknowledged.

References

Araujo H, Danziger N, Cordier J, Glowinski J and Chneiweiss H. (1993). *J. Biol. Chem.*, **268,** 5911–5920.

Baldi A, Santini D, Russo P, Catricala C, Amantea A, Picardo M, Tatangelo F, Botti G, Dragonetti E, Murace R, Tonini G, Natali PG, Baldi F and Paggi MG. (2004). *Exp. Dermatol.*, **13,** 93–97.

Balmain A and Harris CC. (2000). *Carcinogenesis*, **21,** 371–377.

Burns FJ, Vanderlaan M, Snyder E and Albert RE. (1978). *Carcinogenesis, Mechanisms of Tumour Promotion and Co-Carcinogenesis* Slaga TJ and Boutwell RK (eds). Raven Press, Ltd: New York.

Calle EE and Kaaks R. (2004). *Nat. Rev. Cancer*, **4,** 579–591.

Condorelli G, Trencia A, Vigliotta G, Perfetti A, Goglia U, Cassese A, Musti AM, Miele C, Santopietro S, Formisano P and Beguinot F. (2002). *J. Biol. Chem.*, **277,** 11013–11018.

Condorelli G, Vigliotta G, Iavarone C, Caruso M, Tocchetti CG, Andreozzi F, Cafieri A, Tecce MF, Formisano P, Beguinot L and Beguinot F. (1998). *EMBO J.*, **17,** 3858–3865.

Condorelli G, Vigliotta G, Cafieri A, Trencia A, Andalo P, Oriente F, Miele C, Caruso M, Formisano P and Beguinot F. (1999). *Oncogene*, **18,** 4409–4415.

Debatin KM and Krammer PH. (2004). *Oncogene*, **23,** 2950–2966.

Dong G, Loukinova E, Chen Z, Gangi L, Chanturita TI, Liu ET and Van Waes C. (2001). *Cancer Res.*, **61,** 4797–4808.

Formstecher E, Ramos JW, Fauquet M, Calderwood DA, Hsieh JC, Canton B, Nguyen XT, Barnier JV, Camonis J, Ginsberg MH and Chneiweiss H. (2001). *Dev. Cell.*, **2,** 239–250.

Gaumont-Leclerc MF, Mukhopadhyay UK, Goumard S and Ferbeyre G. (2004). *J. Biol. Chem.*, **279,** 46802–46809.

Hao C, Beguinot F, Condorelli G, Trencia A, Van Meir EG, Yong VW, Parney IF, Roa WH and Petruk KC. (2001). *Cancer Res.*, **61,** 1162–1170.

Harada H and Grant S. (2003). *Rev. Clin. Exp. Hematol.*, **7,** 117–138.

Kamata H, Honda S, Maeda S, Chang L, Hirata H and Karin M. (2005). *Cell*, **120,** 649–661.

Kitsberg D, Formstecher E, Fauquet M, Kubes M, Cordier J, Canton B, Pan G, Rolli M, Glowinski J and Chneiweiss H. (1999). *J. Neurosci.*, **19,** 8244–8251.

Macpherson I and Montagnier L. (1964). *Virology*, **23,** 291–294.

Portella G, Cumming SA, Liddell J, Cui W, Ireland H, Akhurst RJ and Balmain A. (1998). *Cell Growth Differ.*, **9,** 393–404.

Ramos JW, Hughes PE, Renshaw MW, Schwartz MA, Formstecher E, Chneiweiss H and Ginsberg MH. (2000). *Mol. Biol. Cell*, **11,** 2863–2872.

Trencia A, Fiory F, Maitan MA, Vito P, Barbagallo AP, Perfetti A, Miele C, Ungaro P, Oriente F, Cilenti L, Zervos AS, Formisano P and Beguinot F. (2004). *J. Biol. Chem.*, **279,** 46566–46572.

Trencia A, Perfetti A, Cassese A, Vigliotta G, Miele C, Oriente F, Santopietro S, Giacco F, Condorelli G, Formisano P and Beguinot F. (2003). *Mol. Biol. Cell*, **23,** 4511–4521.

Tsukamoto T, Yoo J, Hwang SI, Guzman RC, Hirokawa Y, Chou YC, Olatunde S, Huang T, Bera TK, Yang J and Nandi S. (2000). *Cancer Lett.*, **149,** 105–113.

Vaidayanathan H and Ramos WJ. (2003). *J. Biol. Chem.*, **278,** 32367–32372.

Vigliotta G, Miele C, Santopietro S, Portella G, Perfetti A, Maitan MA, Cassese A, Oriente F, Trencia A, Fiory F, Romano C, Tiveron C, Tatangelo L, Troncone G, Formisano P and Beguinot F. (2004). *Mol. Cell. Biol.*, **24,** 5005–5015.

Diabetologia (2006) 49:3058–3066
DOI 10.1007/s00125-006-0455-5

ARTICLE

The *PEA15* gene is overexpressed and related to insulin resistance in healthy first-degree relatives of patients with type 2 diabetes

R. Valentino · G. A. Lupoli · G. A. Raciti · F. Oriente · E. Farinaro · E. Della Valle · M. Salomone · G. Riccardi · O. Vaccaro · G. Donnarumma · G. Sesti · M. L. Hribal · M. Cardellini · C. Miele · P. Formisano · F. Beguinot

Received: 2 June 2006 / Accepted: 27 July 2006 / Published online: 5 October 2006

Abstract
Aims/hypothesis Overexpression of the gene encoding phosphoprotein enriched in astrocytes 15 (PEA15), also known as phosphoprotein enriched in diabetes (PED), causes insulin resistance and diabetes in transgenic mice and has been observed in type 2 diabetic individuals. The aim of this study was to investigate whether *PEA15* overexpression occurs in individuals at high risk of diabetes and whether it is associated with specific type 2 diabetes subphenotypes.
Subjects and methods We analysed *PEA15* expression in euglycaemic first-degree relatives (FDR) of type 2 diabetic subjects.
Results The expression of *PEA15* in peripheral blood leucocytes (PBLs) paralleled that in fat and skeletal muscle tissues. In PBLs from the FDR, PEA15 expression was two-fold higher than in euglycaemic individuals with no family history of diabetes (control subjects), both at the protein and the mRNA level ($p<0.001$). The expression of *PEA15* was comparable in FDR and type 2 diabetic subjects and in each group close to one-third of the subjects expressed *PEA15* levels more than 2 SD higher than the mean of control subjects. Subjects with IFG with at least one type 2 diabetes-affected FDR also overexpressed *PEA15* ($p<0.05$). In all the groups analysed, *PEA15* expression was independent of sex and unrelated to age, BMI, waist circumference, systolic and diastolic BP, and fasting cholesterol, triacylglycerol and glucose levels. However, in euglycaemic FDR of type 2 diabetic subjects, *PEA15* expression was inversely correlated with insulin sensitivity ($r=-557$, $p=0.01$).
Conclusions/interpretation We conclude that *PEA15* overexpression represents a common defect in FDR of patients with type 2 diabetes and is correlated with reduced insulin sensitivity in these individuals.

Keywords Insulin resistance · *PED* · *PEA15* · Type 2 diabetes

R. Valentino · G. A. Lupoli · G. A. Raciti · F. Oriente · C. Miele · P. Formisano · F. Beguinot (✉)
Department of Cellular and Molecular Biology and Pathology 'L. Califano' and C.N.R. Institute of Experimental Endocrinology and Oncology 'G. Salvatore', University of Naples 'Federico II', Via Sergio Pansini, 5,
Naples 80131, Italy
e-mail: beguino@unina.it

E. Farinaro · E. Della Valle · M. Salomone
Occupational Medicine Section,
Department of Preventive Medical Sciences,
Naples, Italy

G. Riccardi · O. Vaccaro · G. Donnarumma
Department of Experimental and Clinical Medicine,
University of Naples 'Federico II',
Naples, Italy

G. Sesti · M. L. Hribal · M. Cardellini
Department of Experimental and Clinical Medicine,
University of Catanzaro 'Magna Graecia',
Naples, Italy

Abbreviations

ERK	extracellular-regulated kinase
EUGENE	European Network on Functional Genomics of Type 2 Diabetes
FDR	first-degree relatives
PBL	peripheral blood leucocyte

PEA15	phosphoprotein enriched in diabetes/phosphoprotein enriched in astrocytes
PKC	protein kinase C
PLD1	phospholipase D1

Introduction

Phosphoprotein enriched in astrocytes 15 (PEA15), also known as phosphoprotein enriched in diabetes (PED) is a small scaffold protein widely produced in different tissues and highly conserved among mammals [1–3], whose gene (*PEA15*) maps on human chromosome 1q21–22 [4]. Several studies in cultured cells and in rodent tissues have revealed that *Pea15* regulates multiple cellular functions by binding components of major intracellular transduction pathways. PEA15 activates extracellular-regulated kinase (ERK) 1/2 [3, 5]. It binds ERKs in the nucleus, exporting them into the cytoplasm, thus preventing cell cycle entry caused by sustained phospho-ERK nuclear accumulation [5, 6]. PEA15 also interacts with protein kinase B (Akt/PKB) and p90 ribosomal S6 kinase isozyme (RSK2), two key components of the phosphoinositide 3-kinase (PI3-K) and ERK signalling pathways, whose activation is central to control of cell survival [7, 8]. In addition, PEA15 exerts a wide anti-apoptotic action. It binds Fas-associated death domain (FADD) and caspase-8, thereby protecting against cytokine-induced apoptosis [9–11]. PEA15 also binds to Omi/HtrA2 to inhibit apoptosis triggered by stress and physical agents [12]. Importantly, there is evidence indicating that PEA15 anti-apoptotic action has an important role in the development and progression of certain cancers in humans as well as in rodents [13–15].

Recent reports further revealed that PEA15 binds to and enhances phospholipase D stability, resulting in increased intracellular levels of diacylglycerol [16, 17]. This effect deregulates protein kinase C (PKC) signalling and generates resistance to insulin action on glucose transport in muscle and adipose cells and in tissues from transgenic mice overexpressing the *Pea15* gene [17, 18]. Inhibited glucose-regulated insulin secretion has also been reported in these animals, contributing to their impaired glucose tolerance. The *Pea15* transgenic mice develop diabetes upon weight gain, indicating an important interaction between obesity and the *Pea15* gene [18].

Earlier findings in humans evidenced that the *PEA15* gene is overexpressed in skeletal muscle and fat tissues as well as in cultured skin fibroblasts from individuals with type 2 diabetes, and this effect occurs independently of obesity, suggesting that it may be a primary component of insulin resistance in these subjects [4]. Whether *PEA15* overexpression is also detectable in more easily accessible cells, such as peripheral blood leucocytes, and whether it represents a common abnormality in type 2 diabetes is unknown. Whether the overexpression occurs in individuals at high risk of diabetes, whether it associates with diabetes risk factors other than obesity, and whether it relates to specific type 2 diabetes phenotypes also remains to be determined. The aim of the present work was to investigate these issues in first-degree relatives of type 2 diabetic individuals.

Subjects and methods

Subjects The subjects investigated in the present study were recruited consecutively at the outpatient facilities of the Department of Preventive Medical Sciences (DSMP), the Metabolic Unit (DMCS) at the University of Naples Federico II Medical School and the Metabolic Unit at the University of Catanzaro 'Magna Graecia' (offspring from the European Network on Functional Genomics of Type 2 Diabetes [EUGENE2] study). Written informed consent was obtained from all participants. The study protocol was approved by the ethics committees of the participating institutions and conducted in accordance to the principles of the Declaration of Helsinki as revised in 2000. The euglycaemic individuals (n=150) were healthy employees of the Campania Region who were not receiving pharmacological treatment, and were undergoing a routine health survey at the DSMP. The presence of type 2 diabetes-affected first-degree relatives (FDR) was ascertained through a written questionnaire and further verified through the medical history. The average number of relatives with type 2 diabetes in the subgroup of FDR was 1.1. The type 2 diabetic patients (n=142) were recruited at the DMCS. Of these individuals, 19% were treated with diet alone, 48% with sulfonylureas and/or metformin, 30% with insulin alone, and 3% with insulin and oral hypoglycaemic agents. The mean diabetes duration was 11±9 years. The mean HbA_{1c} level of the diabetic patients was 7.0±1.0%. Of the diabetic patients, 48% showed no evidence of long-term complications; 24% had microvascular and 12% had macrovascular complications; 16% had both microvascular and macrovascular complications. Anthropometric indexes (BMI was calculated by dividing the weight in kilograms by the square of the height in metres; waist circumference was measured midway between the lowest rib margin and the iliac crest to the nearest 0.5 cm) and detailed medical history (including information on type 2 diabetes-affected relatives and smoking habit) were obtained from all of the participants through identical procedures at each participating institution. Blood pressure values were measured in the left arm of the supine patient, after 5 min of quiet rest, with a mercury sphygmomanometer. For each subject, whole-

blood samples were drawn from an antecubital vein in the morning after an overnight fast on two separate occasions. Plasma glucose, total cholesterol, HDL cholesterol, triacylglycerol and serum insulin levels were determined in a centralised facility as described previously [19, 20]. Diagnoses of type 2 diabetes and IFG were established according to criteria listed previously [21]. For studies in matched groups (n=115) further individuals were recruited at the DSMP. Inclusion criteria in this arm of the study were as follows: age 52–58 years, BMI 26–32 kg/m^2, waist circumference 90–100 cm, systolic BP 120–140 mmHg, diastolic BP 70–85 mmHg, total cholesterol 4.9–5.4 mmol/l, HDL cholesterol 1.2–1.4 mmol/l, serum triacylglycerol 1.4–1.6 mmol/l. Fifty-six type 2 diabetic individuals (mean disease duration 11±4 years, mean HbA_{1c} level 7.2±4.0%) and 59 healthy euglycaemic subjects (of which 34 had no family history of type 2 diabetes and 25 had at least one type 2 diabetes-affected FDR) were consecutively enrolled. Studies in euglycaemic offspring of type 2 diabetic patients were performed using the EUGENE2 cohort http://www.eugene2.com, last accessed in August 2006; [20, 22, 23] at the University of Catanzaro Magna Graecia. The clinical characterisation of these individuals has been previously reported [20, 22, 23]. The OGTT and euglycaemic–hyperinsulinaemic clamp procedures have also been previously reported [20]. Briefly, for clamp studies, insulin (Humulin; Eli Lilly, Indianapolis, IN, USA) was given as a prime continuous infusion to produce plasma insulin levels of ~420 pmol/l. Thereafter, the insulin infusion rate was fixed at 40 mU m^{-2} min^{-1}. Blood glucose was maintained at a constant level throughout the study by infusing 20% glucose at varying rates according to blood glucose measurements performed at 5-min intervals. Lean body mass was assessed by bioimpedence. Duration of the clamp was 120 min. Glucose disposal is expressed as milligrams per kilogram of lean body per mass per minute. Insulin secretion was estimated by the homeostasis model assessment of pancreatic beta cell function (HOMA-B) index [24] and the insulinogenic index as the difference between the 30- and 0-min OGTT plasma insulin values divided by the difference between the corresponding plasma glucose values, ($\Delta I_{30}/\Delta G_{30}$), as described previously [25].

Separation of white blood cells and tissue sampling For peripheral blood leucocyte (PBL) separation, EDTA-treated whole-blood samples were first centrifuged at 300 ×g for 10 min and the plasma removed. PBLs were separated using a 6% dextran gradient in filtered PBS, pH 7.4, as previously described [26], washed in PBS three times, counted and resuspended in 1 ml of PBS for subsequent use. Neutrophils and other major leucocyte subpopulations were further separated as previously described [26, 27]. The purity of the different cell populations was confirmed by microscopic examination. Subcutaneous adipose tissue from the anterior abdominal wall and skeletal muscle (rectus abdominis) biopsies were obtained simultaneously from patients undergoing elective abdominal surgery for gall bladder disease. For this part of the study, the diabetic patients and the euglycaemic subjects (with and without type 2 diabetic FDR in their pedigree) were consecutively recruited to achieve a 1:1:1 ratio between the three groups (total n=21). Tissues were rinsed and dissected free of erythrocytes and connective tissues, as previously described [28]. PBLs were collected at the same time as fat and muscle specimens.

Cell and tissue harvesting and western blotting PBL and tissue samples were solubilised at 4°C in TAT buffer (50 mmol/l HEPES, pH 7.5, 150 mmol/l NaCl, 10 mmol/l EDTA, 10 mmol/l $Na_4P_2O_7$, 2 mmol/l Na_3VO_4, 100 mmol/l NaF, 10% glycerol, 1% Triton X-100) supplemented with 1 mmol/l phenylmethanesulfonylfluoride and 10 μg/ml aprotinin, as described previously [28]. Lysates were centrifuged at 500 ×g for 20 min and supernatant fractions were frozen at −20°C until used. For Western blotting, 50 μg of lysate proteins were heated at 100°C in Laemmli buffer [29]. Proteins were separated by 15% SDS-PAGE and then transferred to 0.45-mm Immobilon-P membranes (Millipore, Bedford, MA, USA). Filters were probed with phospholipase D1 (PLD1) (BioSource International, Camarillo, CA, USA) or PEA15 antibodies [4], revealed by enhanced chemiluminescence and autoradiography, and PEA15 bands were quantitated by laser densitometry. Inter-assay variation was <15%.

RNA samples and real-time RT-PCR RNA from white blood cells were immediately extracted following cell isolation using the QIAamp RNA Blood Mini Kit (Qiagen, Valencia, CA, USA) according to the manufacturer's instructions. *PEA15* gene expression was measured by real-time RT-PCR (SYBRGreen with iCycler IQ Multicolor Real-Time Detection System, Biorad, Richmond, VA, USA). The following primer pairs were designed using the Beacon Designer Software (Biorad) based on published gene sequences (GeneBank Accession nos. AH008227 and M10277, respectively). Human hped1 (forward) 5′-GAGCGCTCAGCTCCAGAGG-3′; human hped3 (reverse) 5′-CAGGACGGCGGGAGATCT-3′; human β-actin (forward) 5′-TGCGTGACATTAAGGAGAAG-3′; human β-actin (reverse) 5′-GCTCGTAGCTCTTCTCCA-3′. Real-time RT-PCR was performed with a cDNA input of 50 ng total RNA with all combinations of primers. Data acquisition and analysis were automatically performed by the iCycler IQ Multicolour Real-Time Detection System Optical System Software, version 3.1 (Biorad). Primers for real-time detection of *PLD1* were as follows. Human PLD1

(forward) 5′-TGGGACCAAAGGGCATAGAAGG-3′ human PLD1 (reverse) 5′-TACCAGCAGGACGAAGG CAATG-3′.

Statistical analysis Data are means±SEM. Comparisons between groups were tested by the unpaired Student's *t* test or the Mann–Whitney *U* test, and among groups by ANOVA. Mean values, after adjusting for covariates, were evaluated by ANCOVA. A p value of < 0.05 was considered significant. Analyses were performed using the statistical package SPSS, version 12 (SPSS, Chicago, IL, USA).

Results

To identify tissues for which *PEA15* expression can be non-invasively quantified in a large number of subjects, we first analysed lysates from PBLs by immunoblotting with specific PEA15 antibodies [4]. In samples from 21 subjects (seven with type 2 diabetes, seven euglycaemic subjects with diabetic FDR [EuF+], and seven euglycaemic subjects with no family history of diabetes [EuF−]), these assays revealed the expression of PEA15, with no significant differences between the granulocyte, lymphocyte and monocyte cells (Fig. 1a). On a per-mg-protein basis, PEA15 levels in these cells were 30% higher than those in human skeletal muscle and adipose tissues ($p<0.001$). Importantly, in these same subjects, there were significant correlations between PEA15 levels in the PBLs and those in fat and in skeletal muscle tissues ($p<0.001$; Fig. 1a,b).

We then compared the levels of PEA15 in PBL lysates from 30 EuF+ individuals (these subjects are known to be at increased risk of diabetes [30, 31]) with those in PBL lysates from 120 EuF− subjects. Their clinical characteristics are shown in Table 1. A two-fold increase in PEA15 levels was found in the EuF+ subjects ($p<0.001$; Fig. 2a). This increase was of a similar magnitude to that observed in an additional group of 142 type 2 diabetic patients, whose clinical features are also shown in Table 1. As in the case of the type 2 diabetic patients, close to one-third of the EuF+ subjects expressed amounts of PEA15 protein that were more than two SDs higher than the mean for the EuF− subjects. As previously demonstrated in isolated fibroblasts, skeletal muscle and adipose tissues from type 2 diabetic individuals [4], the increased levels of PEA15 protein detected in PBLs from the EuF+ and the type 2 diabetic subjects occurred in parallel with an increase in *PEA15* mRNA (Fig. 2b). Also, the increased *PEA15* gene expression in the EuF+ and the type 2 diabetic individuals was paralleled by a three-fold increase in levels of the PEA15 downstream target PLD1 ($p=0.001$; Fig. 2c), with no change in *PLD1* mRNA (data not shown).

As in our previous report [4], in the present study we found no difference in *PEA15* expression between the obese and lean individuals, irrespective of whether they were euglycaemic or diabetic (data not shown). To address

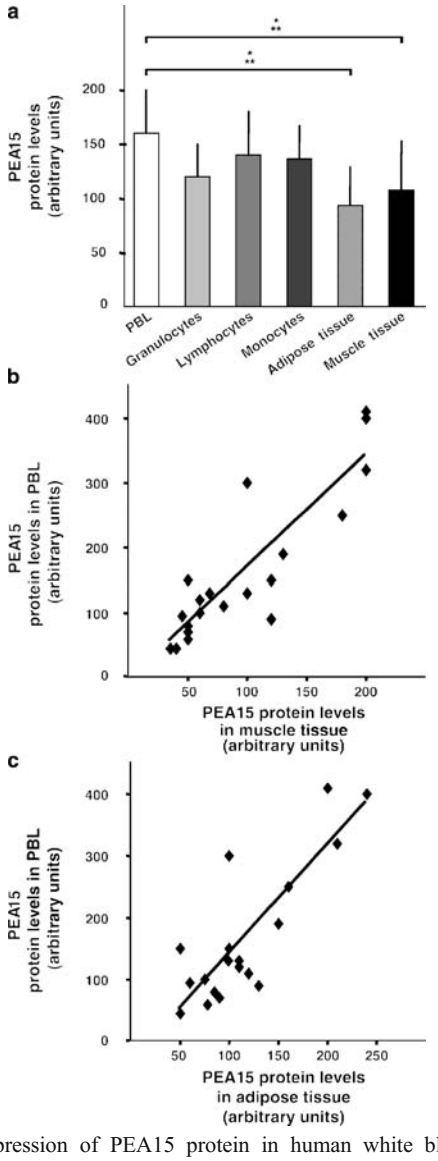

Fig. 1 Expression of PEA15 protein in human white blood cells. **a** PBLs and the relative granulocyte, lymphocyte and monocyte fractions were prepared from samples from 21 individuals (type 2 diabetic, EuF+ and Eu− subjects at a 1:1:1 ratio). Biopsy specimens of skeletal muscle and adipose tissues from these same patients were collected at the time they underwent elective abdominal surgery, as described in the Subjects and methods section. Cells and tissues were solubilised and analysed by western blotting PEA15 antibodies [4]. Blots were revealed by enhanced chemiluminescence and autoradiography, and PEA15 levels quantified by laser densitometry. *Bars* represent the means ± SEM of four independent experiments. *Asterisks* indicate statistical significance between *bracketed columns* ($p<0.001$). Correlation between PEA15 levels in PBLs and muscle ($r=0.881$, $p<0.001$) (**b**) or fat ($r=0.845$, $p<0.001$) (**c**) was tested by linear regression analysis, as described in Subjects and methods

Table 1 Clinical and biochemical features of the euglycaemic and type 2 diabetic individuals

Parameter	EuF− subjects (n=120)	EuF+ subjects (n=30)	Type 2 diabetic subjects (n=142)
Sex (male/female)	84/36	14/16	90/52
Age (years)	49±9	49±6	58±10*
Smokers (%)	27	20	21
BMI (kg/m^2)	28±5	28±3	29±4
Systolic BP (mmHg)	126±15	128±16	134±21**
Diastolic BP (mmHg)	79±9	81±9	80±9
Total serum cholesterol (mmol/l)	6.1±1.2	5.8±1	5.2±0.9**
HDL cholesterol (mmol/l)	1.4±0.4	1.4±0.3	1.2±0.4**
Serum triacylglycerol (mmol/l)	1.5±0.7	1.3±0.5	1.9±1.6**
Fasting plasma glucose (mmol/l)	5.0±0.4	5.0±0.3	9.4±3**
Fasting plasma insulin (μU/ml)	4±3	9±3*	–

Data are presented as the means±SEM or %
*p<0.01 vs EuF− subjects
**p<0.001 vs EuF− subjects

the effect of other major risk factors for type 2 diabetes, we analysed the levels of PEA15 in 55 further individuals diagnosed with IFG according to a previous report [21]. Ten of these subjects had at least one type 2 diabetes-affected FDR (IFG-F+), while the others had no family history of disease (IFG-F−). PBL levels of PEA15 in IFG-F− subjects were found to be very comparable to those detected in EuF− subjects (Fig. 3a). As in the case of the euglycaemic individuals, however, IFG-F+ subjects exhibited PEA15 levels that were significantly greater than those detected in the IFG-F− subjects (p<0.05), further pointing to an important effect of family history on PEA15 levels in euglycaemic and IFG humans.

In the euglycaemic subjects (both EuF+ and EuF−) and in the type 2 diabetic patients described in Table 1, there were no sex-related differences in PEA15 level. Also, no significant correlation was found between the production of PED15 and the age, BMI, waist circumference, systolic BP or diastolic BP, fasting cholesterol, triacylglycerol or glucose levels of the subjects (data not shown), indicating that PEA15 levels are independent of these variables in humans. To further examine this hypothesis, we compared PEA15 levels in three additional groups of consecutively recruited euglycaemic (EuF+ and EuF−) and type 2 diabetic individuals matched for age, BMI, waist circumference, systolic BP and diastolic BP, and fasting HDL cholesterol

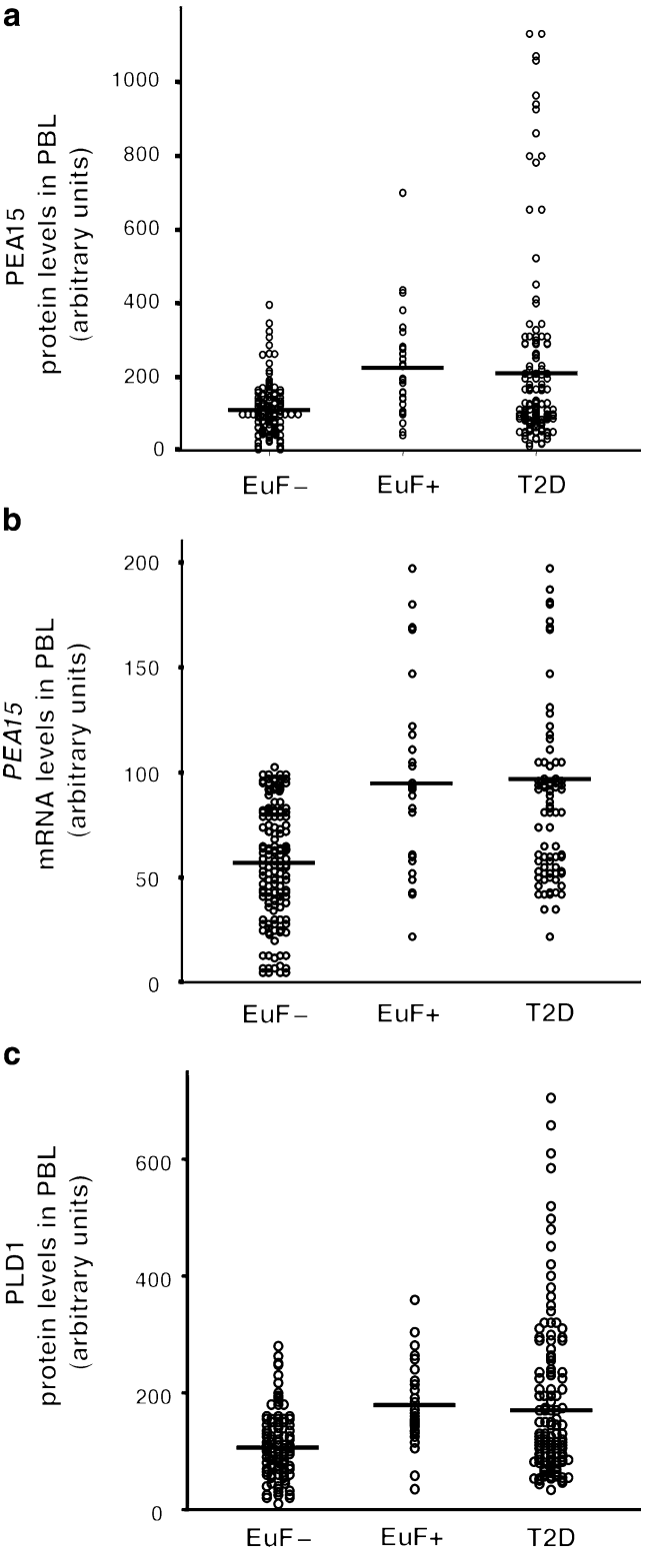

Fig. 2 Expression of *PEA15* in PBLs from euglycaemic subjects. **a** PBLs from 30 euglycaemic individuals with at least one type 2 diabetic FDR (EuF+) and 120 euglycaemic subjects lacking a family history of diabetes (EuF−) were consecutively collected. For comparison, PBLs from 142 type 2 diabetic patients (T2D) were also analysed. Cells were solubilised and PEA15 (**a**) and PLD protein levels (**c**) were quantified in the lysates as outlined in the legend to Fig. 1. Data points represent the mean of three independent determinations in each individual subject. RNA was extracted from PBLs and *PEA15* mRNA (**b**) quantified by real-time PCR as described in the Subjects and methods section. Data points are the means of three independent determinations in each individual subject

and triacylglycerol levels (Table 2). A two-fold increase in PEA15 levels was again observed in both the diabetic subjects and the EuF+ subjects compared with the EuF− subjects ($p<0.01$; Fig. 3b), providing corroborating evidence that PEA15 is independent these variables in humans.

To address the functional significance of *PEA15* overexpression in type 2 diabetic FDR, we searched for associations with diabetes-related phenotypes. We analysed an additional group of 25 euglycaemic offspring of type 2 diabetes-affected couples from the EUGENE2 cohort http://www.eugene2.com, last accessed in August 2006; [20, 22, 23]. PBL expression levels of *PEA15* in these offspring were comparable to those of the other type 2 diabetic FDR investigated in this study (Table 3). The other clinical characteristics of these subjects are also shown in Table 3. A negative correlation was evidenced between the individual levels of PEA15 in PBLs and insulin-stimulated glucose disposal according to fat-free mass, as determined by the euglycaemic–hyperinsulinaemic clamp ($r=-557$, $p=0.01$; Fig. 3c). Insulin-stimulated glucose disposal also negatively correlated with BMI in these individuals ($r=-0.64$, $p=0.01$). However, the correlation with PEA15 levels remained significant after adjustment for age, sex and BMI ($r=-491$, $p=0.02$). As in the case of the other FDR investigated in this study, PEA15 levels did not correlate with age, BMI, waist circumference, SBP or DBP, or fasting cholesterol, triacylglycerol or glucose levels in these offspring (data not shown). Thus, the overexpression of *PEA15* may induce insulin-resistance in euglycaemic offspring of type 2 diabetes-affected couples.

Discussion

Previous studies have reported that PEA15 is a multifunctional protein that controls a number of cellular functions, including proliferation, apoptosis and insulin-regulated glucose transport [4–12, 17, 18, 32]. In transgenic mice fed high-fat diets, the overexpression of *Pea15* leads to diabetes [18]. In humans, no genetic variability accounting for the differential expression of the *PEA15* gene has been identified to date. However, *PEA15* overexpression was shown to occur in skeletal muscle and adipose tissues from type 2 diabetic patients, independently of drug treatment and obesity [4]. Whether this abnormality is associated with other risk factors for type 2 diabetes is unknown, as is whether it contributes to specific phenotype(s) associated with diabetes in humans. In the present work we have addressed these questions in FDR of type 2 diabetic subjects. These individuals have a very high risk of type 2 diabetes [30, 31] and develop different diabetes-related phenotypes years before diabetes onset, independently of the metabolic abnormalities associated with this disorder [33–35]. We have shown that the *PEA15* gene is overexpressed in PBLs from EuF+ subjects. As previously shown

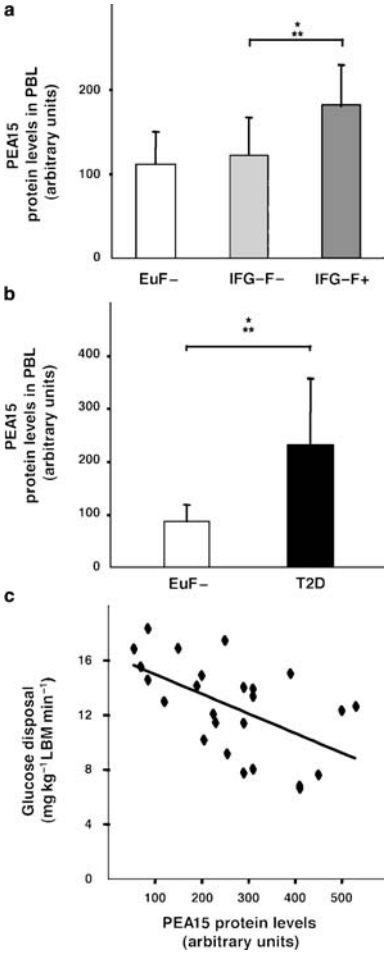

Fig. 3 Type 2 diabetes-associated phenotypes and risk-factors related to *PEA15* expression. **a** PBL were obtained from 55 consecutive individuals with IFG diagnosed as described previously [21]. Ten of these subjects had at least one type 2 diabetes-affected FDR (IFG-F+), while the others had no family history of diabetes ($n=45$; IFG-F−). Cells were solubilised and PEA15 protein levels were quantified in the lysates as outlined in the legend to Fig. 1. For comparison, data obtained from PBL from the euglycaemic subjects lacking a family history of diabetes and shown in Fig. 2 (EuF−) are also presented. **b** Two further groups of euglycaemic subjects with ($n=25$; EuF+) or without ($n=36$; EuF−) a family history of type 2 diabetes and of type 2 diabetic subjects ($n=58$; T2D) were matched for age, BMI, waist circumference, systolic BP and diastolic BP and fasting cholesterol and triacylglycerol levels as described in the Subjects and methods section. PBLs from these subjects were obtained and solubilised, and PEA15 protein levels quantitated in the lysates as outlined in the legend to Fig. 1. *Bars* represent the mean ± SEM of three (**a**) or four (**b**) independent experiments, each in duplicate. *Asterisks* indicate statistical significance between bracketed columns ($p<0.001$). **c** PEA15 protein levels were determined in PBLs from 25 euglycaemic offspring of couples, one of which was affected by type 2 diabetes. Glucose disposal was assessed by the euglycaemic–hyperinsulinaemic clamp as described in the Subjects and methods section and corrected for fat-free mass. Linear regression analysis performed as described in the Subjects and methods section revealed a correlation between PEA15 levels in PBLs and glucose disposal ($r=-0.557$, $p=0.01$)

Table 2 Clinical and biochemical features of matched euglycaemic and type 2 diabetic individuals

Parameter	EuF− subjects (n=34)	EuF+ subjects (n=25)	Type 2 diabetic subjects (n=56)	p value
Sex (male/female)	20/14	10/15	33/23	–
Age (years)	54±2	56±1	55±2	NS
Smokers (%)	25	23	24	NS
BMI (kg/m^2)	29±3	28±2	29±2	NS
Waist circumference (cm)	93±6	94±3	95±3	NS
Systolic BP (mmHg)	132±6	128±7	130±8	NS
Diastolic BP (mmHg)	82±5	80±4	79±10	NS
Total serum cholesterol (mmol/l)	5.2±0.3	5.2±0.2	5.3±0.1	NS
HDL cholesterol (mmol/l)	1.2±0.1	1.2 ±0.1	1.2±0.1	NS
Serum triacylglycerol (mmol/l)	1.4±0.1	1.4±0.1	1.5±0.1	NS
Fasting plasma glucose (mmol/l)	5.0±0.3	5.1±0.3	9.5±3.1	<0.001

Data are presented as the means ± SEM or %. Statistical significance was assessed by comparing all three groups of subjects

in cells from type 2 diabetic subjects [4], this overexpression occurs at both the mRNA and protein level indicating that, as previously demonstrated in cells from type 2 diabetic subjects [4], it is caused, at least in part, by a transcriptional abnormality. Earlier studies in isolated cells and in vivo showed that PEA15 binds to and increases the cellular stability of PLD1, deregulating PKC signalling and impairing insulin-dependent glucose disposal [17, 18]. We now show that enhanced PLD1 stability also appears to occur in PBLs from type 2 diabetic subjects and FDR, suggesting that it occurs in individuals who overexpress *PEA15*. Indeed, in parallel with PEA15, cells from both type 2 diabetic and EuF+ individuals exhibit PLD protein levels that are three times higher than those seen in EuF− individuals, with no change in mRNA. PEA15 levels in the PBLs are closely correlated with those in fat and skeletal muscle tissues. Thus, although PBLs do not represent a classical target for insulin, they do allow the non-invasive investigation of the role of *PEA15* overexpression during progression towards type 2 diabetes. In this study the overexpression of *PEA15* relative to the expression seen in EuF− individuals was demonstrated in almost one-third of the EuF+ subjects and in a similar proportion of the type 2 diabetic subjects. It appears therefore that increased PEA15 levels represent a common abnormality in both type 2 diabetic subjects and individuals at increased risk of this disease, suggesting that it might precede diabetes onset in the latter.

In both type 2 diabetic subjects and their FDR, PEA15 levels were independent of BMI, waist circumference, systolic and diastolic blood pressure, HDL cholesterol, triacylglycerol and glucose levels, indicating that expression of the *PEA15* gene is independent of the main variables associated with the metabolic syndrome in humans. PEA15 levels were also not related to sex or age, or to reduced physical activity or smoke habit, two recognised risk factors for type 2 diabetes and insulin resistance. Interestingly, we report that, similar to EuF+ individuals, individuals with IFG who are FDR of type 2 diabetic individuals (IFG-F+) also exhibit high levels of PEA15. In contrast, IFG subjects lacking a family history of type 2 diabetes (IFG-F−) do not, further indicating familiar clustering of this trait. The overexpression of the *PEA15* gene in the type 2 diabetic subjects and their FDR may be genetically or environmentally determined, or determined by both factors. Indeed, previous studies [4] have shown that the overexpression persists in human skin fibroblasts after several generations in culture, suggesting that the occurrence of similarly high PEA15 levels in the EuF+, IFG+ and type 2 diabetic individuals is at least partly a genetically determined effect. At variance with these euglycaemic and IFG individuals, the presence of a FDR affected by type 2 diabetes had no effect on PEA15 levels in patients with an established diagnosis of type 2 diabetes (data not shown). Once deranged glucose tolerance enables overt diabetes to occur, factors secondary to the disease might modify *PEA15* gene expression and/or PEA15 protein levels, thereby masking the primary overexpression. Consistent with this possibility, recent studies by

Table 3 Clinical and biochemical features of the type 2 diabetic offspring

Parameter	Mean ± SEM
Number (male/female)	13/12
Age (years)	30.1±8.3
BMI (kg/m^2)	24.5±4.1
Waist circumference (cm)	83.5±12.2
Systolic BP (mmHg)	112±11
Diastolic BP (mmHg)	75±6
Total cholesterol (mmol/l)	4.8±0.9
HDL cholesterol (mmol/l)	1.5±0.3
Triacylglycerol (mmol/l)	1±0.7
Fasting plasma glucose (mmol/l)	4.8±0.5
2-h glucose (mmol/l)	5.8±1.4
Fasting plasma insulin (pmol/l)	55.6±20.8
Fat-free mass glucose disposal (mg kg LBM^{-1} min^{-1})	12±3
HOMA-IR	1.8±0.9
HOMA-B	174±65
Insulinogenic index ($\Delta I_{30}/\Delta G_{30}$)	18±12
PEA15 (arbitrary units)	257±35

Data are presented as the means ± SEM

HOMA-B Homeostasis model assessment of pancreatic beta cell function, *HOMA-IR* homeostasis model assessment of insulin resistance, *LBM* lean body mass

our own as well as other laboratories have shown that PEA15 is highly regulated at the post-translational level [1, 2, 7, 12].

Previous studies in cultured cells and in transgenic mice have shown that overexpression of the gene encoding PEA15 determines resistance to insulin action and impairs glucose-induced insulin secretion. In this study, we investigated whether *PEA15* overexpression is associated with impaired insulin action and/or secretion in euglycaemic offspring of type 2 diabetes-affected couples. In these individuals, who are at increased risk of diabetes, insulin resistance and reduced non-oxidative glucose metabolism appear years before the onset of hyperglycaemia [33, 34]. Using results from euglycaemic–hyperinsulinaemic clamp studies, a negative correlation was established between PEA15 levels and the insulin-stimulated glucose disposal by the fat-free mass of the offspring, suggesting that high levels of PEA15 protein contribute to development of skeletal muscle resistance to insulin action in these individuals. PEA15 levels were also weakly correlated with fasting plasma insulin in these FDR, but not in euglycaemic individuals lacking a family history of type 2 diabetes (data not shown). *PEA15* might induce insulin resistance only in conjunction with other diabetes-related genes enriched in at-risk individuals. In this case, as previously demonstrated by Mootha et al. [36], gene enrichment analysis [37] may help to further unravel the mechanistic significance of increased levels of PEA15 in human diabetes. However, whether the *PEA15* effect is weaker in individuals lacking a particular, as-yet-undefined, genetic background cannot be concluded from these studies. Indeed, unlike the hyperglycaemic–euglycaemic clamp, fasting plasma insulin is a very crude index of insulin sensitivity [38]. In addition to insulin resistance, offspring of type 2 diabetes-affected couples may also have beta cell dysfunction, as evidenced by decreases in insulin and amylin secretion in response to glucose stimulation [35]. However, PEA15 levels were not correlated with any index of beta cell function in the offspring. Overexpression of the gene may impair glucose-triggered insulin secretion in transgenic mice but not in humans. This is unlikely, however, as transfection of a *PEA15* cDNA in human beta cell lines grossly impairs the insulin response to glucose (data not shown). Alternatively, in the type 2 diabetic FDR, the consequence of the high PEA15 levels on insulin action might occur earlier during life than the PEA15 effect on beta cell function.

In conclusion, in the present study we have shown that *PEA15* overexpression represents a common abnormality in both type 2 diabetic patients and their FDR and can be conveniently detected in PBLs. In at-risk individuals, this defect is associated with the presence of a type 2 diabetes-affected FDR and not with other major type 2 diabetes risk factors. In euglycaemic FDR of type 2 diabetic patients, high PEA15 levels are strongly correlated with resistance to insulin action in the lean mass, suggesting that PEA15 contributes to the early appearance of insulin resistance in these individuals. Follow-up studies are in progress to further elucidate the effect of PEA15 levels in type 2 diabetes.

Acknowledgements This work was supported in part by the European Community's FP6 EUGENE2 (LSHM-CT-2004-512013), grants from the EFSD to F. Beguinot, the Associazione Italiana per la Ricerca sul Cancro (AIRC) (Italian Association for Cancer Research) to F. Beguinot and P. Formisano, and the Ministero dell'Università e della Ricerca Scientifica (Ministry of Education) (PRIN to F. Beguinot and P. Formisano and FIRB RBNE0155LB to F. Beguinot). The financial support of Telethon – Italy is gratefully acknowledged. The authors also warmly thank R. Napoli (University of Naples 'Federico II') for continuous advice during the course of this work and for critical reading of the manuscript, and G. Fratellanza for technical help.

Duality of interest The authors declare that there are no competing financial interests.

References

1. Danziger N, Yokoyama M, Jay T, Cordier J, Glowinski J, Chneiweiss H (1995) Cellular expression, developmental regulation, and phylogenic conservation of PEA-15, the astrocytic major phosphoprotein and protein kinase C substrate. J Neurochem 64:1016–1025
2. Estelles A, Yokoyama M, Nothias F et al (1996) The major astrocytic phosphoprotein PEA-15 is encoded by two mRNAs conserved on their full length in mouse and human. J Biol Chem 271:14800–14806
3. Ramos JW, Hughes PE, Renshaw MW et al (2000) Death effector domain protein PEA-15 potentiates Ras activation of extracellular signal receptor-activated kinase by an adhesion-independent mechanism. Mol Biol Cell 11:2863–2872
4. Condorelli G, Vigliotta G, Iavarone C et al (1998) *PED/PEA-15* gene controls glucose transport and is overexpressed in type 2 diabetes mellitus. EMBO J 17:3858–3866
5. Formstecher E, Ramos JW, Fauquet M et al (2001) PEA-15 mediates cytoplasmic sequestration of ERK MAP kinase. Dev Cell 1:239–250
6. Brunet A, Roux D, Lenormand P, Dowd S, Keyse S, Pouyssegur J (1999) Nuclear translocation of p42/p44 mitogen-activated protein kinase is required for growth factor-induced gene expression and cell cycle entry. EMBO J 18:664–674
7. Trencia A, Perfetti A, Cassese A et al (2003) Protein kinase B/Akt binds and phosphorylates PED/PEA-15, stabilizing its antiapoptotic action. Mol Cell Biol 23:4511–4521
8. Vaidyanathan H, Ramos JW (2003) RSK2 activity is regulated by its interaction with PEA-15. J Biol Chem 278:32367–32372
9. Estelles A, Charlton CA, Blau HM (1999) The phosphoprotein protein PEA-15 inhibits Fas- but increases TNF-R1-mediated caspase-8 activity and apoptosis. Dev Biol 1999 216:16–28
10. Kitsberg D, Formstecher E, Fauquet M et al (1999) Knock-out of the neural death effector domain protein PEA-15 demonstrates that its expression protects astrocytes from TNFalpha-induced apoptosis. J Neurosci 19:8244–8251
11. Condorelli G, Vigliotta G, Cafieri A et al (1999) PED/PEA-15: an anti-apoptotic molecule that regulates FAS/TNFR1-induced apoptosis. Oncogene 18:4409–4415
12. Trencia A, Fiory F, Maitan MA et al (2004) Omi/HtrA2 promotes cell death by binding and degrading the anti-apoptotic protein ped/pea-15. J Biol Chem 279:46566–46572

13. Xiao C, Yang BF, Asadi N, Beguinot F, Hao C (2002) Tumor necrosis factor-related apoptosis-inducing ligand-induced death-inducing signaling complex and its modulation by c-FLIP and PED/PEA-15 in glioma cells. J Biol Chem 277:25020–25025
14. Hao C, Beguinot F, Condorelli G et al (2001) Induction and intracellular regulation of tumor necrosis factor-related apoptosis-inducing ligand (TRAIL) mediated apoptosis in human malignant glioma cells. Cancer Res 61:1162–1170
15. Formisano P, Perruolo G, Libertini S et al (2005) Raised expression of the antiapoptotic protein ped/pea-15 increases susceptibility to chemically induced skin tumor development. Oncogene 24:7012–7021
16. Zhang Y, Redina O, Altshuller YM et al (2000) Regulation of expression of phospholipase D1 and D2 by PEA-15, a novel protein that interacts with them. J Biol Chem 275:35224–35232
17. Condorelli G, Vigliotta G, Trencia A et al (2001) Protein kinase C (PKC)-alpha activation inhibits PKC-zeta and mediates the action of PED/PEA-15 on glucose transport in the L6 skeletal muscle cells. Diabetes 50:1244–1252
18. Vigliotta G, Miele C, Santopietro S et al (2004) Overexpression of the *PED/PEA-15* gene causes diabetes by impairing glucose-stimulated insulin secretion in addition to insulin action. Mol Cell Biol 24:5005–5015
19. Di Paola R, Frittitta L, Miscio G et al (2002) A variation in 3′ UTR of *hPTP1B* increases specific gene expression and associates with insulin resistance. Am J Hum Genet 70:806–812
20. Marini MA, Frontoni S, Mineo D et al (2003) The Arg972 variant in insulin receptor substrate-1 is associated with an atherogenic profile in offspring of type 2 diabetic patients. J Clin Endocrinol Metab 88:3368–3371
21. Genuth S, Alberti KG, Bennett P et al (2003) Follow-up report on the diagnosis of diabetes mellitus. Diabetes Care 26:3160–3167
22. Prudente S, Hribal ML, Flex E et al (2005) The functional Q84R polymorphism of mammalian *Tribbles* homolog *TRB3* is associated with insulin resistance and related cardiovascular risk in Caucasians from Italy. Diabetes 54:2807–2811
23. Cardellini M, Perego L, D'Adamo M et al (2005) C-174G polymorphism in the promoter of the interleukin-6 gene is associated with insulin resistance. Diabetes Care 28:2007–2012
24. Matthews DR, Hosker JP, Rudenski AS, Naylor BA, Treacher DF, Turner RC (1985) Homeostasis model assessment: insulin resistance nad beta-cell function from fasting plasma glucose and insulin concentrations in man. Diabetologia 28:412–419
25. Hanson RL, Pratley RE, Bogardus C et al (2000) Evaluation of simple indices of insulin sensitivity and insulin secretion for use in epidemiologic studies. Am J Epidemiol 151:190–198
26. Metcalfe P, Waters AH (1992) Location of the granulocyte-specific antigen LAN on the Fc-receptor III. Transfus Med 2:283–287
27. Seager Danciger J, Lutz M, Hama S et al (2004) Method for large scale isolation, culture and cryopreservation of human monocytes suitable for chemotaxis, cellular adhesion assays, macrophage and dendritic cell differentiation. J Immunol Methods 288:123–134
28. Miele C, Formisano P, Condorelli G et al (1997) Abnormal glucose transport and GLUT1 cell-surface content in fibroblasts and skeletal muscle from NIDDM and obese subjects. Diabetologia 40:421–429
29. Laemmli UK (1970) Cleavage of structural proteins during the assembly of the head of bacteriophage T4. Nature 227:680–685
30. Klein BE, Klein R, Moss SE, Cruickshanks KJ (1996) Parental history of diabetes in a population-based study. Diabetes Care 19:827–830
31. Bennet PH (1990) Epidemiology of diabetes mellitus. In: Rifkin H, Porte D Jr (eds) Hellenberg and Rifkin's diabetes mellitus. Elsevier, New York, pp 363–377
32. Condorelli G, Trencia A, Vigliotta G et al (2002) Multiple members of the mitogen-activated protein kinase family are necessary for PED/PEA-15 anti-apoptotic function. J Biol Chem 277: 11013–11018
33. Beck-Nielsen H, Groop LC (1994) Metabolic and genetic characterization of prediabetic states. Sequence of events leading to non-insulin-dependent diabetes mellitus J Clin Invest 94:1714–1721
34. Eriksson J, Franssila-Kallunki A, Ekstrand A et al (1989) Early metabolic defects in persons at increased risk for non-insulin-dependent diabetes mellitus. N Engl J Med 321:337–343
35. Knowles NG, Landchild MA, Fujimoto WY, Kahn SE (2002) Insulin and amylin release are both diminished in first-degree relatives of subjects with type 2 diabetes. Diabetes Care 25:292–297
36. Mootha VK, Lingren CM, Eriksson KF et al (2003) PGC-1α-responsive genes involved in oxidative phosphorylation are coordinately downregulated in human diabetes. Nat Genet 34:267–273
37. Subramanian A, Tamayo P, Mootha VK et al (2005) Gene set enrichment analysis: a knowledge-based approach for interpreting genome-wide expression profiles. Proc Natl Acad Sci USA 102:15545–15550
38. Castillo MJ (2002) Simple assessment of insulin sensitivity and secretion. Int Diabetes Monitor 14:1–7